CENTRAL NERVOUS SYSTEM INTRINSIC INFLAMMATION AS DRIVER AND THERAPEUTIC TARGET OF PROGRESSION IN MULTIPLE SCLEROSIS

DISSERTATION
for the award of the degree
"Doctor rerum naturalium"

of the Georg-August University Göttingen
within the PhD program Molecular Medicine
of the Georg-August University School of Science

submitted by
ANASTASIA GELADARIS
from Wuppertal

Göttingen, October 2021

1ST MEMBER OF THE THESIS COMMITTEE:

Prof. Dr. Martin Sebastian Weber

Department of Neuropathology
University Medical Centre, Georg-August University Göttingen

2ND MEMBER OF THE THESIS COMMITTEE:

Prof. Dr. Dr. Hannelore Ehrenreich

Clinical Neuroscience
Max Planck Institute of Experimental Medicine Göttingen

3RD MEMBER OF THE THESIS COMMITTEE:

Prof. Dr. Jutta Gärtner

Department of of Pediatrics and Adolescent Medicine
University Medical Centre, Georg-August University Göttingen

FURTHER MEMBERS OF THE EXAMINATION BOARD

Prof. Dr. Frauke Alves

Institute of Molecular Biology of Neuronal Signals
Max Planck Institute of Experimental Medicine Göttingen

Prof. Dr. Alexander Flügel

Institute for Neuroimmunology and Multiple Sclerosis Research
University Medical Center, Georg-August-University Göttingen

Dr. Sebastian Kügler

Department. of Neurology
University Medical Center Göttingen

DATE OF ORAL EXAMINATION: 01.12.2021

FÜR ALLE MÄUSE, DIE DIESE ARBEIT ERMÖGLICHT HABEN

LIST OF PUBLICATIONS

ABSTRACTS

XIV European Meeting on Glial Cells in Health and Disease, Porto, July 10-13. 2019, poster presentation: B cell-derived IL-10 modulates the inflammatory response of microglia and astrocytes.

Geladaris, A., Häusler, D., Brück, W., Weber, M.S.

8th joint European Committee for Treatment and Research in Multiple Sclerosis-Americas Committee for Treatment and Research in Multiple meeting (MSVirtual 2020), September 11-13, 2020: B cells regulate chronic CNS inflammation in an IL-10-dependent manner.

Geladaris, A., Häusler, D., Brück, W., Weber, M.S.

XV European Meeting on Glial Cells in Health and Disease, Online, July 5-9, 2021, poster presentation: The role of B cell-derived IL-10 in regulation of chronic CNS inflammation.

Geladaris, A., Häusler, D., Brück, W., Weber, M.S.

37th Congress of the European Committee for Treatment and Research in Multiple Sclerosis, October, 13-15, 2021: poster presentation: Targeting BTK in chronic CNS autoimmunity inhibits activation of microglia.

Geladaris, A., Torke, S., Grenningloh, R., Boschert, U., Brück, W., Weber, M.S

REVIEW ARTICLE

Geladaris, A., Häusler, D., & Weber, M. S. (2021). Microglia: The Missing Link to Decipher and Therapeutically Control MS Progression?. International Journal of Molecular Sciences, 22(7), 3461.

CONTENTS

List of Figures

ABBREVIATIONS

Ab	Antibody
AF	AlexaFluor
ANOVA	Analysis of variance
APC	Allophycocyanin
APC	Antigen-presenting cell
BCR	B cell receptor
BTK	Bruton's tyrosine kinase
BV	Brilliant violet
B2M	Beta-2-Microglobulin
CD	Cluster of differentiation
CFA	Complete Freund's adjuvant
CFSE	Carboxyfluorescein succinimidyl ester
CIS	Clinical isolated syndrome
CNS	Central nervous system
CSF	Cerebrospinal fluid
Ctrl	control
DAB	3,3'-Diaminobenzidine
DAPI	4',6-diamidino-2-phenylindole
dH_2O	Distilled water
ddH_2O	Bidistilled water
DMEM	Dulbecco's Modified Eagle Medium
DMSO	Dimethyl sulfoxide
DNA	Deoxyribonucleic acid
EAE	Experimental autoimmune encephalomyelitis
e.c.	Extracellular
EDSS	Expanded disability status scale
EDTA	Ethylenediamine Tetraacetic Acid Disodiumsalt Dihydrate
e.g.	Exempli gratia
FACS	Fluorescence activated cell sorting
FCS	Fetal calf serum
FITC	Fluorescein isothiocyanate
G	Gramm
GAPDH	Glycerinaldehyd-3-phosphat-Dehydrogenase
GFAP	Glial fibrillary acidic protein
GM-CSF	Granulocyte-macrophage colony-stimulating factor
H	Hour(s)
H&E	Haematoxilin and eosin
H_2O_2	Hydrogen peroxide
Iba1	Ionized calcium-binding adapter molecule 1
i.c.	Intracellular
IFN	Interferon
IL	Interleukin
i.p.	Intraperitoneal
KO	Knock-out
L	Liter
mAb	Monoclonal antibody
MACS	Magnetic activated cell sorting
MBP	Myelin basic protein
MFI	Mean fluorescence intensity
MHC	Major histocompatibility complex
µl	Microliter
µm	Micrometer
µM	Micromolar

mg	Milligram
ml	Milliliter
mm	Millimeter
mM	Millimolar
min	Minute(s)
MOG	Myelin oligodendrocyte glycoprotein
MS	Multiple Sclerosis
OVA	Ovalbumin
PB	Pacific Blue
PBS	Phosphate buffered saline
PCR	Polymerase chain reaction
PE	Phycoerithrin
PFA	Paraformaldehyde
p.i.	Post immunization
PLL	Poly-L-lysine
PLP	Proteolipid-Protein
PMA	Phorbol 12-Myristate 13-Acetate
PPMS	Primary progressive multiple sclerosis
PTX	Pertussis Toxin
q	Quantitative
RNA	Ribonucleic acid
RPMI-1640	Roswell Park Memorial Institute-1640
RRMS	Relapsing-remitting multiple sclerosis
RT	Room temperature
S	Second (s)
SD	Standard deviation
SDS	Sodium dodecyl sulfate
SEM	Standard error
SPMS	Secondary progressive multiple sclerosis
TCR	T cell receptor
Th	T helper cells
TNF	Tumor necrosis factor
Tris	Tris (Hydroxymethyl) Aminomethane

ABSTRACT

Controlling disease progression in multiple sclerosis (MS) remains a major challenge. Progression of MS is defined as an increase in neurological disability occurring independently of relapses or focal MRI-detectable inflammatory lesions. Whereas the exact mechanisms of progression are still unknown, it is assumed to be driven by an interplay of central nervous system (CNS)-resident cells and hematopoietic cells within the CNS.

The potential of B cells to modulate CNS-compartmentalized inflammation in progressive disease is of growing interest, since B cells are known to persist in the inflamed MS CNS and B cell-follicle like structures were found in the meninges of MS patients. Whether and how B cells interact with CNS-resident cells, such as microglia and astrocytes, to possibly modulate chronic progression of MS remains unclear.

In the first part of this study, the interaction of B cells with CNS-resident cells in modulation of chronic CNS inflammation was investigated. It was observed that B cells are capable of shaping the activity of microglia and astrocytes. B cells and their supernatant showed an upregulation of pro-inflammatory molecules on homeostatic microglia and astrocytes, while under inflammatory conditions the pro-inflammatory cytokine profile of microglia was reduced. It was identified that this effect is attributed to a soluble factor of B cells and showed that B cell-derived IL-10 has the potential of limiting microglia activity and function. In contrast, astrocyte activity was unaffected by B cell-derived IL-10. Taken together, these data demonstrate that the sole presence of B cells within the CNS is not by definition associated with pathogenic functions and reveal an immunoregulatory potential for controlling CNS-intrinsic inflammation, which is associated with disease progression.

The second part of this study aimed at analyzing the potential of Bruton's tyrosine kinase (BTK) inhibition as a therapeutic strategy on CNS-resident cells in halting disease progression. BTK is an enzyme involved in B cell and myeloid cell activation and function. In the present study it was shown that the majority of CNS-resident cells expressing BTK are microglia cells and that its expression is increased upon activation. Evobrutinib inhibited microglial M1 polarization and enhanced the phagocytic capacity of microglia in vitro. Additionally, in the passive experimental autoimmune encephalomyelitis (EAE) animal model of MS, which vastly excludes an involvement of peripheral immune cells, evobrutinib reduced the expression of markers involved in activation and antigen presentation on microglia. Furthermore, in the cuprizone model, evobrutinib treatment increased the number of

oligodendrocyte precursor cells and induced remyelination. In conclusion, these data suggest that BTK-dependent inflammatory signaling in microglia cells can be modulated by evobrutinib. These findings highlight the therapeutic potential of BTK inhibition in counteracting chronic progression of MS.

1 INTRODUCTION

1.1 MULTIPLE SCLEROSIS

Multiple sclerosis (MS) is the most common chronic inflammatory demyelinating disease of the central nervous system (CNS) leading to the formation of focal demyelinating lesions in the white and grey matter as well as to diffuse damage and neurodegeneration in the entire brain (Lassmann, Bruck, & Lucchinetti, 2007). Around 2.8 million people are affected worldwide (Walton et al., 2020). The large variety of symptoms often includes partial or complete loss of vision, changes in the sensation in the extremities and fatigue. Due to the chronic nature of the disease, it can further extend to an impairment of balance, muscle spasms, problems with speech as well as bladder and bowel difficulties (Smith & McDonald, 1999). There are four clinical MS subtypes defined. The most common disease type is the relapsing-remitting MS (RRMS), affecting about 85 % of patients. RRMS is characterized by relapses, followed by periods of recovery with remission. Most of these patients transitioning gradually from RRMS to a progressive disease, termed as secondary progressive MS (SPMS). The remaining 10-15 % of patients have a slow and continuous neurological deterioration from onset without definable relapses, termed as primary progressive MS (PPMS) (Lublin et al., 2014). With magnetic resonance imaging (MRI) and the better understanding of the disease mechanisms, the classification of MS includes active or non-active in both the relapsing and the progressive forms of the disease. The classification reflects the inflammatory component of MS, which can be visualized by MRI (Lublin et al., 2014). Furthermore, patients with SPMS and PPMS are classified into those with or without progression measured by the assessment of ongoing progression of disability, which is associated with diffuse inflammation and neurodegenerative mechanisms (Lublin et al., 2014).

1.1.1 PATHOLOGY & PATHOGENESIS

The pathological hallmark of MS is the presence of multifactorial lesions in the grey and white matter of the CNS. These lesions are characterized by an inflammatory infiltrate and gliosis resulting in demyelination and axonal damage (Bruck, 2005; Kutzelnigg & Lassmann, 2014). These so-called MS plaques are present throughout the CNS with predominant occurrence in the spinal cord, optic nerve, periventricular areas and brain stem (Gilmore et al., 2009; Green, McQuaid, Hauser, Allen, & Lyness, 2010). In the early disease stage, most lesions detected are termed as active lesions, which arise quickly and vanish after a while (Lassmann et al., 2007).

In contrast, smoldering lesions, which are present over a longer period of time and slowly expand, are more prominent in chronically diseased patients. However, active lesions can still arise in progressive MS patients. In addition to the focal lesions, patients with progressive MS show profound alterations in the so-called normal-appearing white matter (NAWM) (D. H. Mahad, Trapp, & Lassmann, 2015). Changes in NAWM are characterized by diffuse inflammation and potential axonal injury in non-demyelinated areas (D. H. Mahad et al., 2015). Pathological differences between early and chronic MS lesions can be described by their amount of infiltrating inflammatory cells, overall demyelinating and axonal damage. Early lesions are characterized by a dominant accumulation of macrophages and activated microglia containing myelin fragments, whereas the density of T cells, B cells and plasma cells can vary, and incomplete demyelination and acute axonal damage can be observed. Remyelination is often more pronounced in early lesions compared to chronic lesions (Kuhlmann et al., 2017; Kutzelnigg & Lassmann, 2014). Lymphocytes and macrophages are not as dominant in chronic lesions and oligodendrocyte precursor cells are present, whereas mature oligodendrocyte numbers are reduced. Furthermore, the axonal density is often decreased in areas of chronic MS lesions. For active lesions four neuropathological patterns have been described in MS based on infiltrating immune cells, deposition of humoral factors and loss of oligodendrocyte and/or myelin proteins, which are homogenous in a single patient but vary interindividually (Lucchinetti et al., 2000). Pattern I lesions show demyelination associated with activated macrophages/microglia, while in pattern II lesions, complement activation is prominent, suggesting the involvement of antibodies. Pattern III lesions are characterized by the presence of oligodendrocytes with nuclear condensation and fragmentation, resembling apoptotic cell death. This is associated with a selective loss of myelin-associated glycoprotein. Pattern IV lesions are exceptionally rare and show extensive non-apoptotic oligodendrocyte degeneration in the periplaque white matter adjacent to the active lesion, with limited repair, and no evidence for either complement deposition or loss of the myelin-associated glycoprotein (Kuhlmann et al., 2017; Lucchinetti et al., 2000).

The cause of MS is still unknown, but the understanding of the major processes and MS pathogenesis has grown. Inflammation in the CNS is believed to be the primary site of damage in MS. There is an accumulation of peripheral immune cells after initial activation within the CNS, resulting in demyelination. This hypothesis mainly stems from the experimental autoimmune encephalomyelitis (EAE) model, in which the disease can be induced by immunization with myelin- or CNS-derived proteins or peptides and is largely driven by CNS-specific $CD4^+$ T cells, whereas in contrast MS is most strongly associated with $CD8^+$ T cells

(Lassmann & Bradl, 2017). The site of activation of these autoreactive T cells is still unknown in MS. However, it is assumed to be influenced by both genetic and environmental factors (Dendrou, Fugger, & Friese, 2015). Once in the CNS, autoreactive effector $CD4^+$ T cells are locally reactivated by antigen-presenting cells (APCs), leading to the release of various pro-inflammatory cytokines like Interferon (IFN)-γ and Tumor-necrosis factor (TNF)-α causing the disruption of the blood-brain barrier (BBB) and easing the transmigration of peripheral immune cells through the BBB (Goverman, 2009). These recruited T cells, B cells and macrophages lead to an established inflammation within the CNS by interfering with CNS-resident cells (Hochmeister et al., 2006; Lisak et al., 2009). Thereby causing myelin loss, oligodendrocyte destruction, axonal damage and leading to neurological destruction. In parallel, immune-modulatory networks are triggered to limit inflammation and to initiate repair, which results in at least partial remyelination and is associated with clinical remission (Franklin & Goldman, 2015). However, further attacks alleviate the capacity to compensate axonal loss and recovery mechanisms are less effective, therefore an imbalance between damage and repair is ultimately leading to progression of MS (Nave & Trapp, 2008). Inflammation is an important feature of both relapsing and progressive forms of MS, although the number of inflammatory cells is smaller in PPMS than in SPMS (Nave & Trapp, 2008).

1.1.2 Pathomechanisms of MS progression

The pathophysiology of MS progression is not completely understood, but the current understanding is that progression of MS is characterized by chronic inflammation behind a relatively closed BBB with activation of microglia and continuous involvement of hematopoietic cells. Release of reactive oxygen species (ROS) and nitrogen species (RNS) contributes to mitochondrial and axonal damage. Ultimately leading to neurodegeneration, which is characteristic for progressive MS (Faissner, Plemel, Gold, & Yong, 2019).

Inflammation is likely to continuously drive these processes, but as already mentioned, this inflammation is considered to be compartmentalized at both the leptomeningeal and the blood vessel within the CNS parenchyma (Serafini, Rosicarelli, Magliozzi, Stigliano, & Aloisi, 2004). Several observations make such contribution of T cells and B cells plausible. In MS patients with disease progression $CD8^+$ T cells were found in cortical plaques, interacting with mononuclear phagocytes composed of macrophages, microglia and monocytes (Konjevic Sabolek et al., 2019; Smolders et al., 2018) Furthermore, a high number of B cells and plasma cells were found in progressive MS patients. These plasma cells are apparently the source for oligoclonal bands in the cerebrospinal fluid (CSF) (Machado-Santos et al., 2018). Interestingly,

neuropathological studies showed that demyelination and axonal damage occurred in the cortical and deep grey matter of MS patients, which are associated with microglial activation, while lymphocytes are located in the meninges (Magliozzi et al., 2007). Therefore, it is likely, that the activation of microglia is driven by soluble factors produced by T cells and/or B cells. In this regard, pro-inflammatory cytokines such as TNF-α and IFN-γ have been detected in progressive MS patients (Gardner et al., 2013; Rossi et al., 2014). Along the same lines, activated microglia and astrocytes can contribute to the persistence of B cells within the CNS by the secretion of specific molecules, such as BAFF or IL-6, which are known to support B cell survival (Krumbholz et al., 2005).

Furthermore, axonal damage and demyelination are deemed as other major mechanisms leading to neurodegeneration and therefore to progression of MS. Reduced repair and impaired axonal regeneration are probably the main driver, in part caused due to age and a lifelong oxidative stress environment, which itself causes both dysfunctions of the mitochondria and nuclear/mitochondrial DNA mutations (Murphy, 2009). The mitochondrial damage results in energy deficiency. Once exceeding a certain threshold, energy deficiency can cause an imbalance in cell ion exchange through mechanisms linked to calcium channels, which finally may lead to axonal degeneration and cell death (Trapp & Stys, 2009). Another result of demyelination and oligodendrocyte loss may be the activation of microglia and their production of ROS and nitric oxide (NO). NO can directly inhibit the mitochondrial respiratory chain complex IV as well as the cytochrome c oxidase and can thereby lead to axonal injury (D. J. Mahad et al., 2009). Notably, in patients with progressive MS, an increased number of neurons with respiratory deficits are present in the cerebral cortex (Campbell et al., 2011). Finally, extracellular iron, released by injured oligodendrocytes and microglia, increases tissue susceptibility to oxidative damage caused by free radicals (Hametner et al., 2013). These processes likely cause a vicious cycle of tissue destruction contributing to progression of MS.

1.2 CELL TYPES INVOLVED IN MS PROGRESSION

1.2.1 B CELLS

The historical view of MS as a T cell-mediated disease has changed through various findings. The observation that B cell depletion with anti-CD20 monoclonal antibodies substantially limits new relapses and disease activity in MS has made it clear, that B cells probably are equally important in the initiation and propagation of MS (Hauser et al., 2008). B cells

modulate the immune response in multiple ways: they differentiate into plasmablasts which secrete effector antibodies, modulate effector T cell responses through antigen presentation and produce cytokines. (M. Duddy et al., 2007; Nutt, Hodgkin, Tarlinton, & Corcoran, 2015; Rivera, Chen, Ron, Dougherty, & Ron, 2001). In detail, as APCs they recognize even low concentrations of antigens with their B cell receptor (BCR) and initiate T cell responses through co-stimulatory molecules such as CD40, CD80 and CD86 as well as major histocompatibility complex class II (MHCII) (Rivera et al., 2001). The process of antigen presentation not only activates responding T cells but in turn induces the proliferation of the presenting B cells and leads to their differentiation into memory cells and antibody-producing cells (Nutt et al., 2015). The presence of oligoclonal immunoglobulins within the CSF of MS patients, which result from local antibody production, has long been described and served as a biomarker for the diagnosis of the disease (Link & Huang, 2006). Whether oligoclonal bands contribute to the pathogenesis and progression of MS still remains unclear but the immunoglobulins (Ig) were shown to localize within lesions and near damaged myelin and were demonstrated, ex vivo and in vitro, to cause axonal damage by inducing complement-mediated tissue injury (Link & Huang, 2006; Magraner et al., 2012). In addition, in SPMS patient's lymphoid follicle-like structures were observed, which correlate with an early onset of disease and an early irreversible disability (Howell et al., 2011; Magliozzi et al., 2007). As cytokine producing cells, B cells are able to regulate immune responses in a pro-and anti-inflammatory manner (M. Duddy et al., 2007; Fillatreau, Sweenie, McGeachy, Gray, & Anderton, 2002). Cytokines are small, secreted proteins that facilitate interactions and communications between cells (Zhang & An, 2007). B cells can release pro-inflammatory cytokines such as IL-6, granulocyte macrophage colony-stimulating factor (GM-CSF), TNF-α and lymphotoxin, which can all influence the development of effector and memory $CD4^+$ T cell responses. (Barr et al., 2012; Korn et al., 2008; Li et al., 2015). B cells isolated from the blood of MS patients, showed an overall shift from the naïve status towards activation and memory cell differentiation. Compared to healthy controls, B cells from MS patients produced enhanced levels of pro-inflammatory cytokines, such as IL-6, lymphotoxin and TNF-α, while producing less IL-10 (Barr et al., 2012; M. Duddy et al., 2007). Importantly, B cells can release anti-inflammatory cytokines, such as IL-10 and IL-35 (Fillatreau et al., 2002). Both cytokines are essential for the resolution of CNS inflammation, as mice deficient for B cell-derived IL-10 or IL-35 fail to recover from EAE and instead chronically deteriorate (Fillatreau et al., 2002; Shen et al., 2014) However, it is still unclear whether these cytokines are produced simultaneously by one or individually by different B cell populations.

1.2.2 ASTROCYTES

Astrocytes are the most abundant and heterogenous cell type of glia cells in the CNS. They play a pivotal role in CNS development and homeostasis by the modulation of synaptic activity, and provide nutrients and support needed for neuronal survival as well as they play a major role in BBB formation (Clarke & Barres, 2013; Rouach, Koulakoff, Abudara, Willecke, & Giaume, 2008). Although most astrocytes are tissue embedded, positionally stable and nonmotile, they express numerous receptors and secrete various molecules which on the one hand, enable them to respond to neuroactive compounds, such as neurotransmitters, neuropeptides, growth factors, cytokines and toxins and on the other hand, regulate surrounding cells (Ponath, Park, & Pitt, 2018). Through the contact of the neurons pre- and post-synaptic terminals, astrocytes regulate synaptic formation, activity and plasticity e.g., by releasing glutamate, D-serine, and ATP (Chung, Allen, & Eroglu, 2015). They prune synapses through phagocytosis, modify gene expression, secrete neurotrophic factors and participate in the production of neurosteroids.

Astrocytes respond to changes in the CNS environment by a complex process of activation, including morphological transformations and transcriptional and biochemical changes (Sofroniew & Vinters, 2010). Environmental changes lead to a rapid upregulation of molecules secreted by astrocytes, including TNF-α, IL-1β and IL-6, neurotrophic factors, such as nerve growth factor (NGF), brain-derived neurotropic factor (BDNF) vascular endothelial growth factor (VEGF) and leukemia inhibitory factor, as well as chemokines like CCL2, CCL5 and CXCL10. Furthermore, reactive astrocytes express cell adhesion molecules such as ICAM-1 and VCAM-1, as well as iNOS (Ponath et al., 2018). These than so-called reactive astrocytes have recently been categorized accordingly to their transcriptome profile as A1 or A2 in parallel to the M1 and M2 phenotype categories for macrophages and microglia (Liddelow & Barres, 2017; Liddelow et al., 2017). A1 astrocytes are induced by neuroinflammation and upregulate many genes that have been shown to be destructive to synapses, suggesting that A1 type astrocytes might have harmful functions (Liddelow et al., 2017). By contrast, A2 astrocytes are induced by ischemia and upregulate many neurotrophic factors, which promote survival and growth of neurons and synaptic repair (Liddelow et al., 2017). Since the classification of the dichotomy of this classification is already questionable for macrophages and may be oversimplified, reactive astrocytes might have more than these two states of polarization.

Traditionally, astrocytes have been assigned to play a negligible role in MS by the formation of a glia scar, once demyelination occurred (Brosnan & Raine, 2013). However, in neuroinflammation astrocytes were shown to control CNS infiltration by peripheral inflammatory immune cells and are suggested to regulate the activity of microglia and oligodendrocytes. Reactive astrocytes are present in lesions and the NAWM of MS patients (Brosnan & Raine, 2013; Ponath et al., 2017). Observations in EAE, the animal model of MS showed that astrocytes are even activated before significant immune cell infiltration takes place (Wang et al., 2005). Reactive astrocytes and the loss of the end-feed around small vessels are an early event in lesion development, linked to the loss of BBB function (Brosnan & Raine, 2013). However, progression is supposed to be a CNS-compartmentalized process behind a relatively closed BBB, therefore the mechanism how astrocytes contribute to MS progression may be different.

Astrocytes secrete a variety of molecules by which they may contribute to progression of MS. For example, IL-15 and BAFF secreted by astrocytes support B cell proliferation and survival (Michel et al., 2015). Importantly, B cell activating factor (BAFF) levels were shown to be increased in the CSF of MS patients compared to healthy controls (Ragheb et al., 2011). Furthermore, progression is assumed to be driven by the activation of glia cells within the CNS. Molecules secreted by reactive astrocytes like IL-6, lymphotoxin-alpha promote activation of microglia (Aharoni, Eilam, & Arnon, 2021). A study in a chronic progressive model of EAE has shown that astrocytes produce and response to sphingolipid lactosylceramide (LacCer) (Mayo et al., 2014). LacCer induces production of iNOS in astrocytes and was found to control the recruitment and activation of microglia and macrophages in the CNS (Mayo et al., 2014). Furthermore, secretion of Fibroblast growth factors (FGF)-2 promotes oligodendrocyte precursor cell (OPC) proliferation and survival but prevents maturation (Goddard, Berry, & Butt, 1999).

Astrocytes may also dampen inflammation and promote repair. In EAE, ablation of BDNF-derived by astrocytes resulted in a more severe clinical course and enhanced axonal loss in the chronic disease phase (Linker et al., 2010). Whereas an enhanced BDNF production by astrocytes resulted in enhanced remyelination (Fulmer et al., 2014). Indicating that BDNF released by astrocytes exhibits neuroprotective effects. In MS lesions, BDNF is expressed in high levels by immune cells and neurons as well as reactive astrocytes (Stadelmann et al., 2002).

The pivotal roles of astrocytes make them an attractive therapeutic target. Understanding astrocyte function and diversity and the mechanism by which they are regulated as well as how they regulate other cells may lead to the development of novel approaches to target disease progression.

1.2.3 MICROGLIA

Microglia are the resident immune cells of the CNS (Kreutzberg, 1996; Perry & Gordon, 1988). They develop from immature yolk sac progenitor cells during early embryogenesis and persist throughout life (Ginhoux, Lim, Hoeffel, Low, & Huber, 2013). Microglia permanently monitor their microenvironment, even slight abnormalities can be detected, affecting neural tissue homeostasis, deviations from normal neuronal firing activity or unusual appearance and concentrations or formats of certain molecules like neurotransmitters or cytokines (Kettenmann, Hanisch, Noda, & Verkhratsky, 2011). Microglia have been shown to be highly plastic and heterogenous cells, which can rapidly switch between different phenotypes after CNS injury (Kettenmann et al., 2011). Depending on the inflammatory milieu, microglia change their morphology, gene expression and function and thereby can either trigger neurotoxic pathways leading to progressive neurodegeneration or exert important roles in promoting neuroprotection, downregulation of inflammation and stimulation of repair (Kettenmann et al., 2011). The diverse microglia phenotypes were classified into M1, M2a, M2b or M2c subset and were characterized by the presence of particular cell surface molecules and the expression of specific cytokines as well as chemokines (Martinez, Sica, Mantovani, & Locati, 2008). Under homeostatic conditions, microglia cells reveal a ramified morphology and are considered as 'resting' microglia. The homeostatic phenotype of microglia expresses several immune receptors, such as TREM2, SIRP1A, CXC3CR1, CSF-1R and CD200R (Aguzzi, Barres, & Bennett, 2013; Ginhoux et al., 2013). Upon activation, a drastic morphological transformation to an amoeboid cell type takes place. This phenotype is defined as the classically activated M1 microglia, which is cytotoxic and exhibits pro-inflammatory markers. Thus, some of the homeostatic genes are downregulated while genes linked to phagocytosis, antigen presentation and oxidative injury are upregulated (Aguzzi et al., 2013). In detail, potentially neurotoxic microglia, which promote inflammation and oligodendrocyte damage, present cell-surface-expressed molecules such as MHCII and CD86, which allow T cells to recognize and bind small fragments of pathogens (Schetters, Gomez-Nicola, Garcia-Vallejo, & Van Kooyk, 2017). Furthermore, M1 microglia produce pro-inflammatory molecules, such as NO, reactive ROS, IL-1β, and TNF-α (Colton & Gilbert, 1987; Ding, Nathan, & Stuehr, 1988).

In contrast, the alternative M2 phenotype is defined as a neuroprotective microglial phenotype, which regulates immune functions, promotes repair and is characterized by increased phagocytosis and the production of diverse factors including arginase 1 (Arg1), CD206, insulin-like growth factor (IGF-2) and anti-inflammatory cytokines such as IL-10 (Martinez et al., 2008). The M2 phenotype is further categorized into three different subtypes: M2a and M2b/c. M2a microglia are involved in repair and regeneration, M2b microglia are associated with an immunoregulatory phenotype and M2c with an acquired-deactivating phenotype with repair and wound healing functions (Chhor et al., 2013). However, as for astrocytes the classification of these phenotypes is likely to be over-simplified but at the same time a useful tool to study and understand the role of microglia in health and disease.

The role of microglia during disease progression was manifested from neuropathological studies of MS patients. Progressive MS patients reveal a chronic active (smoldering or expanding) lesion pattern with microglial activation at the edge of a burned-out plaque (Frischer et al., 2009) and microglial activity was observed in areas surrounding the focal lesion, the NAWM (De Groot et al., 2001; van der Poel et al., 2019). As a biomarker for microglia activity, the mitochondrial translocator protein (TSPO) is studied by positron emission tomography (PET). TSPO expression in the CNS is low under healthy conditions, but increases under neuroinflammation in microglia (Giannetti et al., 2014). In progressive MS patients it was observed, that microglial activity correlates with disease disability and prognosis, but not with disability in relapsing MS patients, which could be associated with compartmentalized inflammation and neurodegeneration (Giannetti et al., 2014). Furthermore, the phenotype of microglia in patients with progressive MS was investigated by a single-cell mass cytometry analysis (Bottcher et al., 2020). The study revealed, that highly phagocytic and activated microglia downregulated the expression of homeostatic markers such as P2Y12 and GPR56, while upregulating the expression of proteins involved in phagocytic activity and microglial activation including CD68, CCR2, CD64, CD32, CD95 and CCL4 (Bottcher et al., 2020). Besides the physical presence of microglia at sites of demyelination and an upregulation of various markers, the pathophysiological function of microglia in progression is largely unclear. However, once activated microglia can produce numerous pro-inflammatory molecules, which may induce bystander effects to neighboring glial cells and neurons. For example, microglia derived TNF-α and C1q are involved in the induction of a neurotoxic A1 astrocyte phenotype, which can cause the rapid killing of both neurons and oligodendrocytes (Liddelow et al., 2017; Rothhammer et al., 2018). Due to their high metabolic activity, oligodendrocytes are especially susceptible to microglia-derived

factors. As already mentioned, microglia are also capable of a neuroprotective function. Key mechanisms, how microglia contribute to neuronal repair and therefore induce remyelination, are myelin debris clearance by phagocytosis and the production of anti-inflammatory cytokines like IL-4, IL-10 and IL-13 (Karamita et al., 2017; Lampron et al., 2015). In general, myelin debris clearance and the secretion of pro-inflammatory cytokines by microglia benefit the recruitment of oligodendrocyte precursors cells (OPCs) to the lesion site, thereby enhancing remyelination. However, histopathological studies from progressive MS patients, showed a decreased number of OPCs in the lesion (Boyd, Zhang, & Williams, 2013; Franklin & Goldman, 2015). The failure of remyelination may be one mechanism of MS progression, which could be in part explained through the lack of the neuroprotective M2 microglia.

1.3 THERAPY IN MS

1.3.1 BRUTON'S TYROSINE KINASE

Bruton's Tyrosine Kinase (BTK), a member of the Tec family of kinases, is a cytoplasmic non-receptor tyrosine kinase, expressed in cells of hematopoietic origin, including B cells, myeloid cells and platelets, but not T cells, NK cells or plasma cells (Hendriks, Yuvaraj, & Kil, 2014). Besides the well-established mediation of the BCR signaling, including the regulation of survival, activation, proliferation and differentiation to antibody-producing plasma cells, BTK is assumed to be involved in various signaling downstream to Fc, integrin, chemokine and toll-like receptors (Hendriks et al., 2014; Lopez-Herrera et al., 2014).

BTK is phosphorylated by Lyn or Syk, leading to the activation of PLC-γ, which initiates the stimulation and production of IP3, DAG and PKC (Humphries et al., 2004). The levels of calcium are increased and the MAPK/ERK path is triggered, affecting the transcriptional expression of genes involved in proliferation, survival and cytokine secretion (Brullo, Villa, Tasso, Russo, & Spallarossa, 2021).

Dysfunctional mutations of BTK cause the failure of B cell development, resulting in X-linked agammaglobulinemia in humans, a prototypic primary humoral immunodeficiency (Shillitoe & Gennery, 2017). Moreover, deficiency in BTK or BTK inhibition alleviates Th17-cell-related inflammatory responses in various inflammatory mouse models (Martin et al., 2020; Pal Singh, Dammeijer, & Hendriks, 2018). Within the CNS, BTK is mainly expressed in microglia (Keaney, Gasser, Gillet, Scholz, & Kadiu, 2019). Furthermore, neuropathological studies from

progressive MS patients revealed an increased expression of BTK in the CNS (Glendenning et al., 2020; Martin et al., 2020). Due to the involvement of BTK in various cell signaling pathways inhibition of BTK may have a potential to target innate immunity within the CNS, associated with disease progression.

1.3.2 BTK INHIBITION

In the past years, a large number of BTK inhibitors have been developed and tested for the treatment of a number of diseases. The most studied compound is ibrutinib, which is approved for the treatment of B cell malignancies, as well as chronic graft-vs-host disease (Deeks, 2017; Miklos et al., 2017). However, ibrutinib has shown side effects, which have been attributed, in part to off-target to kinases other than BTK. Thus, to improve the tolerability of BTK inhibitors, while maintaining the efficacy of ibrutinib, new BTK inhibitors have been developed with high potency, enhanced selectively profiles, and reduced off-target effects (Brullo et al., 2021). According to their mechanism of action and binding mode, BTK inhibitors can be classified into two types based on their mode of binding to BTK: Irreversible inhibitors form a covalent bond with the amino acid residue Cys481 in the ATP binding site of BTK or reversible inhibitors, which bind to specific pockets in the SH3 domain by weak, reversible forces (hydrogen bonds or hydrophobic interactions), inducing an inactive conformation of the kinase (Carnero Contentti & Correale, 2020; Roskoski, 2020). Importantly, a mutation in the Cys481 region can lead to a reduction in the compound potency and might reduce the therapeutic efficacy in patients with these mutations. In contrast, noncovalent BTK inhibitors retain potent inhibition against these mutations (Brullo et al., 2021). Evobrutinib is a potent, covalent BTK inhibitor with high kinase selectivity that has shown efficacy in animal models of rheumatoid arthritis, systemic lupus erythematosus and MS (Caldwell et al., 2019; Park et al., 2016; Torke et al., 2020). Furthermore, evobrutinib has already met its primary endpoint in the treatment of RRMS, defined as total number of T1 gadolinium-enhancing lesions in a Phase II clinical trial. However, evobrutinib showed no effect on progression of disability (Montalban et al., 2019).

1.4 AIMS OF THE STUDY

1.4.1 AIM 1: THE ROLE OF REGULATORY B CELLS IN CONTAINMENT OF CHRONIC CNS INFLAMMATION

The mechanisms leading to disease progression remain unknown. However, several mechanisms have been proposed to drive disease progression, including sustained compartmentalized inflammation behind a relatively closed BBB with continued involvement of hematopoietic cells and activation of CNS-resident cells, such as microglia and astrocytes. Therefore, the first part of this study aimed at analyzing the interaction of B cells with CNS-resident cells to investigate whether B cells can attenuate the activity of these cell types in a self-sustained circuit of inflammation within the CNS, which is associated with disease progression. Thus, B cells or B cell-derived supernatant were directly co-cultured with purified microglia or astrocytes, addressing whether direct cell-cell contact or a soluble factor attenuated the activity of CNS-resident cells. Furthermore, to distinctively investigate the effect of B cell-derived molecules on CNS-resident cells, specific cytokine function was blocked using specific antibodies. Microglial and astrocytic phenotype, activation and functionality were analyzed.

1.4.2 AIM 2: THE THERAPEUTIC POTENTIAL OF BTK INHIBITION IN CHRONIC CNS AUTOIMMUNITY

Targeting disease progression of MS remains a major challenge. Inhibition of BTK already showed promising results in a phase II trial of RRMS. However, due to molecular size and properties of BTK inhibitors, targeting BTK within the CNS may be a promising candidate to halting or slowing disease progression. Therefore, in the second project, the potential of BTK inhibition on CNS-resident cells was analyzed in vitro and in vivo in animal models of MS. First, the expression of BTK in CNS-resident cells was analyzed. Second, especially the influence of BTK inhibition on microglia, the mainly BTK expressing cell type in the CNS, was analyzed in terms of differentiation, activation and functionality.

2 MATERIAL & METHODS

2.1 MATERIAL

2.1.1 REAGENTS

TABLE 1: REAGENTS

REAGENT	SOURCE OF SUPPLY
Acetic acid	Merck, Millipore, Germany
Agarose	Starlab Gmbh, Germany
β-Mercaptoethanol	Sigma Aldrich, USA
BD FACS Clean™	BD Biosciences, USA
BD FACS Flow™	BD Biosciences, USA
BD FACS Rinse™	BD Biosciences, USA
BD FACS™ Lysing Solution, 10x	BD Biosciences, USA
BD Pharm Lyse™, 10x	BD Biosciences, USA
BD PhosFlow™ Buffer I 10x	BD Biosciences, USA
BD PhosFlow™ Lyse Fix 5x	BD Biosciences, USA
CFSE	BioLegend, USA
Cytofix/Cytoperm™	BD Biosciences, USA
Cytofix™	BD Biosciences, USA
Chloral Hydrate	Merck Millipore, Germany
Citric acid	Merck Millipore, Germany
DAB	Sigma-Aldrich Chemie Gmbh, Germany
DAPI	Sigma-Aldrich Chemie Gmbh, Germany
DEPEX	VWR International, Germany
DMEM	PAN Biotech, Germany
DMSO	Sigma Aldrich, USA
DNase I	Roche, Switzerland
EDTA	Carl Roth, Germany
Ethanol, 100 %	Merck Millipore, Germany
FCS	Sigma Aldrich, USA
FoxP3 Fix/Perm Concentrate	eBioscience, USA
FoxP3 Fix/Perm Diluent	eBioscience, USA
FoxP3 Perm Buffer, 10x	eBioscience, USA
GelRed	Biotium, Inc., Fremont, USA
Gibco® GlutaMax™	Thermo Fisher Scientific, USA

Go-Taq® DNA Polymerase Buffer, 5x	Promega, USA
GolgiPlug™	BD Biosciences, USA
HCl	Merck Millipore, Germany
H_2O_2, 30 %	Merck Millipore, Germany
HyperLadder™ 50 bp	Meridian Bioscience, BioCat GmbH, Germany
Ionomycin	Sigma Aldrich, USA
Isopropyl alcohol	Th. Geyer GmbH & Co. KG, Germany
L-Glutamine, 200 mM	Sigma Aldrich, USA
LIVE/DEAD™ Fixable NIR Dead Cell Stain Kit	Thermo Fisher Scientific, USA
Mayer's Hemalum	Merck Millipore, Germany
MOG_{35-55} peptide	GenScript Biotech, Netherlands
MOG_{1-117} protein	GenScript Biotech, Netherlands
NaCl, 0.9 % solution, sterile	B. Braun Melsungen Ag, Germany
$NaCO_3$	Merck Millipore, Germany
$NaHCO_3$	Merck Millipore, Germany
Paraffin Oil	Carl Roth, Germany
PBS, sterile	Sigma Aldrich, USA
Penicillin, 10 000 Units	Sigma Aldrich, USA
Perm/Wash™ Buffer, 10x	BD Biosciences, USA
PLL	Sigma Aldrich, USA
POX (Peroxidase conjugated Avidin)	Sigma Aldrich, USA
PFA, powder	Merck Millipore, Germany
PMA	Sigma Aldrich, USA
PTX	Sigma Aldrich, USA
RPMI-1640	Sigma Aldrich, USA
Sodium Pyruvate, 100 mM	Sigma Aldrich, USA
qPCRBIO SyGreen	Nippon Genetics Europe GmbH, Germany
TMB	Moss Inc., Maryland, USA
Tris	Carl Roth, Germany
Trypan Blue	Sigma Aldrich, USA
Trypsin 2.5 %	PAN Biotech, Germany
Trypsin/EDTA 0.05%	PAN Biotech, Germany
Tween® 20	Merck Millipore, Germany
Xylol	Th. Geyer GmbH & Co. KG, Germany

2.1.2 SOLUTIONS, BUFFERS AND CELL CULTURE MEDIA

TABLE 2: SOLUTIONS, BUFFERS AND CELL CULTURE MEDIA

SOLUTION	COMPOSITION
Blocking buffer for immunohistochemistry	PBS 10 % FCS
CFA	Paraffin oil 15 % mannide monooleate 6.7 mg/ml Mycobacterium tuberculosis H37RA
Chloral hydrate, 14 %	distilled water 14 % chloral hydrate
Citric acid buffer, 10 Mm	2.1 g citric acid 1 l distilled water NaOH, adjust to pH 6
Coating buffer	8.4 g NaHCO3 3.5 g NaCO3 1 l distilled water Stir filter, adjust to pH 9.5
Cryo medium	60 % RPMI complete 20 % DMSO 20 % FCS
3,3'-Diaminobenzidine tetrachloride (Dab) working solution	PBS 0.5 mg/ml DAB add 20 µl 30 % hydrogen peroxidase per 50 ml DAB solution before use
DMEM complete	DMEM 10 % FCS 1 % GlutaMax® 100 units penicillin
ELISA wash buffer	1 ml Tween® 20 1.8 l distilled water 200 ml 10x PBS
ELISA stop solution	1 N H_2SO_4 solution
1 % Eosin	70 % isopropyl alcohol 1 % eosin G stir filter, before use add 0.5 % acetic acid
Fluorescence-activated cell sorting (FACS) buffer	PBS, sterile

	2 % FCS
1 % HCl	1 % HCl absolute 70 % ethanol
Magnetic Activated Cell Sorting (MACS) buffer	PBS, sterile 0.5 % FCS 2 mM EDTA pH 7.2
10x PBS	95.5 g PBS 1 l distilled water
RD1 buffer (ELISA block buffer)	200 ml 10x PBS 20 g BSA 1.8 l distilled water
RPMI complete	RPMI-1640 10 % FCS 1 mM sodium pyruvate 50 µM β-Mercaptoethanol 100 units penicillin 2 mM L-glutamine
TAE (Tris, acetic acid, EDTA) buffer	40 mM Tris 20 mM acetic acid 1 mM EDTA 1 l distilled water (adjusted to pH 8)

2.1.3 MONOCLONAL ANTIBODIES FOR FLOW CYTOMETRY

TABLE 3: ANTIBODIES

SPECIFICITY	FLUOROCHROME	CLONE	DILUTION	SOURCE OF SUPPLY
B220	PE-Cy7	RA3-6B2	1:100	BD Bioscience
CD3e	PE	145-2C11	1:100	BioLegend
CD3e	BUV395	145-2C11	1:100	BD Bioscience
CD4	BV510	GK1.5	1:100	BioLegend
CD8a	FITC	53-6.7	1:100	BioLegend
CD11b	FITC	M1/70	1:100	BioLegend
CD11b	PacificBlue™	M1/70	1:100	BioLegend
CD11c	PE-Dazzle	N418	1:100	BioLegend
CD16	AlexaFluor700	FAB19601N	1:100	R&D systems
CD19	BV510	6D5	1:100	BioLegend

CD19	PerCp-Cy5.5	1D3	1:100	BioLegend
CD20	AlexaFluor647	SA275A11	1:200	BioLegend
CD21/CD35	BV510	7G6	1:100	BioLegend
CD23	APC	B3B4	1:100	BioLegend
CD25	PE	PC61.5	1:100	BioLegend
CD32	FITC	S17012B	1:100	BioLegend
CD40	PE-CF594	3/23	1:100	BD Biosciences
CD44	APC	IM7	1:100	BioLegend
CD45	BUV395	30-F11	1:100	BD Biosciences
CD45	PerCP-Cy5.5	30-F11	1:100	BioLegend
CD64	PE	X54-5/7.1	1:100	BioLegend
CD68	PE	FA-11	1:100	BioLegend
CD69	PE-Dazzle	H1.2F3	1:100	BioLegend
CD80	PE-CF594	16-10A1	1:100	BD Biosciences
CD86	APC	GL1	1:100	BioLegend
CD93	PE	AA4.1	1:100	BioLegend
CD95 (Fas)	BV421	Jo2	1:100	BioLegend
CD206	PE	C068C2	1:100	BioLegend
CD279	PE	MIH5	1:100	BioLegend
Arginase 1	APC	A1exF5	1:100	Invitrogen
BTK	PE	53/BTK	1:10	BD Biosciences
Foxp3	PE	FJK-16s	1:100	eBioscience
GFAP	FITC	1B4	1:50	BD Biosciences
iNOS	FITC	6/iNOS/NOS Type II	1:100	BD Biosciences
IgMb	FITC	AF6-78	1:100	BD Biosciences
IgD	BV421	11-26c.2a	1:100	BioLegend
Ly6C	APC	HK1.4	1:100	BioLegend
Ly6G	PacificBlue™	1A8	1:100	BioLegend
MHC-II	PE	AF6-120.1	1:100	BioLegend
MHC-II	PB	AF6-120.1	1:100	BioLegend

2.1.4 ANTIBODIES FOR CELL CULTURE

TABLE 4: ANTIBODIES FOR CELL CULTURE

SPECIFICITY	CLONE	SOURCE OF SUPPLY
Anti-mouse IL-6	JES5-2A5	BioXcell
Anti-mouse IL-10	JES5-2A5	BioXcell
Anti-mouse rat IgG1 Isotype	MP5-20F3	BioXcell
leaf™ purified anti-mouse CD3	145-2C11	BioLegend
leaf™ purified anti-mouse CD28	37.51	BioLegend

2.1.5 PRIMARY ANTIBODIES FOR IMMUNOHISTOCHEMICAL STAINING

TABLE 5: PRIMARY ANTIBODIES FOR IMMUNOHISTOCHEMICAL STAINING

SPECIFICITY	SPECIES	ANTIGEN RETRIEVAL/FIXATION	DILUTION	SOURCE OF SUPPLY
Iba1	Rabbit	Citrat	1:500	Fujufilm Wako
GFAP	Rabbit	Citrat	1:300	Citrat
Olig2	Rabbit	TE	1:300	IBL
PLP	Mouse	Citrat	1:500	Bio-Rad

2.1.6 SECONDARY ANTIBODIES FOR IMMUNOHISTOCHEMICAL STAINING

TABLE 6: SECONDARY ANTIBODIES FOR IMMUNOHISTOCHEMICAL STAINING

SECONDARY ANTIBODY	DILUTION	MANUFACTURER
Anti-mouse IgG, biotinylated	1:100	Merck
Anti-rabbit IgG, biotinylated	1:250	Jackson ImmunoResearch
Anti-rat IgG, biotinylated	1:500	Innovative Diagnostic Systems
Anti-mouse IgG, AF488	1:250	Jackson ImmunoResearch
Anti-rabbit IgG Cy3	1:200	Jackson ImmunoResearch

2.1.7 OLIGONUCLEOTIDE PRIMERS

TABLE 7: MURINE OLIGONUCLEOTIDE PRIMERS

GENE	SEQUENCE	AMPLIFICATION SIZE (bp)
Arginase 1	forward: CGCCTTTCTCAAAAGGACAG reverse: CCAGCTCTTCATTGGCTTTC	204
BTK	forward: GGTGGAGAGCACGAGATAAA reverse: CCGAGTCATGTGTTTGGAATAC	113
B2M	forward: CGGCCTGTATGCTATCCAGA reverse: GGGTGAATTCAGTGTGAGCC	227
CCL2	forward: GCATCCACGTGTTGGCTCA reverse: CTCCAGCCTACTCATTGGGATCA	95
CCL3	forward: TGTACCATGACACTCTGCAAC reverse: CAACGATGAATTGGCGTGGAA	109
CCL5	forward: ACTCCCTGCTGCTTTGCCTAC reverse: ACGTGCTGGTGTAGAAATACT	76
CXCL1	forward: TGTTGTGCGAAAAGAAGTGC reverse: CGAGACGAGACCAGGAGAAA	249
GapDH	forward: CATGGCCTTCCGTGTTCCTA reverse: TGTCATCATACTTGGCAGGTTTCT	83
iNOS	forward: GGCAGCCTGTGAGACCTTTG reverse: GCATTGGAAGTGAAGCGTTTC	72

2.1.8 CONSUMABLES

TABLE 8: CONSUMABLES

CONSUMABLE	SOURCE OF SUPPLY
Bottle Top Filter, 0.2 µM	Sarstedt, Germany
Cell culture plates, Flat Bottom (6 Well, 24 Well, 96 Well)	Greiner bio-one, Austria
96-well round bottom plate	Sarstedt, Germany
96-well Transwell plate 0.4 µm	Sigma-Aldrich Chemie Gmbh, Germany
Cell strainer (40, 70 µm)	Greiner bio-one, Austria
FACS Tube, 5 ml	Sarstedt, Germany
gentleMACS™ C Tubes	Miltenyi Biotec, Germany

LS columns	Miltenyi Biotec, Germany
Needles	BD Biosciences, USA
Nunc™ Maxisorp® 96 Well Elisa Plate	Thermo Scientific, USA
Pre-Separation filters, 30 µm	Miltenyi Biotec, Germany
Syringes	BD Biosciences, USA
Tubes (50 ml, 15 ml, 10 ml, 2 ml, 1.5 ml, 0.5 ml)	Sarstedt, Germany

2.1.9 TECHNICAL DEVICES

TABLE 9: TECHNICAL DEVICES

DEVICE	SOURCE OF SUPPLY
Olympus microscope BX63	Olympus, Germany
Centrifuge 5415 R	Eppendorf, Germany
FACS LSR II	BD Biosciences, USA
gentleMACS™ Octo Dissociator	Miltenyi Biotec, Germany
iMark™ Micorplate Reader	Bio-Rad, Germany
Microscope	Olympus, Germany
Microtome	Leica, Germany
Microwave	Bosch, Germany
QuadroMACS™ Separator	Miltenyi Biotec, Germany
T3 Thermocycler	Biometra, Germany

2.1.10 SOFTWARE

TABLE 10: SOFTWARE

SOFTWARE	APPLICATION	SOURCE OF SUPPLY
BD bioscience FACS diva software 8.02	Data acquisition flow cytometry	BD Biosciences, FUSA
FlowJo v10.8.0	Data analysis flow cytometry	Tree Star Inc., USA
GraphPad Prism 6	Graphs & Statistical analysis	GraphPad software Ins., USA

ImageJ 1.47d	Data analysis histology	National Institutes of Health, Bethesda, USA

2.2 ANIMALS

C57BL/6 mice were obtained from Charles River laboratories, Germany. Each experimental group contains 5-10 mice. For primary cell culture C57BL/6 new born mice were obtained from the Central Animal Facility of the University Medical Centre Göttingen (UMG). 2D2 animals were generated and characterized by Bettelli and colleagues in 2003. 90-95 % of the $CD4^+$ T cells in 2D2 mice express the MOG_{35-55} specific T cell receptor Vα3.2/Vβ11 (Bettelli et al., 2003), breed and obtained from Central Animal Facility of the UMG. All animals were housed under standard laboratory conditions at the animal facility of the UMG and had access to food and water ad libitum and a 12 h/12 h light/dark cycle under SPF conditions. Mice were allowed to adapt to the new environment for seven days before each experiment. All experiments were approved by the Lower Saxony authorities for animal experimentation.

2.3 METHODS

2.3.1 GENOTYPING

For the genotyping of 2D2 mice, tissue was obtained via tail biopsy. After DNA extraction, transgenes were amplified with specific primers and separated by agarose gel electrophoresis as described below. All genotyping was performed by Ms. Katja Grondey and Mr. Julian Koch (Department of Neuropathology, University Medical Center Germany).

2.3.1.1 DNA EXTRACTION

DNA was isolated from tail biopsies of 2D2 mice. The tissue was digested in 100 µl lysis buffer at 99 °C for 30 min. Afterwards 100 µl neutralization buffer was added.

2.3.1.2 PCR REACTION

Each reaction sample contains 1 µl genomic DNA, 10 µl Dream Taq® PCR Mix 2x, 1 µl of each primer and 7 µl nuclease free water.

Primer 1: 5'-CCC GGG CAA GGC TCA GCC ATG CTC CTG-3'

Primer 2: 5'-GCG GCC GCA ATT CCC AGA GAC ATC CCT CC-3'

2.3.1.3 PCR CONDITIONS

PCR reactions were run in the Eppendorf thermocycler at the following cycling conditions:

Temperature	Time	Step
94 °C	2 min	Initial denaturation
94 °C	1 min	Denaturation
58 °C	1 min	Annealing
72 °C	1 min	Extension
72 °C	1 min	Final extension
4 °C	∞	Storage

To analyze the amplified PCR product, the samples (5 µl) were loaded on an agarose gel in TAE buffer, containing ethidium bromide. Electrophoresis was performed in a Sub-Cell GT Agarose Gel electrophoresis System at 120 V for 45 min. Evaluation of the PCR product was done by visualization and documentation by UV-light.

2.3.2 CUPRIZONE TREATMENT

Seven to eight-week-old C57BL/6 mice were fed with cuprizone at 0.25 % dose in normal chow ad libitum. Mice were treated from 2 weeks up to 6 weeks. To analyze remyelination the 0.25 % cuprizone diet was removed after 5 weeks and mice were fed with a normal diet for 3 days. Body weights of the animals were measured weekly.

2.3.3 EAE INDUCTION

Female C57BL/6J mice were immunized by subcutaneous injection with 75 µg MOG_{35-55} peptide (GenScript) emulsified in complete Freund´s adjuvant, containing 250 µg killed *Mycobacterium tuberculosis* H37 Ra. Directly and 48 h after immunization, 200 ng Bordetella pertussis toxin (Sigma Aldrich) was intraperitoneally (i.p.) injection. The EAE score, the measure of disease severity, was evaluated daily and illustrated in a scale from 0 to 5: 0 = no clinical signs; 1.0 = tail paralysis; 2.0 = hindlimb paresis; 3.0 = severe hindlimb paresis; 4.0 = paralysis of both hindlimbs; 4.5 = hindlimb paralysis and beginning forelimb paresis, 5.0 = moribund/death.

2.3.4 ADOPTIVE TRANSFER EAE

Donor mice were immunized with 200 µg MOG_{35-55} peptide. Inguinal lymph node cells were isolated at d12 after immunization and activated in cell culture with a mixture of 25 µg/ml

MOG_{35-55} peptide, 25 µg/ml recombinant IL-12 and 20 µg/ml anti-IFN-γ antibodies for 3 days. Purified T cells were generated by magnetic cell separation and encephalitogenic T cells were transferred by i.p. injection into recipient mice. Mice were weighted and scored as described in 3.3.3.

2.3.5 EVOBRUTINIB TREATMENT

Evobrutinib was formulated in 20 % Kleptose (Roquette) in 50 mM Na-Citrate buffer pH 3.0. The compound was administrated daily at a concentration of 3 mg/kg or 10 mg/kg by oral gavage. Control animals received 20 % Kleptose in 50 mM Na-Citrate buffer.

2.3.6 HISTOLOGY AND IMMUNOHISTOCHEMISTRY

To perform histology analysis, mice were transcardially perfused with 4 % paraformaldehyde (PFA) in PBS. Brain, spinal cord, spleen and liver were collected and stored in 4 % PFA at 8 °C for at least 2 days. After post-fixation, the tissue was transferred to PBS and embedded in paraffin. Therefore, the brains were cut into 2-3 mm coronal sections, spinal cord were dissected into 10-12 sections, washed in water, dehydrated overnight by a graded alcohol/xylene/paraffin series. Paraffin blocks were sliced in 1 µm thick sections, using a sliding microtome and mounted on glass slides. The tissue sections were then deparaffinized and rehydrated. Therefore, the slices were incubated for 60 min at 54 °C and rehydrated as follows:

4x 10 min	Xylol
1x 5 min	Isoxylol
2x 5 min	100 % isopropyl alcohol (IPA)
1x 5 min	90 % IPA
1x 5 min	70 % IPA
1x 5 min	50 % IPA
∞	Distilled water (dH_2O)

After histochemistry or immunohistochemistry sections were dehydrated by performing the xylene/isopropyl series described above in reverse order with an incubation time of 2-3 min. Finally, the stained sections were mounted either with DePex medium or fluorescence mountain medium.

2.3.6.1 HEMATOXYLIN AND EOSIN (HE) STAINING

To obtain a general overview of the tissue, a HE staining was performed. Hematoxylin stains basic nucleoproteins which results in blue coloured cell nuclei. Eosin is binding acidophilic and basic extra- and intracellular proteins and marks thereby the parenchyma red. For the staining, sections were deparaffinized and rehydrated as described above. Slides then were incubated in Mayer's hemalaun for 5 min. Afterwards, tissue sections were rinsed with dH_2O. The sections were differentiated by shortly dipping them in 1 % HCL-alcohol (1 % HCl-alcohol in 90 % isopropyl alcohol). The sections were then blued by rinsing them under tap water. For the staining of the parenchyma the slides were incubated in 1 % eosin for 5 min (1 % eosin in 70 % isopropyl alcohol + 10 drops glacial acetic acid). Finally, the sections were rinsed with dH_2O, dehydrated and mounted in DePex medium.

2.3.6.2 LUXOL FAST BLUE – PERIODIC ACID SCHIFF (LFB-PAS) STAINING

LFB/PAS staining was performed to visualize myelin. Myelin is stained deep blue by LFB through its binding to lipoproteins. In contrast, PAS stains demyelinated parenchyma and grey matter in pink. At first, the sections were deparaffinized and rehydrated up to the 90 % IPA step. Following the 90 % IPA, the slides were put directly into the LFB solution over night at 60 °C. The next day, the slides were washed in 90 % IPA and differentiated by shortly dipping them into 0.05 % lithium carbonate solution followed by a short dip into 70 % IPA and a rinsing step with dH_2O. Then the sections were incubated in 1 % periodic acid for 5 min and rinsed for 5 min under flowing tap water. Slides were shortly washed with dH_2O and afterwards incubated in Schiff's solution for 20 min. Slides were washed under tap water for 5 min and incubated in Mayer's hemalaun for 2 min. Slides were shortly dipped in dH_2O and afterwards differentiated in 1 % HCl-alcohol (1 % HCl-alcohol in 90 % isopropyl). Sections were blued by rinsing under tap water for 10 min. Finally, the tissue was dehydrated and mounted in DePex medium.

2.3.6.3 IMMUNOHISTOCHEMICAL STAINING

For the detection of specific cell markers, immunohistochemical stainings with antibodies were performed. Primary and secondary antibodies used for immunohistochemistry (IHC) and fluorescence immunocytochemistry are listed in table 5 and 6 section 2.1.5.

Many epitopes are masked in formalin fixed tissue. For de-masking epitopes, sections were harvested in a microwave either in citric acid- or Tris-EDTA buffer 5 times for 3 min. The

epitope retrieval buffer used for each primary antibody is listed in table 5 in section 2.1.5. For the antigen retrieval with the proteinase solution the slides were incubated in a 37 °C warm proteinase solution for 10 min and rinsed two times with dH_2O. The slides were washed with PBS and incubated with 3 % H_2O_2 for 20 min at 4 °C to block endogenous peroxidase and reduce unspecific signals. Afterwards the slides were rinsed 3 times with PBS. The slides were pre-incubated with 10 % FCS (in PBS) for 20 min at RT in a humidified chamber to prevent unspecific antibody binding. The slides were then incubated with the primary antibody (diluted in 10 % FCS/PBS) over night at 4 °C in a humidified chamber. The slides were rinsed 3 times with PBS and incubated with biotin conjugated secondary antibody (diluted in 10 % FCS/PBS) for 1 h at RT in a humidified chamber. The slides were rinsed with PBS for 3 times and incubated with 0.1 % streptavidin conjugated peroxidase (POX) (diluted in 10 % FCS/PBS) for 1 h at RT in a humidified chamber. Afterwards, the slides were again rinsed with PBS 3 times. For the signal development, the slides were put into DAB solution for several minutes and then rinsed 3 times with PBS. The nuclei were counterstained with Meyer's hemalaun solution for 30 sec followed by a short dip (1 s) in dH_2O and a short wash step in dH_2O. The slides were dehydrated and mounted in DePex medium.

Fluorescence IHC was performed for Iba1 and GFAP. For that purpose, the sections were incubated consecutively with the primary and secondary antibodies. Between each antibody incubation step, the sections were washed three times with PBS. The primary antibodies were visualized with Fluorophore conjugated antibodies. Finally, sections were incubated with DAPI (1:10.000) for 10-15 min at RT to counterstain the nuclei.

2.3.7 Analysis of CNS-resident cells ex vivo

To analyze CNS-resident cells, tissue was isolated and dissociated into a single-cell suspension by combining mechanical dissociation with enzymatic degradation using the gentleMACS™ Dissociator and Tissue Dissociation Kits.

2.3.7.1 Microglia

To analyze microglia from adult mice, the Multi Tissue Dissociation Kit I (Miltenyi Biotec, Germany) was used. Therefore, the mice were transcardially perfused with cold PBS. Brain and spinal cord were isolated and cut either into approximately 8 sagittal slices (brain) or into pieces of approximately 5 mm length (spinal cord). The tissue was transferred into a genlteMACS™ C tube containing 2500 µl of enzyme mix and dissociated, according to the manufacturer's instructions, for 45 min. After termination of the program, the samples were

resuspended and transferred to a 70 µm cell strainer, washed with DPBS and centrifuged 10 min at 300 x g. Next, debris removal was performed using a gradient with appropriated volumes as described in manufacturers protocol. Therefore, the cell pellet was resuspended in an appropriate volume of cold DPBS and cold debris removal solution (Miltenyi Biotec, Germany) and finally overlayed with the appropriate volume of cold DPBD and centrifugated at 4 °C and 3000 x g for 15 min without acceleration and brake.

After centrifugation, three phases were formed, the two top phases were completely discarded, and the pellet washed with DPBS, by gently inverting the tube 3 times and centrifuge at 4 °C and 1000 x g 10 min. To remove the red blood cells, a red blood cell removal was performed. Therefore, the cell pellet was resuspended in 1 ml Red blood cell removal solution (Miltenyi Biotec, Germany) and incubated in the refrigerator (2-8 °C) for 10 min. The reaction was stopped by adding 10 ml of DPBS containing 0.5 % FSC and centrifugation at 4 °C and 300 x g for 10 min. The cell pellet was resuspended in DPBS and cells were further analyzed by flow cytometry.

2.3.7.2 ASTROCYTES

To isolate astrocytes from adult mice, the Adult Brain Tissue Dissociation Kit (Miltenyi Biotec, Germany) was used. Therefore, the mice were transcardially perfused with cold PBS. Brain and spinal cord were isolated and cut either into approximately 8 sagittal slices (brain) or into pieces of approximately 5 mm length (spinal cord). The tissue was transferred into a genlteMACS C tube containing enzyme mix, according to manufactures protocol, and dissociated for 35 min. After termination of the program the samples were resuspended and transferred to a 70 µm cell strainer, washed with DPBS and centrifuged 10 min at 300 x g. Debris- and red blood cell removal was performed as described in section 3.3.7.1. To further isolate purified astrocytes magnetic activated cell sorting (MACS) separation using ACSAII beads was performed and the cells were resuspended in 350 µl RLT buffer and stored at -80 °C until further analysis by qualitative PCR (qPCR).

2.3.8 PRIMARY MIXED GLIAL CELL CULTURE

Primary microglia and astrocytes were isolated from newborn to 2-day-old C57BL/6 mice. The preparation of microglia and astrocytes was performed on ice in Hank's balanced salt solution (HBSS, Biochrome). The animals were sacrificed by decapitation. Brains were excised and the meninges removed. After washing three times with HBSS, the tissue was incubated with 2.5 % trypsin (Pan Biotech) for 5 min at 37 °C, carefully vortexed and further incubated

5 min at 37 °C. The reaction was stopped by adding Dulbecco's modified Eagle's medium (DMEM) containing 10 % fetal calf serum (FCS), 1 % GlutaMax™ (Thermo Fisher), 100 units/ml penicillin, and 100 µg/ml streptomycin and finally incubated with 0.4 mg DNase (Roche). Cells were mechanically separated and centrifuged at 129 x g for 10 min at 4 °C. The pellet was resuspended and one brain per T75 flask was cultivated at 37 °C and 5 % CO_2. After 24 h cells were washed twice with PBS and complete DMEM was exchanged every 2-3 days until confluency.

2.3.8.1 MICROGLIA

To obtain an enriched microglia culture after cell confluency, flasks were shaken off by 90 rpm for 10 min at 37 °C, cell culture medium was removed, and the cells were stimulated with complete medium containing 30 % culture supernatant from mouse fibroblast cell line L929 (routinely cultured in DMEM and split once a week; L929 medium was collected and stored at -20 °C until use). After 5 days microglia were harvested by gentle shaking at 90 rpm for 30 min at 37 °C to separate microglial cells from other glia cells. The cells were seeded depending on the experimental setting described in table 11 on Poly-L-Lysine (Sigma) coated plates. Cultures usually contained > 95% microglial cells.

2.3.8.2 ASTROCYTES

For obtaining an enriched astrocyte culture, mixed glial cells were shaken off by 170 rpm for 1 h at 37 °C to remove other glial cells. The supernatant was removed, and the cells were washed twice with PBS and detached with 0.05 % trypsin, 0.02 % EDTA (w/v) for 4 min. The reaction was stopped with complete medium and the cells were centrifuged at 129 x g for 10 min at 4°C. Finally, microglia cells were isolated by MACS separation using a mouse anti-CD11b Biotin-labeled antibody (BD Bioscience), followed by an incubation with anti-Biotin magnetic microbeads (Miltenyi Biotech). Cultures usually contained > 95 % astrocytes

TABLE 11: OVERVIEW OF SEEDED CNS-RESIDENT CELLS IN VITRO

PURPOSE	CULTURE DISH	PLL COATING/ WELL IN µL	CELLS AMOUNT/WELL	VOLUME OF CULTURE MEDIUM
Elisa	96 well plate	50	30.000	100 µl
FACS	12 well plate	500	200.000 – 300.000	500 µl
qPCR	12 well plate	500	200.000 – 300.000	500 µl
ICC	8- Chamber slide	50	150.000	200 µl

2.3.9 STIMULATION OF MICROGLIA AND ASTROCYTES

In general, the cells rested for at least 3-24 h with complete medium. Afterwards, medium was removed and medium containing stimuli were added. Depending on the experiment microglial cells were stimulated to either differentiate into the M1 or M2 phenotype. To induce a pro-inflammatory M1 phenotype the cells were either stimulated with Lipopolysaccharide (LPS, Sigma) or recombinant Interferon-γ (rIFN-γ, R&D). The M2 phenotype was induced by a mix of recombinant interleukin (IL-)-4, IL-10, and IL-13 (Sigma). Astrocytes were stimulated with a mix of IFN-γ and IL-1β (Sigma).

2.3.9.1 INHIBITION OF BTK

To investigate the potential of BTK inhibition in CNS-resident cells the BTK inhibitor evobrutinib (Merck) was diluted in DMSO to a 10 mM stock solution and cells were pre-incubated with appropriate working concentrations 30 min before stimulation was added.

2.3.9.2 ISOLATION OF IMMUNE CELLS EX VIVO

To analyze immune cells ex vivo, a single cell suspension of murine spleens was prepared. Therefore, the spleen was isolated and cells were distributed by mechanical force through a 70 µM cell strainer. After two washing steps with ice cold PBS and centrifugation at 300 x g a 4 °C, splenocytes were further processed depending on the following experiment. Murine splenic B cells were purified by MACS separation using mouse CD19 beads (BioLegend). Murine T cells were isolated by negative MACS separation, using the mouse pan T cell isolation kit II (Miltenyi Biotech).

2.3.9.3 GENERATION OF B CELL SUPERNATANT & NEUTRALIZATION

To isolate B cell supernatant, B cells were isolated as described in 3.3.3 and stimulated with 5 µg/ml LPS or CpG for 24 or 48 h. Supernatant was collected and LPS removal was performed using Pierce™ high capacity endotoxin removal spin columns (ThermoFisher) according to manufacturer's instructions.

For neutralization of IL-6 or IL-10 in the supernatant, antibodies against IL-6 or IL-10 (BioXcell) were used. Therefore, supernatant was incubated with 1 µg/ml antibodies or appropriate isotype control for 20 min before incubation with the cells.

2.3.9.4 CO-CULTURE OF MICROGLIA AND IMMUNE CELLS

For co-culture settings, microglial cells and astrocytes were plated and stimulated 18 h depending on the experiment. The cells were washed and co-cultured either with purified B cells or T cells.

2.3.9.5 B CELLS

Cells were isolated and purified as described in section 3.3.10 and stimulated for 24 h with 5 µg/ml LPS or CpG. The cells were washed twice with complete medium, cell number was determined, and cells were co-cultured in an amount 1:2 with microglial cells or astrocytes for 24 h. Microglial and astrocyte activity was measured by ELISA and flow cytometry.

2.3.9.6 T CELLS

To investigate the capacity of microglia to act as antigen presenting cells (APC) to activate T cells, microglial cells were stimulated depending on the experimental setup and co-cultured with T cells or carboxyfluorescein succinimidyl ester (CFSE)-labeled T cells. In detail, purified T cells were isolated from 2D2 mice. T cell proliferation was assessed by CFSE-staining of T cells and subsequent flow cytometry analysis of CFSE dilution. CFSE can penetrate the intact cell membrane and binds irreversible to intracellular proteins. Upon proliferation, the cytoplasm is shared between the two daughter cells and therefore the fluorescence intensity of CFSE is halved at each cell division (Parish, 1999). T cells were therefore resuspended in 1 ml chilled PBS and incubated with 1 µM CFSE and incubated for 15 min at 37 °C in the water bath. The reaction was stopped by addition of 48 ml cold complete RPMI medium. Cells were washed twice with complete RPMI medium by centrifugation for 10 min at 300 x g and 4 °C. Finally, the appropriate number of CFSE-labeled T cells were added to the microglial cells and stimulated with MOG_{35-55} peptide and incubated for 48-72 h at 37 °C and 5 % CO_2. T cell proliferation was analyzed by measuring the CFSE dilution via flow cytometry.

2.3.9.7 FLOW CYTOMETRY

To analyze the effect of the interaction of B cells and CNS-resident cells, as well as the potential of BTK inhibition in CNS-resident cells in vivo and in vitro, flow cytometry (FACS) was performed. For this purpose, cells were stained with different combinations of fluorochrome-labeled antibodies and cell populations were analyzed, using BD LSRFortessa II and the BD FACSDiva Software 8.0.2. The staining protocol was performed in 96 well round

bottom plates at 4 °C. Wash steps were performed by adding 200 µl of FACS buffer and centrifugation for 8 min at 4 °C at 300 x g for splenocytes and 129 x g for CNS-resident cells.

In detail, isolated cells were centrifuged and washed with FACS buffer. Necrotic cells were stained with 30 µl LIVE/DEAD™ Fixable NIR Dead Cell Stain Kit (Thermo Fisher Scientific) 1:500 diluted in chilled PBS for 10 min at room temperature in the dark. Unspecific Fc receptors binding was blocked via monoclonal antibodies specific for CD16/CD32 diluted 1:100 in FACS buffer and incubated for 10 min at 4 °C. The cells were washed and incubated with 30 µl of a fluorophore-labeled antibody mix diluted 1:100 in FACS buffer for 15 min at 4 °C in the dark. After incubation, the cells were washed twice and fixed with 4 % PFA for 30 min. After washing the cells twice, the cells were resuspended in FACS buffer and transferred to a 5 ml FACS tube and analyzed within 48 h.

2.3.9.8 PREPARATION OF MICROGLIA FOR FLOW CYTOMETRY ANALYSIS

For the analysis of microglial using flow cytometry, the cells were first detached form the cell culture plate. All used solutions were pre-warmed in the water bath at 37 °C. Microglial cells were washed twice with pre-warmed PBS. The cells were detached from the cell culture dish upon addition of 300 µl 0.05 % trypsin, 0.02 % EDTA (w/v) in PBS, for 4 min at 37 °C, 5 % CO_2. The reaction was stopped by addition of 600 µl culture medium. Cells were scratched off, transferred to 10 ml reaction tubes, washed with chilled PBS, transferred to a 96 well round bottom plate, and stained for flow cytometric analysis as described previously.

2.3.10 PHOSFLOW

To investigate the phosphorylation of specific proteins, as well as intracellular proteins by flow cytometric analysis, a PhosFlow protocol was utilized. Therefore, after stimulation the cells were washed twice with pre-warmed PBS and directly stained with fixable viability stain 520 (BD Bioscience) for 10 min in the dark (diluted 1:5000 in PBS). The staining solution was removed, and the cells were directly fixed with pre-warmed 1x Lyse Buffer I (BD Bioscience) for 10 min at 37 °C in the dark. Cells were detached by scraping and centrifuged by 600 x g for 6 min. Cells were washed with 1x PhosFlow Perm Wash (BD Bioscience) for 15 min at RT in the dark. After centrifugation the cells were stained with specific antibodies labeled with fluorescent dyes for 1 h at RT. Cells were washed once with PhosFlow Perm Wash and finally resuspended in FACS buffer and analyzed within several hours.

2.3.11 PHAGOCYTOSIS ASSAY

To investigate the phagocytosis capacity of microglia, FITC-labeled Ovalbumin (OVA-FITC, Thermo Fisher Scientific) was added to the treated cells and incubated for 2½ h. Thereafter, cells were harvested and stained for flow cytometric analysis as described in section 2.3.13.

2.3.12 QUANTITATIVE PCR ANALYSIS

RNA was isolated using the RNeasy Mini Kit (Qiagen) and reverse transcription was performed using QuantiNova Reverse Transcription kit (Qiagen), according to the manufacturer's instructions. Quantitative (q) PCR was performed using 500 nM Primer and qPCRBIO SyGreen (Nippon Genetics) in a total volume of 10 µl on a QuantStudio 7 (Applied Biosystems). Primers were purchased from Eurofins Genomics (table 7). qPCR was performed at 95 °C denaturating and 70 °C annealing temperature for 30 s and 40 cycles with subsequent melt-curve analysis. Primer specificity was validated by product size, using a 2 % Agarose gel containing GelRed and UV-light illumination. Samples were analyzed in triplicates and considered valid when Ct<35 and SD Ct<0.5. The expression level of each transcript is indicated as the percentage of the housekeeping genes beta-2-microglobulin (B2M) and Glycerinaldehyd-3-phosphat Dehydrogenase (GAPDH).

2.3.13 ENZYME-LINKED IMMUNOSORBENT ASSAY

Cyto- and chemokine release was determined by enzyme-linked immunosorbent assay (ELISA). The production of CCL2, GM-CSF, IFN-ɣ, IL-6, IL-17 and TNF-α was measured with ELISA MAX™ Standard Set kits (BioLegend)., CCL3, CXCL1 and IL-10 was quantified by DuoSet Elisa kits (R&D Systems) according to manufacturer's protocol. The OD was determined at 450 nm with 540 nm wavelength correction using the iMark™ microplate reader (Bio-Rad laboratories).

2.3.14 STATISTICAL ANALYSIS

All statistics were calculated using the software GraphPad Prism 6. In vitro microglial activation, antigen presentation, differentiation, phagocytosis and cytokine production, as well as in vitro T cell proliferation and ex vivo BTK expression are shown as mean ± SEM and were analyzed using the unpaired t test or Mann-Whitney U test. In vitro and in vivo comparison were made to vehicle treated animals. Data are shown as mean ± SEM. In vitro data were analyzed by Kruskal-Wallis test followed by Dunn`s test for multiple comparison.

In vivo data were analyzed by unpaired t test or Mann-Whitney U test, depending on whether values are normally distributed. A value of $p < 0.05$ was considered significant and is shown by one asterisk.

3 RESULTS

3.1 PROJECT 1: THE ROLE OF REGULATORY B CELLS IN CONTAINMENT OF CHRONIC CNS INFLAMMATION

Chronic progression in MS is attributed to a self-sustained circuit of inflammation within the CNS, involving infiltrating hematopoietic cells and CNS-resident cells like microglia and astrocytes. In this context, it is still debated whether and how B cells within the CNS directly or indirectly interact with CNS-resident cells.

3.1.1 B CELL-DERIVED MOLECULES MODULATE MICROGLIA PHENOTYPE AND FUNCTION

To investigate if B cells exert a direct effect on CNS-resident cells, B cells were co-cultured with primary microglia. Therefore, purified B cells were stimulated in the presence of 5 µg/ml LPS or 5 µg/ml CpG for 24 h, medium was exchanged and activated B cells were co-cultured with primary microglia, left either unstimulated or stimulated with LPS. Under homeostatic conditions, the presence of LPS activated B cells resulted in an upregulation of the cell surface markers CD40, CD69, PD-L1 and CD80 on microglia, which are associated with activation and antigen presentation. However, this effect was missing if microglia were driven into a pro-inflammatory state by LPS stimulation (Fig. 1.1a-f). In addition, the production of the pro-inflammatory cytokines TNF-α, CCL3 and IL-6 was enhanced upon co-culture of microglia with B cells in the absence or presence of modest LPS concentrations (Fig. 1.2). However, the level of pro-inflammatory cytokine secretion was exceeded by microglia without B cell co-culture upon stimulation with moderate or high LPS concentrations (Fig. 1.2a-c). By contrast, the production of the anti-inflammatory cytokine IL-10 was enhanced irrespective of LPS stimulation upon co-culture of microglia with B cells (Fig. 1.2d). CpG-activated B cells showed a modest effect on microglia (Fig. 1.3). The expression of MHCII was upregulated under all conditions, while the expression of CD80 and CD86 as well as the secretion of TNF-α was reduced with high LPS concentrations (Fig. 1.3d, e, g).

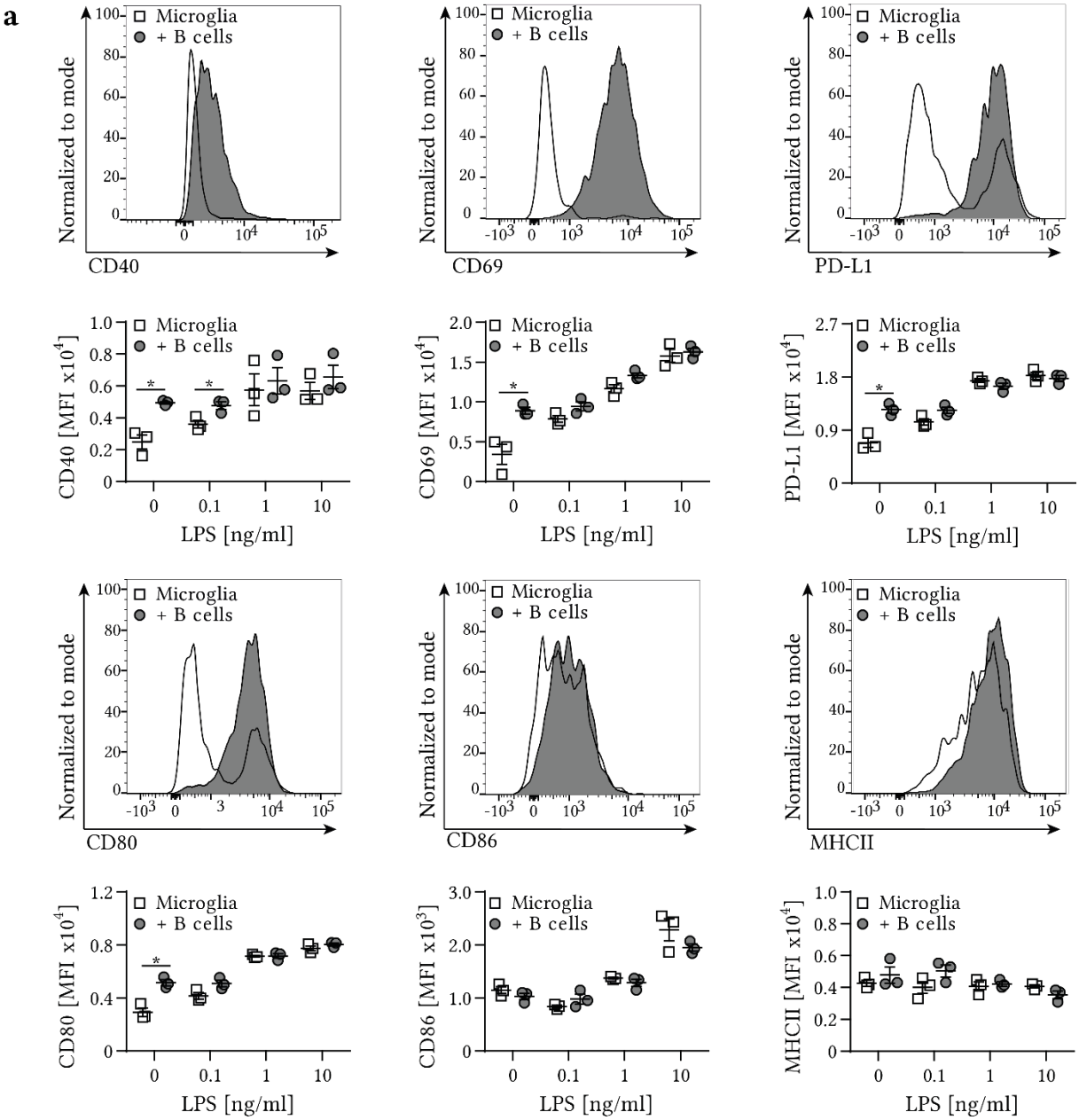

FIGURE 1.1: B CELLS DIRECTLY MODULATE MICROGLIAL ACTIVITY. Purified B cells were cultured in the presence of 5 µg/ml LPS for 24 h. Thereafter, B cells were washed and co-cultured with primary microglia, unstimulated or stimulated with 0.1, 1 or 10 ng/ml LPS for 24 h. **a-f)** Microglial activation and expression of molecules involved in antigen presentation were analyzed using flow cytometry. Mean fluorescence intensity (MFI) ± SEM, n=3. Representative histograms are shown for unstimulated microglia; n=3, representative data of 2-3 independent experiments, unpaired t-test; *p<0.05.

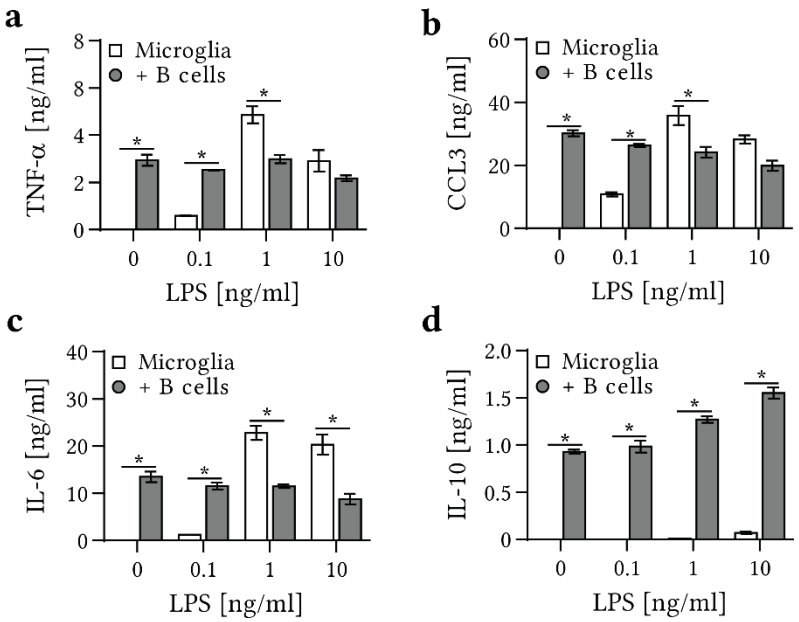

FIGURE 1.2: B CELLS DIRECTLY MODULATE PRO-INFLAMMATORY CYTOKINE SECRETION OF MICROGLIA. Purified B cells were cultured in the presence of 5 µg/ml LPS for 24 h. Thereafter, B cells were washed and co-cultured with primary microglia, unstimulated or stimulated with 0.1, 1 or 10 ng/ml LPS for 24 h. **a-d)** Mean cytokine concentration ± SEM, determined by ELISA; n=3, representative data of 2-3 independent experiments, unpaired t-test; *p<0.05.

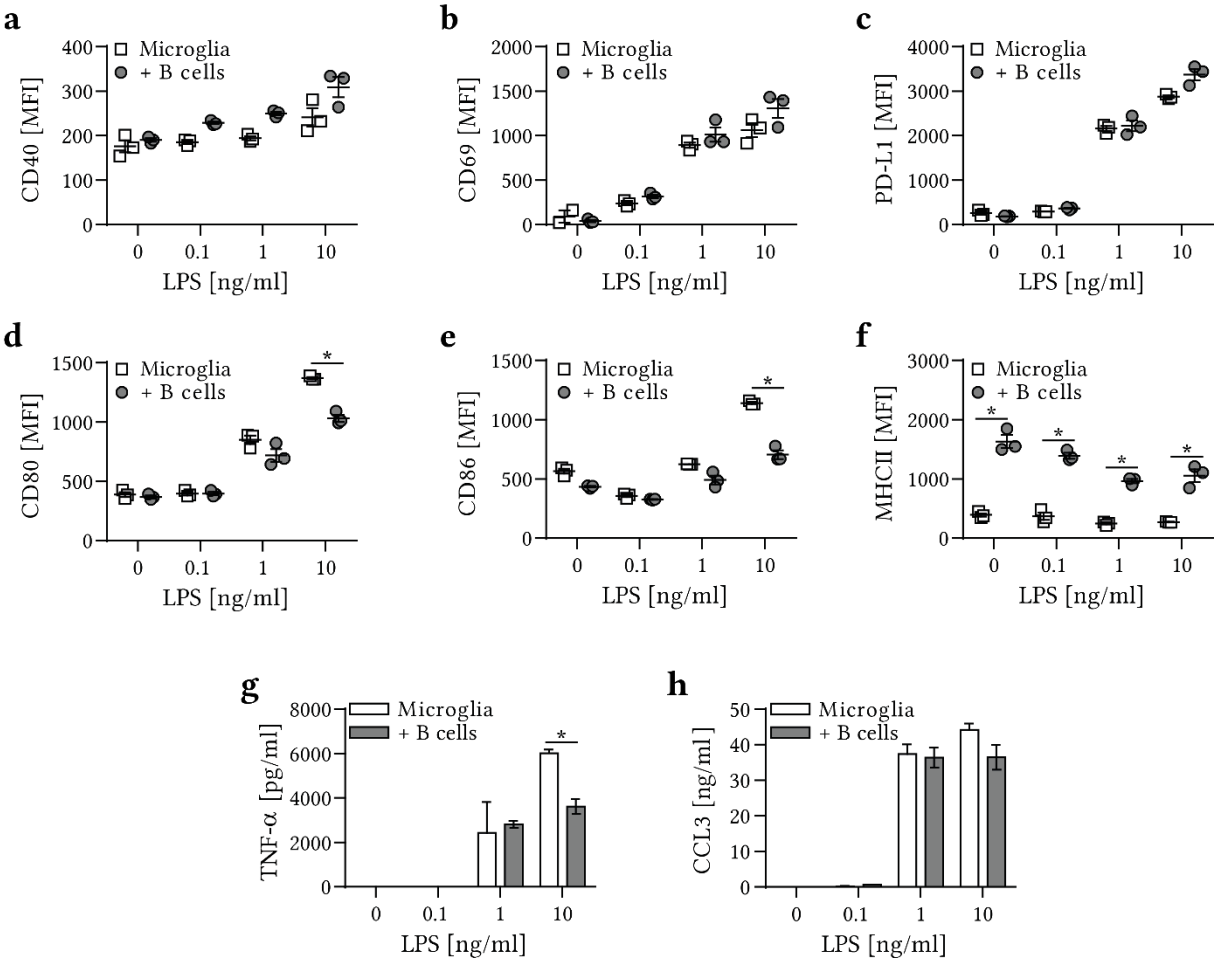

FIGURE 1.3: CPG STIMULATED B CELLS SHOW A GENTLE MODULATION OF MICROGLIA. Purified B cells were cultured in the presence of 5 µg/ml CpG for 24 h. Thereafter, B cells were washed and co-cultured with primary microglia, unstimulated or stimulated with 0.1, 1 or 10 ng/ml LPS for 24 h. **a)** Microglial activation and expression of molecules involved in antigen presentation were analyzed using flow cytometry. Mean fluorescence intensity (MFI) ± SEM, n=3. **b)** Mean cytokine concentration ± SEM, determined by ELISA; n=3, representative data of 2-3 independent experiments, unpaired t-test; *p<0.05.

To clarify, if the observed effects are based on cell-cell contact or on a soluble factor derived by B cells, microglia were cultures with B cells separated by a fluid-permeable membrane termed as transwell. In this approach only, pro-inflammatory microglia were used, which were generated upon LPS stimulation (Fig. 1.4). The experiments revealed an enhanced expression of CD40, CD69, CD80 and MHCII and a reduced expression of PD-L1 after culture of microglia with separated B cells as compared to microglia without B cells (Fig. 1.4b). Interestingly, the culture of microglia with B cells directly showed differences in the expression of CD40, CD86 and MHCII compared to the culture with separated B cells (Fig. 1.4b). These results indicate, that depending on the expression of a specific marker, cell-cell contact has different ramifications than B cell-derived molecules. On the contrary, the secretion of pro-inflammatory cytokines by microglia upon co-culture with B cells or culture

with separated B cells showed the very same results a reduced secretion of pro-inflammatory cytokines (Fig. 1.4c). These results indicate, that a soluble factor secreted by B cells may have a regulatory function on microglia by the modulation of the secreted cytokine pattern.

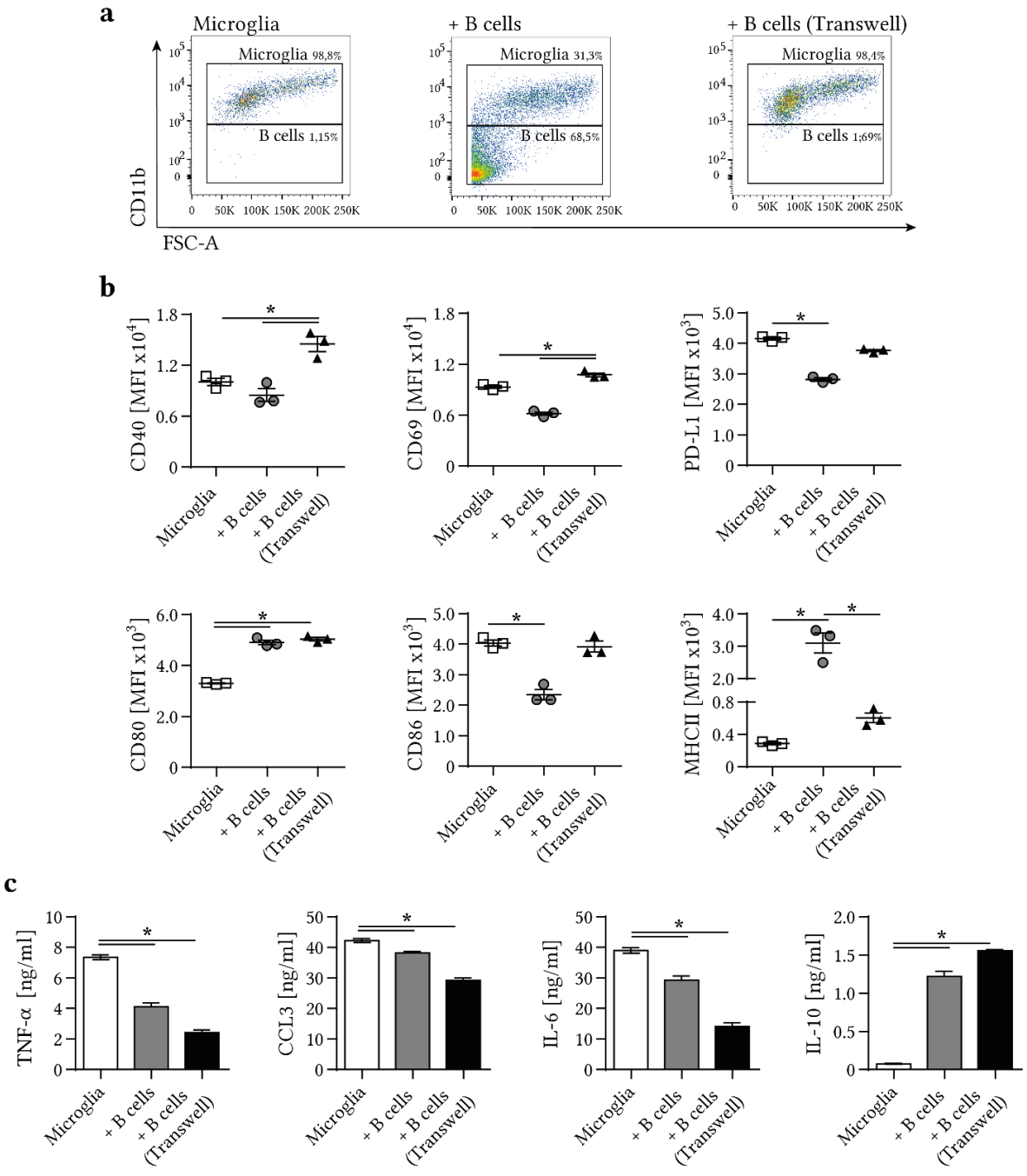

FIGURE 1.4: A SOLUBLE FACTOR DERIVED FROM B CELLS ATTENUATES THE PRO-INFLAMMATORY RESPONSE OF MICROGLIA. Purified B cells were cultured with 5 µg/ml LPS for 24 h, after medium exchange B cells were co-cultured with microglia separated by a fluid-permeable membrane (= Transwell) for 24 h. Microglia without B cell co-culture served as controls. Microglia cells were harvested and stained for flow cytometry. **a)** Representative flow cytometry plots. **b)** Mean fluorescence intensity (MFI) ± SEM, n=3, **c)** Cytokine production measured by ELISA; mean cytokine concentration ± SEM, n=3; Representative data of two independent experiments; one-way ANOVA with Holm-Sidak post hoc test, *p<0.05.

To further investigate this assumption, microglia were next cultured with B cell-derived supernatant. For this purpose, B cells were purified and cultured in the presence of LPS or CpG (Fig. 1.5-1.7). Since microglia are sensitive to LPS, LPS was first removed from the supernatant and primary microglia were left either unstimulated or stimulated with LPS in the presence or absence of B cell-derived supernatant (Fig. 1.5, 1.6). Under homeostatic conditions LPS-stimulated B cell supernatant upregulated the expression of CD40 and CD69 while all the other analyzed markers merely showed a trend towards a higher expression (Fig. 1.5) as well as the production of the pro-inflammatory cytokines TNF-α and CCL3 were enhanced (Fig. 1.6a, b). However, under pro-inflammatory conditions CD69, PD-L1, CD86 and MHCII were upregulated, while CD80 remained unchanged and CD40 was downregulated (Fig. 1.5). Similar to the direct B cell co-culture experiments culture with B cell-derived supernatant enhanced the production of the pro-inflammatory cytokines TNF-α, CCL3 and IL-6 in the absence or presence of modest LPS concentrations (Fig. 1.6). However, the level of pro-inflammatory cytokine secretion was exceeded by microglia without B cell-derived supernatant upon stimulation with moderate or high LPS concentrations. By contrast, the production of the anti-inflammatory cytokine IL-10 was enhanced irrespective of LPS stimulation upon culture of microglia with B cell-derived supernatant (Fig. 1.6).

CpG derived B cell supernatant led to an upregulation of CD69 with high LPS concentrations while no other analyzed marker showed any differences compared to microglia without B cell supernatant (Fig. 1.7). By contrast, the production of TNF-α and CCL3 was enhanced by B cell supernatant under low or no LPS concentrations (Fig. 1.7b). This effect was not observed in the direct co-culture with CpG activated B cells, indicating that the remaining CpG in the supernatant has an impact on the activation of microglia.

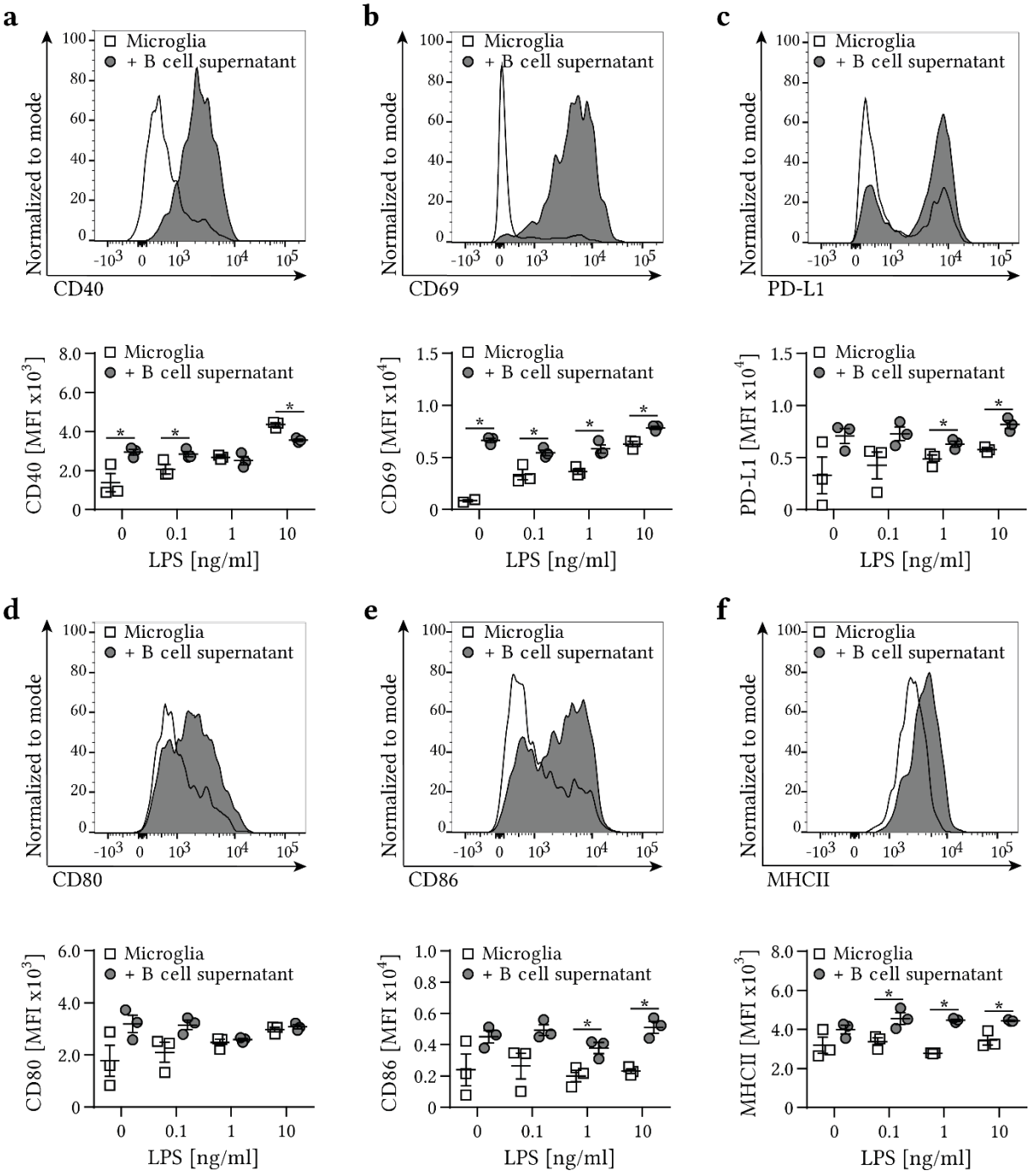

FIGURE 1.5: B CELL SUPERNATANT MODULATES MICROGLIAL ACTIVITY. B cell supernatant modulates microglial activity. Purified B cells were cultured in the presence of 5 µg/ml LPS for 24 h. Supernatant was harvested and LPS removed. Primary microglia were either left unstimulated or stimulated with 0.1, 1 or 10 ng/ml LPS and co-cultured with B cell supernatant for 24 h. **a-f)** Microglial activation and expression of molecules involved in antigen presentation were analyzed using flow cytometry. Mean fluorescence intensity (MFI) ± SEM, n=3. data of 2-3 independent experiments. unpaired t-test, *p<0.05. Representative histograms are shown for unstimulated microglia.

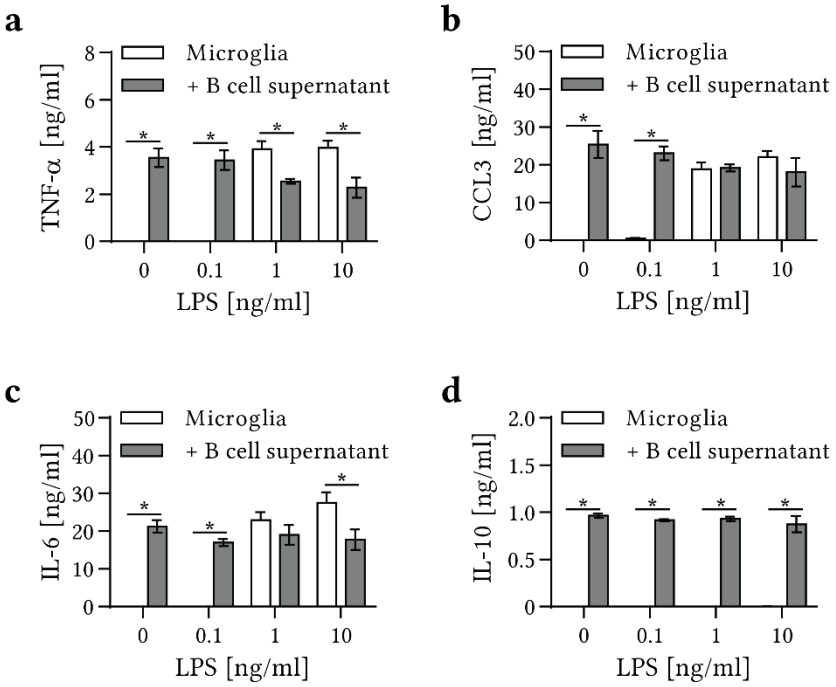

FIGURE 1.6: B CELL SUPERNATANT ALTERS THE CYTOKINE PROFILE OF MICROGLIA. Purified B cells were cultured in the presence of 5 µg/ml LPS for 24 h. Supernatant was harvested and LPS removed. Primary microglia were either left unstimulated or stimulated with 0.1, 1 or 10 ng/ml LPS and co-cultured with B cell supernatant for 24 h. **a-d)** Mean cytokine concentration ± SEM, determined by ELISA; n=3, representative data of 2-3 independent experiments, unpaired t-test; *p<0.05.

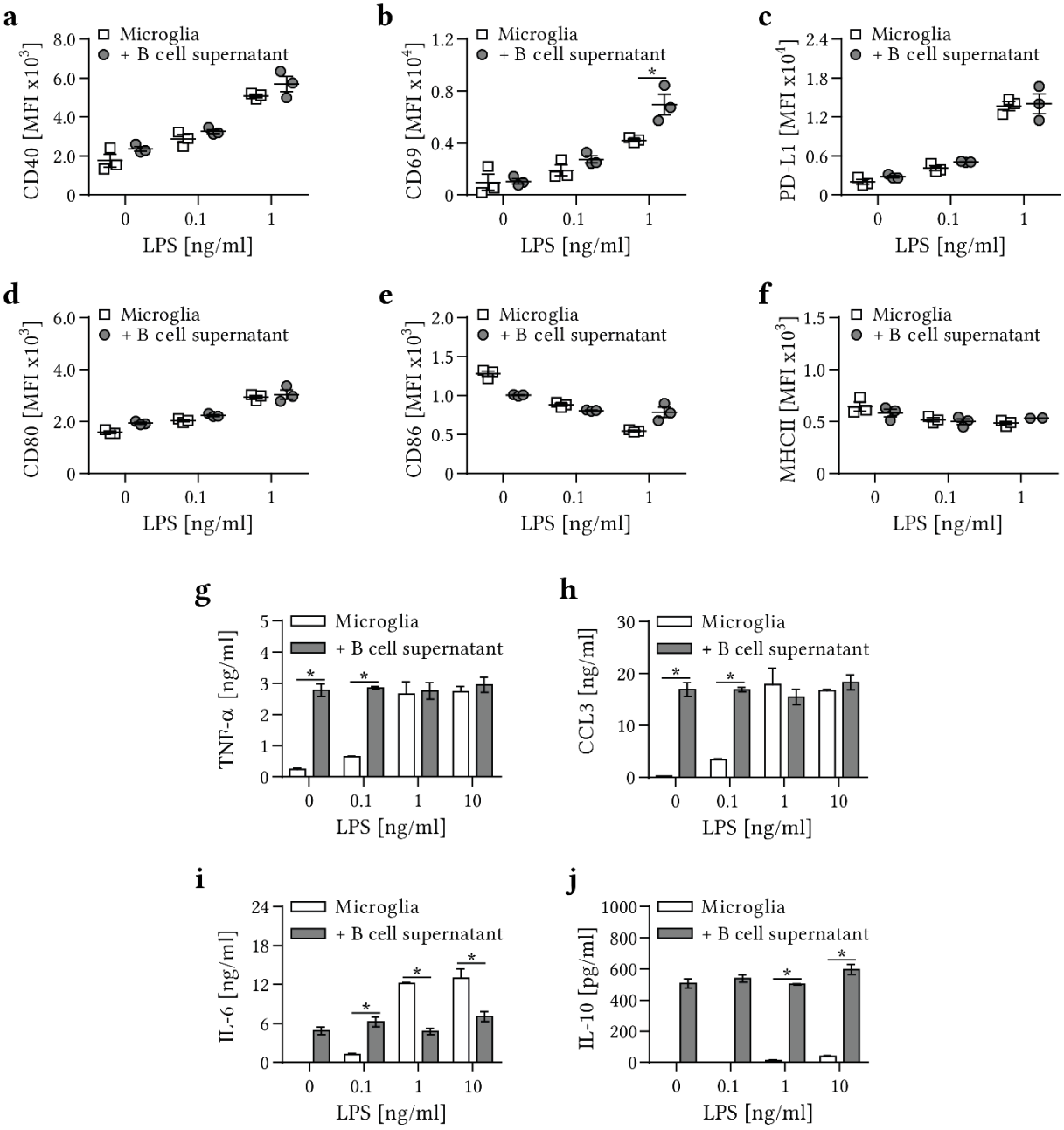

FIGURE 1.7: B CELL SUPERNATANT OF CPG STIMULATED B CELLS INDUCES A MODEST MICROGLIAL MODULATION. Purified B cells were cultured in the presence of 5 µg/ml CpG for 24 h. Supernatant was collected and co-cultured with primary microglia, unstimulated or stimulated with 0.1, 1 or 10 ng/ml LPS for 24 h. **a-f)** Microglial activation and expression of molecules involved in antigen presentation were analyzed using flow cytometry. Mean fluorescence intensity (MFI) ± SEM, n=3. **g-j)** Mean cytokine concentration ± SEM, determined by ELISA; n=3, Representative data of 2-3 independent experiments, unpaired t-test; *p<0.05.

To reveal, to what extent these changes have an impact on microglia function, microglial phagocytosis and the capacity of microglia to act as APCs were investigated. First, the ability to incorporate fluorescence-labeled particles was assessed. Thus, microglia with phenotypic changes through B cell supernatant were cultured in the presence of various concentrations of FITC labeled OVA (OVA-FITC). A dose-dependent phagocytosis of OVA-FITC was

observed, which was reduced by the addition of B cell supernatant (Fig. 1.8a, b). Besides their role in phagocytosis, one major function of microglia is the function as antigen presenting cells, by which they can interact for example with infiltrating T cells and induce T cell proliferation. To assess the potential of B cell supernatant to modulate the APC function of microglia, microglia treated with B cell supernatant were co-cultured with MOG-specific 2D2 T cells. Of note, to enhance the MHCII expression on microglia, which is essential for microglia-T cell interaction, microglia were pre-treated with IFN-γ. MOG_{35-55} peptide clearly induced $CD4^+$ T cell proliferation, while the addition of B cell supernatant decreased this proliferation without effecting the viability of T cells (Fig. 1.8c, d). These findings indicate that in addition to a reduced pro-inflammatory response in activated microglia in the presence of B cells and B cell supernatant, B cell supernatant is also able to reduce the capacity of microglia to phagocyte and to serve as APCs.

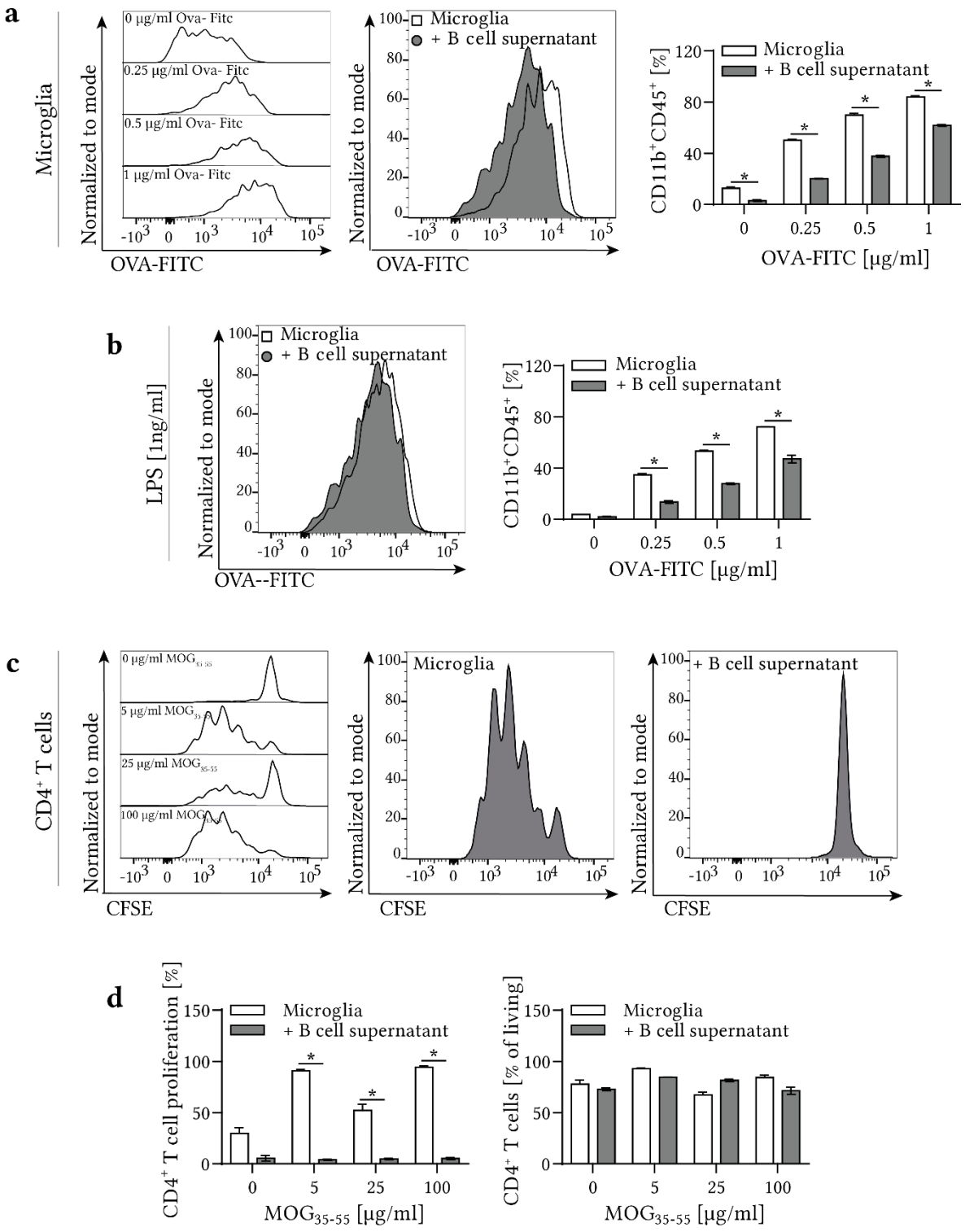

FIGURE 1.8: B CELL-DERIVED SUPERNATANT DIMINISHES PHAGOCYTOSIS CAPACITY AND APC FUNCTION OF MICROGLIA. Primary microglia were left unstimulated (a) or stimulated with 1 ng/ml LPS (b) and co-cultured with B cell supernatant for 24 h. **a, b)** Cells were washed and OVA-FITC was added in indicated concentrations. After 2 h the cells were harvested and stained for flow cytometry analysis. Frequency of OVA-FITC$^+$ microglia cells ± SEM; n=3. **c, d)** After incubation with B cell supernatant microglia cells were co-cultured with CFSE stained MOG-specific T cells and MOG_{35-55} peptide. After 72 h T cells were harvested and stained for flow cytometry. Frequency of CD4$^+$ T cell proliferation assessed by CFSE dilution; Mean ± SEM; n=3. **c)** Representative histograms. Representative data of 2-3 independent experiments. unpaired t-test, $^*p<0.05$.

3.1.2 CYTOKINE PATTERN OF B CELL SUPERNATANT

To better understand through which factor B cells modulate the inflammatory response of microglia, the molecules produced by B cells were analyzed by ELISA (Fig. 1.9). Under both LPS and CpG stimulation, especially the molecules IL-6, IL-10, CCL2, CCL3 and CCL5 were produced at high levels. Of note, the amount of the produced cytokines differed by LPS or CpG stimulation. Since a downregulation of pro-inflammatory cytokines upon treatment with B cells and B cell supernatant was observed in microglia, the anti-inflammatory cytokine IL-10 and on the contrary, the pro-inflammatory cytokine IL-6, which are known to have important roles in MS, were further studied in detail.

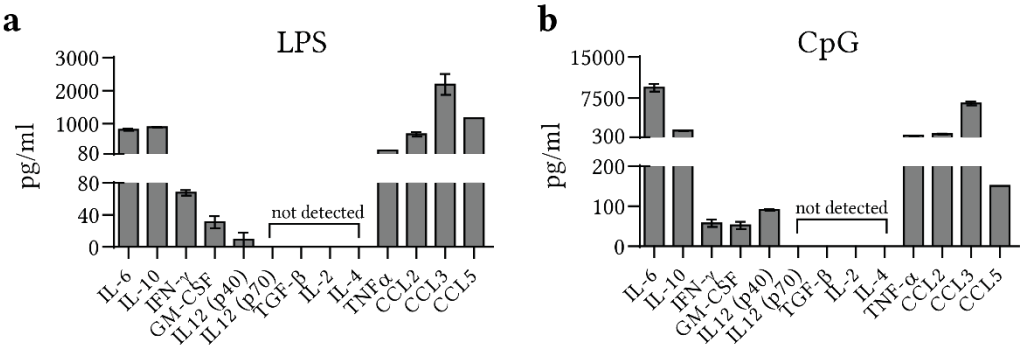

FIGURE 1.9: CYTOKINE PATTERN OF B CELL SUPERNATANT. Purified B cells were cultured in the presence of 5 µg/ml LPS (a) or 5 µg/ml CpG (b) for 24 h. Supernatant was collected and analyzed by ELISA. **a, b)** Mean cytokine production measured by ELISA ± SEM, n=2.

3.1.3 IL-10 REDUCES THE PRO-INFLAMMATORY PROPERTIES OF MICROGLIA

In a first step, the direct effect of IL-6, IL-10 and TGF-β on microglia was investigated. Thus, primary microglia were left unstimulated or stimulated with LPS and treated with recombinant (r) IL-6, rIL-10 or rTGF-β. rIL-10 induced a dose-dependent reduction of the pro-inflammatory cytokines and downregulated the expression of cell surface markers for activation and antigen presentation without changing the viability of the cells (Fig. 1.10b, d). Interestingly, rIL-6 or rTGF-β showed no significant effect, although rTGF-β showed a trend towards downregulation of the pro-inflammatory cytokine TNF-α (Fig. 1.10b, c).

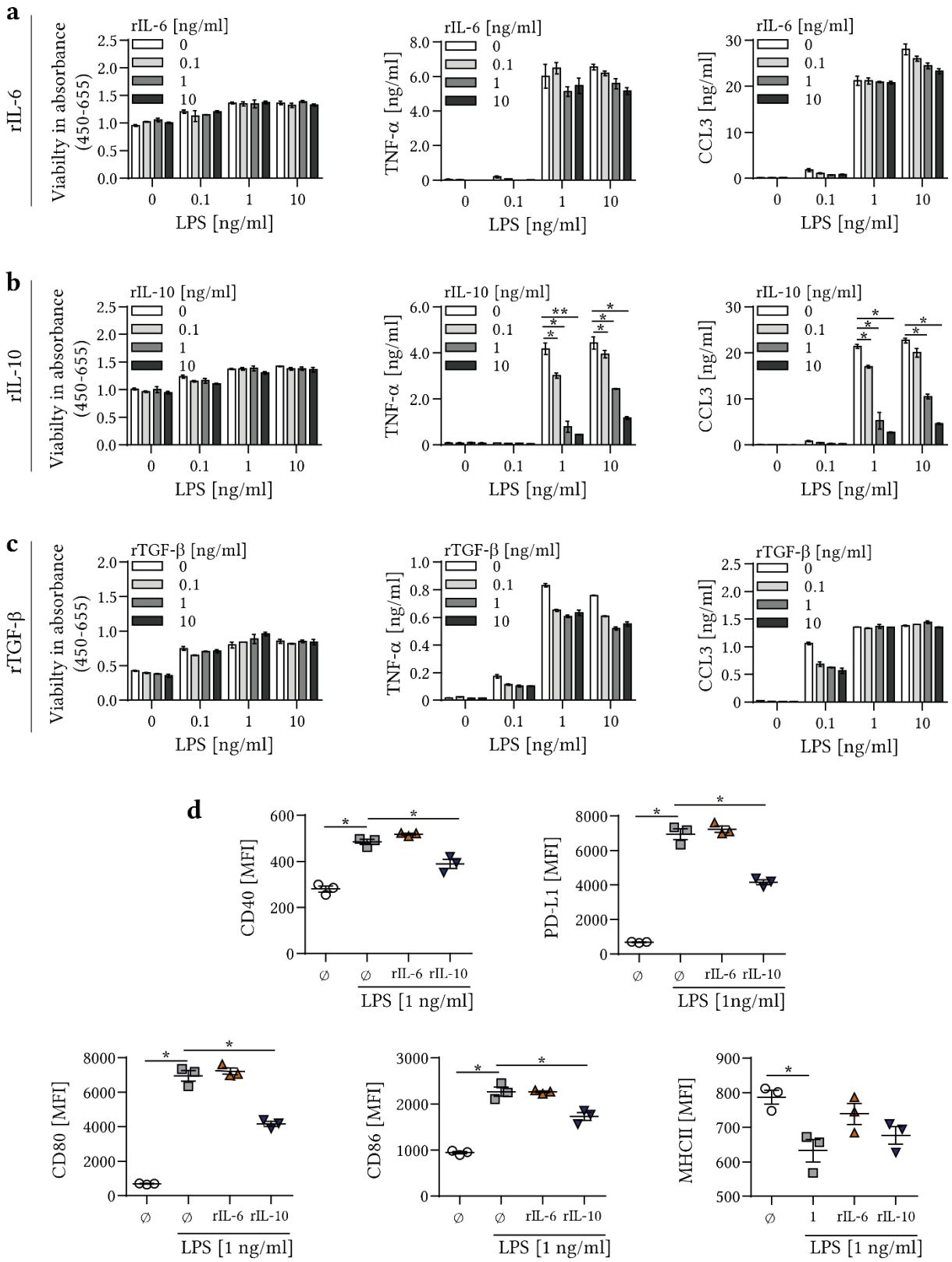

FIGURE 1.10: IL-10 REDUCES THE PRO-INFLAMMATORY PROPERTIES OF MICROGLIA. Primary microglia were left either unstimulated or stimulated with LPS and treated with rIL-6 (a), rIL-10 (b) or rTGF-β (c) for 24 h. **a-c)** Cell viability was determined by WST-1 assay; Mean ± SEM. Mean cytokine concentration ± SEM; n=3. **d)** Cells were harvested and stained for flow cytometry, mean fluorescence intensity ± SEM; n=3. Representative data of 2-3 independent experiments; one-way ANOVA with Holm-Sidak post hoc test; *p<0.05.

In a second step, the impact of rIL-6 and rIL-10 was analyzed on microglia function. As expected rIL-6 had no effect on phagocytosis or APC function, both on unstimulated (Fig. 1.11a, c) and inflammatory microglia (Fig. 1.11b, d), the phagocytic capacity of microglia was not changed dependent on rIL-10 (Fig. 1.11a, b), while the $CD4^+$ T cell proliferation was reduced whereas the viability of T cells was not affected (Fig. 1.11c, d). rIL-10 had a direct anti-inflammatory response on microglial cells.

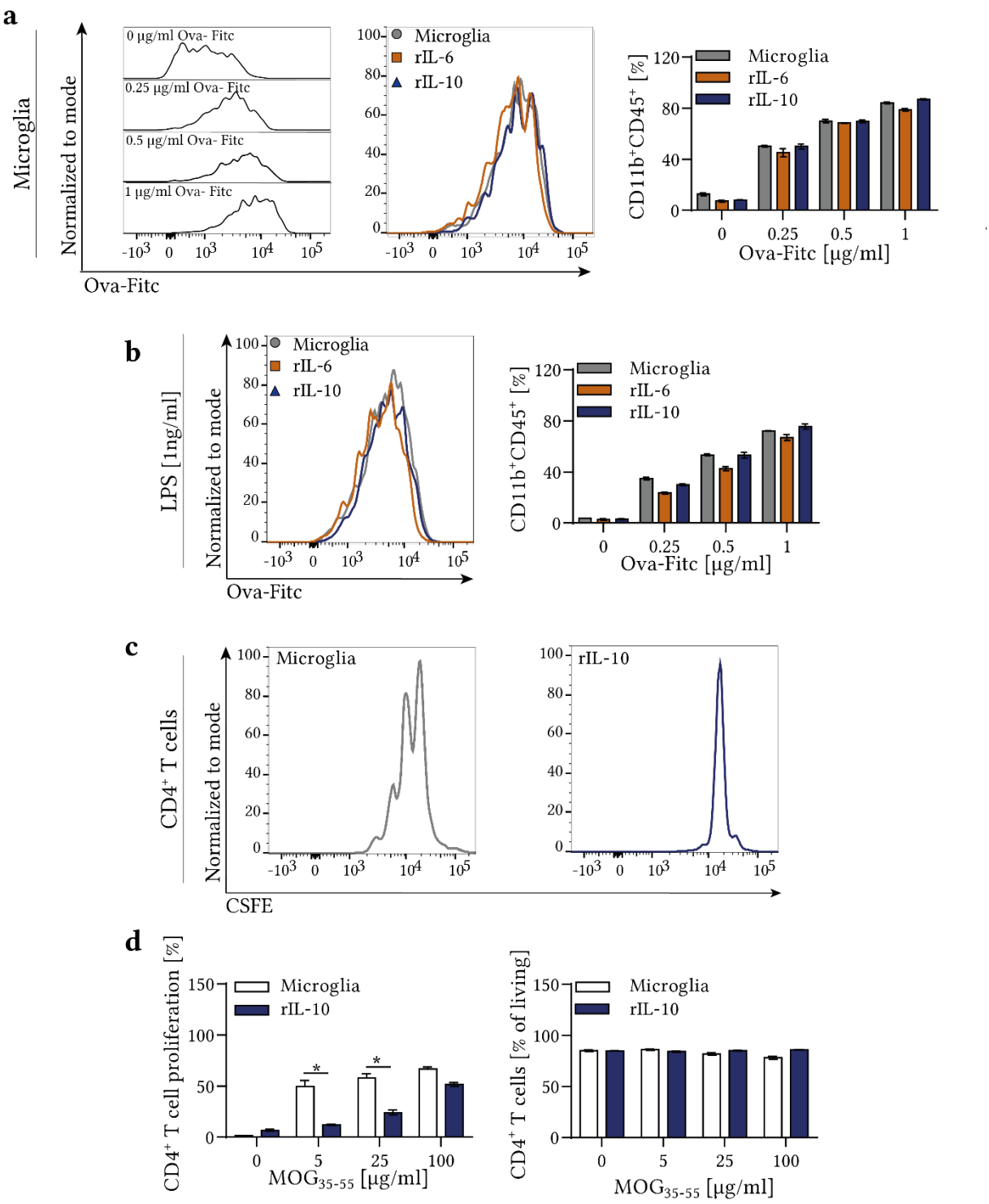

FIGURE 1.11: IL-10 REDUCES MICROGLIAL APC FUNCTION. Primary microglia were left unstimulated (a) or stimulated with 1 ng/ml LPS (b) and treated with rIL-6 or rIL-10. **a, b)** Cells were incubated for 2 h with OVA-FITC, harvested and stained for flow cytometry analysis. Frequency of OVA-FITC$^+$ microglia cells ± SEM; n=3; **a)** Unstimulated microglia. **b)** Microglia were stimulated with 1 ng/ml LPS. **c, d)** Microglia cells were co-cultured with CFSE stained MOG-specific 2D2 T cells and indicated MOG_{35-55} peptide concentrations after incubation with rIL-6 and rIL10. T cells were harvested and stained for flow cytometry. **a, b, c)** Representative histograms of OVA-FITC and rIL-6 or rIL-10 treated microglia (a, b), of CFSE labeled T cells stimulated with 25 µg/ml MOG_{35-55} peptide and treated with rIL-10. **c)** Frequency of CD4$^+$ T cell proliferation by CFSE dilution; Frequency of living of CD4$^+$ T cells; Mean ± SEM; n=3. Representative data of 2-3 independent experiments; unpaired t-test, $^*p<0.05$.

3.1.4 B CELL-DERIVED IL-10 DIMINISHES THE INFLAMMATORY RESPONSE OF MICROGLIA

To distinctively investigate the effect of IL-6 and IL-10 derived by B cells, these cytokines were blocked in the B cell supernatant by addition of functionally neutralizing antibodies. 1 µg/ml of the neutralizing antibodies led to an effective block of the specific cytokines in the B cell supernatant. Whereby the isotype control had no impact on IL-6 or IL-10 levels and anti-IL-6 did not influence the IL-10 levels as well as anti-IL-10 did not alter the IL-6 levels (Fig. 1.12).

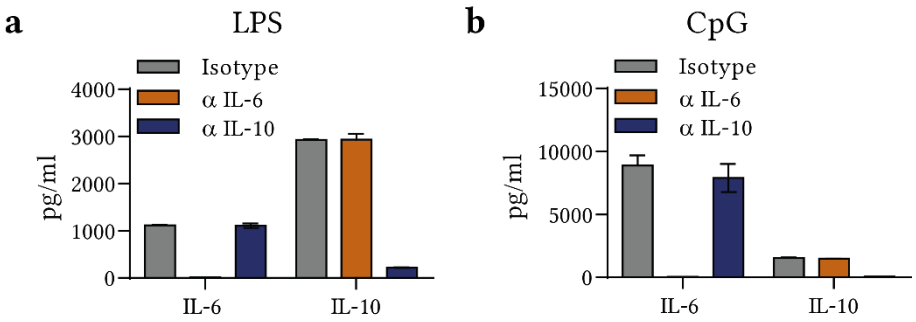

FIGURE 1.12: NEUTRALIZATION OF IL-6 AND IL-10 IN B CELL SUPERNATANT BY SPECIFIC ANTIBODIES. Purified B cells were cultured in the presence of 5 µg/ml LPS (a) or 5 µg/ml CpG (b) for 24 h. B cell supernatant was incubated with 1 µg/ml of antibodies specific against IL-6 or IL-10 or the appropriate isotype control for 20 minutes. Cytokine neutralization was measured by ELISA. Mean cytokine production ± SEM; n=2.

With the functional neutralization of IL-6 and IL-10, it was possible to analyze the specific function of these cytokines produced by B cells. Blocking of IL-6 in the supernatant of B cells showed no effect on microglia phenotype and function. Blocking of IL-10 in the supernatant of B cells had no impact on the expression of cell surface markers on microglia of LPS derived B cell supernatant (Fig 1.13), but reduced the expression of PD-L1 of CpG derived supernatant (Fig. 1.15). By contrast, the inflammatory cytokine production by microglia was highly upregulated when lacking IL-10 in the LPS treated supernatant (Fig. 1.14b). While CpG derived supernatant only upregulated TNF-α and IL-6 when IL-10 was blocked (Fig. 1.15b).

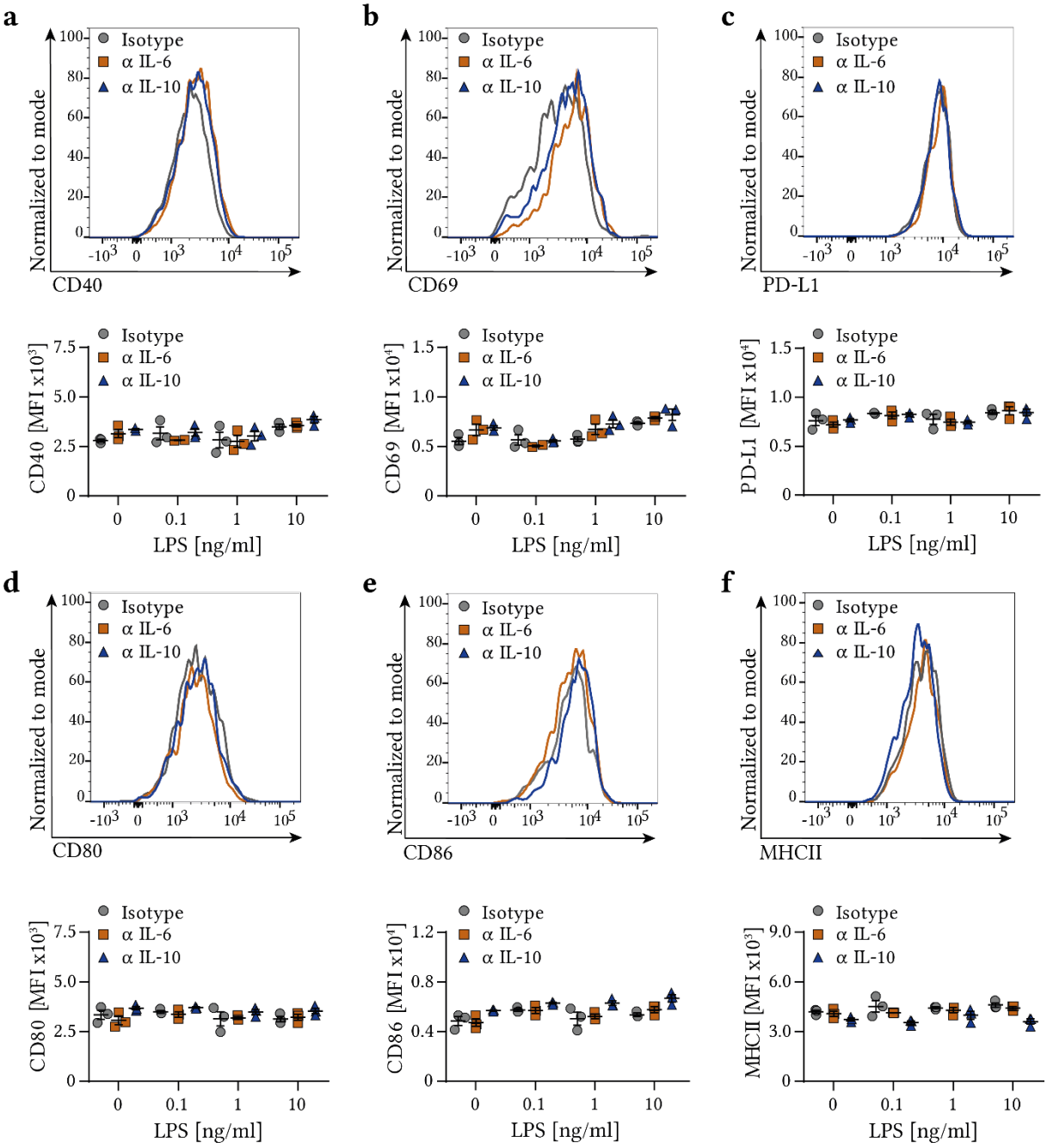

FIGURE 1.13: B CELL DERIVED IL-6 OR IL-10 DO NOT CHANGE THE EXPRESSION OF MARKERS INVOLVED IN ACTIVATION AND ANTIGEN PRESENTATION OF MICROGLIA. IL-6 or IL-10 was blocked with 1 µg/ml in the B cell supernatant by specific antibodies for 20 minutes. Primary microglia were left either unstimulated or stimulated with 0.1, 1 or 10 ng/ml LPS and co-cultured with neutralized B cell supernatant for 24 h. **a-f)** Microglial activation and expression of molecules involved in antigen presentation were analyzed using flow cytometry. Mean fluorescence intensity (MFI) ± SEM; n=3. Representative histograms are shown for LPS stimulated microglia.

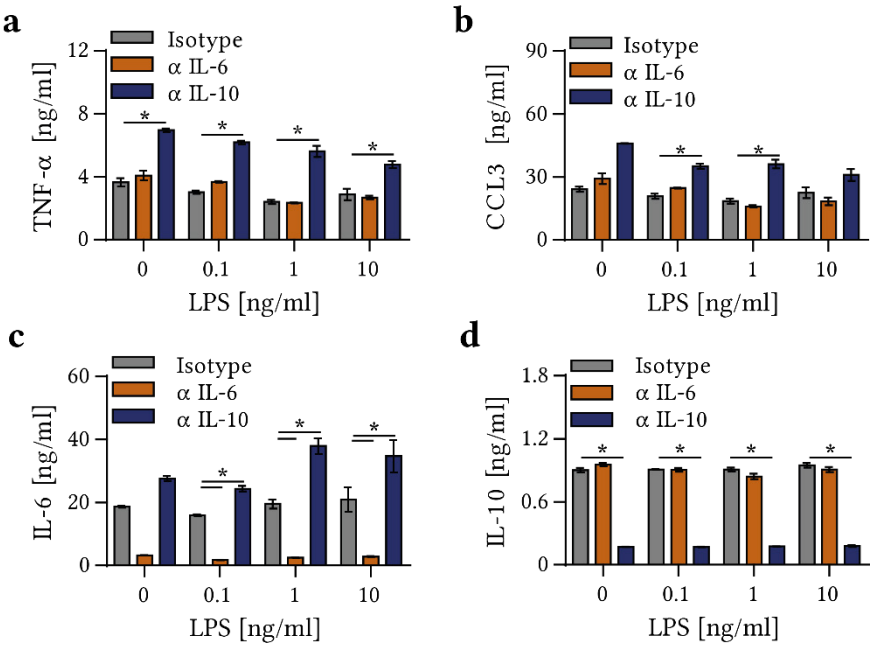

FIGURE 1.14: B CELL DERIVED IL-10 DIMINISHES THE INFLAMMATORY RESPONSE OF MICROGLIA. IL-6 or IL-10 was blocked with 1 µg/ml in the B cell supernatant by specific antibodies for 20 minutes. Primary microglia were left either unstimulated or stimulated with 0.1, 1 or 10 ng/ml LPS and co-cultured with neutralized B cell supernatant for 24 h. **a-d)** Mean cytokine concentration ± SEM, n=3, representative data of 2-3 independent experiments; one-way ANOVA with Holm-Sidak post hoc test; *p<0.05.

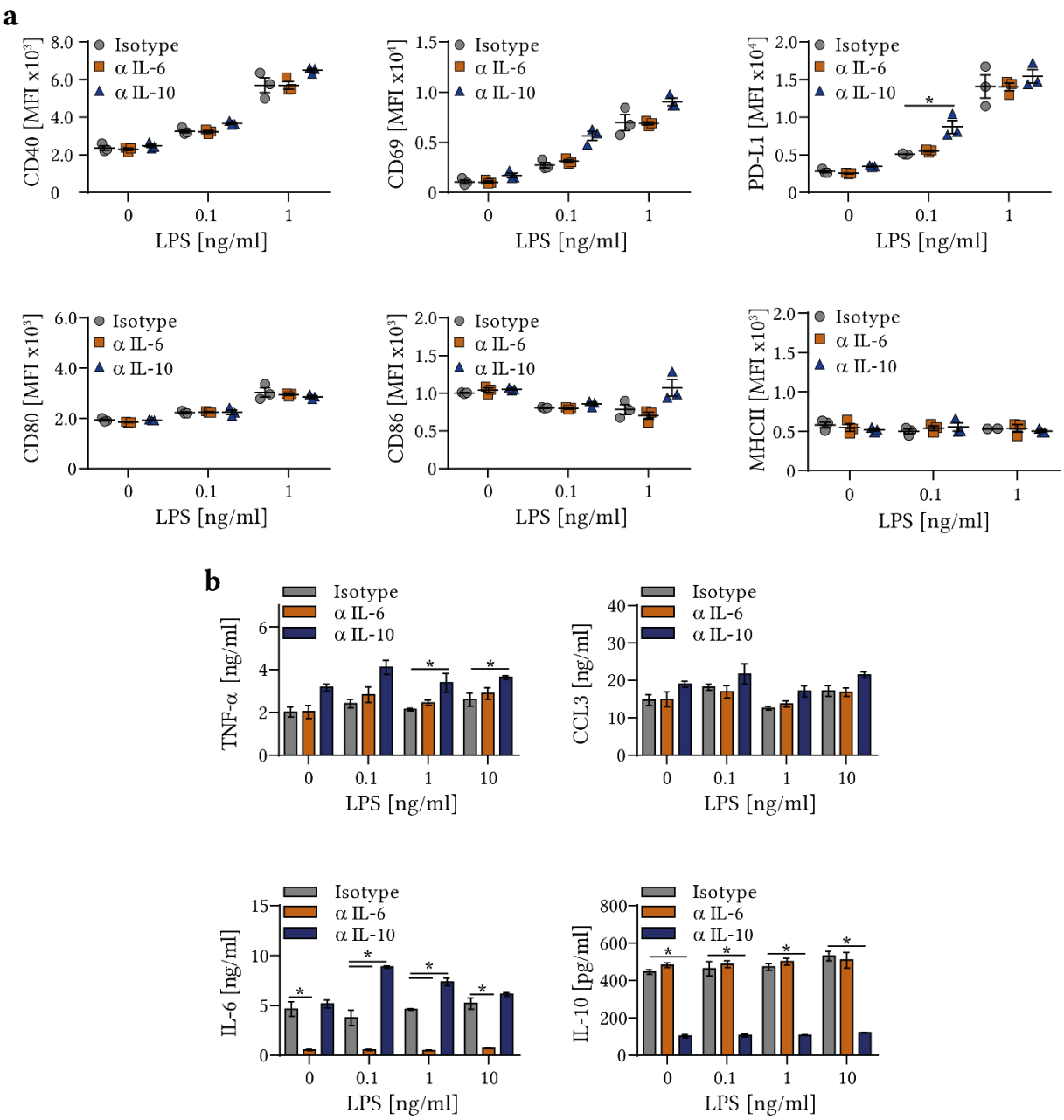

FIGURE 1.15: CPG INDUCED B CELL-DERIVED IL-10 DIMINISHES THE PRO-INFLAMMATORY RESPONSE OF MICROGLIA. Purified B cells were cultured in the presence of 5 µg/ml CpG for 24 h. Supernatant was collected, and IL-6 or IL-10 was blocked in the B cell supernatant with 1 µg/ml of the specific antibodies for 20 min followed by co-culture with microglia, left unstimulated or stimulated with 0.1, 1 or 10 ng/ml LPS for 24 h. **a)** Microglial activation and expression of molecules involved in antigen presentation were analyzed using flow cytometry. Mean fluorescence intensity (MFI) ± SEM, n=3. **b)** Mean cytokine concentration ± SEM, determined by ELISA; n=3, representative data of 2-3 independent experiments, one-way ANOVA with Holm-Sidak post hoc test; *p<0.05.

These data suggest that IL-10 has a regulatory effect on microglial phenotype. Therefore, it was next investigated, if IL-10 has an impact on the phagocytic capacity or APC function of microglia. There were no changes in microglial phagocytosis observed by both blocking IL-6 or IL-10, either in unstimulated or stimulated microglia (Fig. 1.16a). As already observed in

Fig. 1.8, the APC function of microglia is impaired by the treatment of microglia with B cell supernatant. Of note, blocking of IL-10 results in reduced T cell viability (Fig. 1.16b).

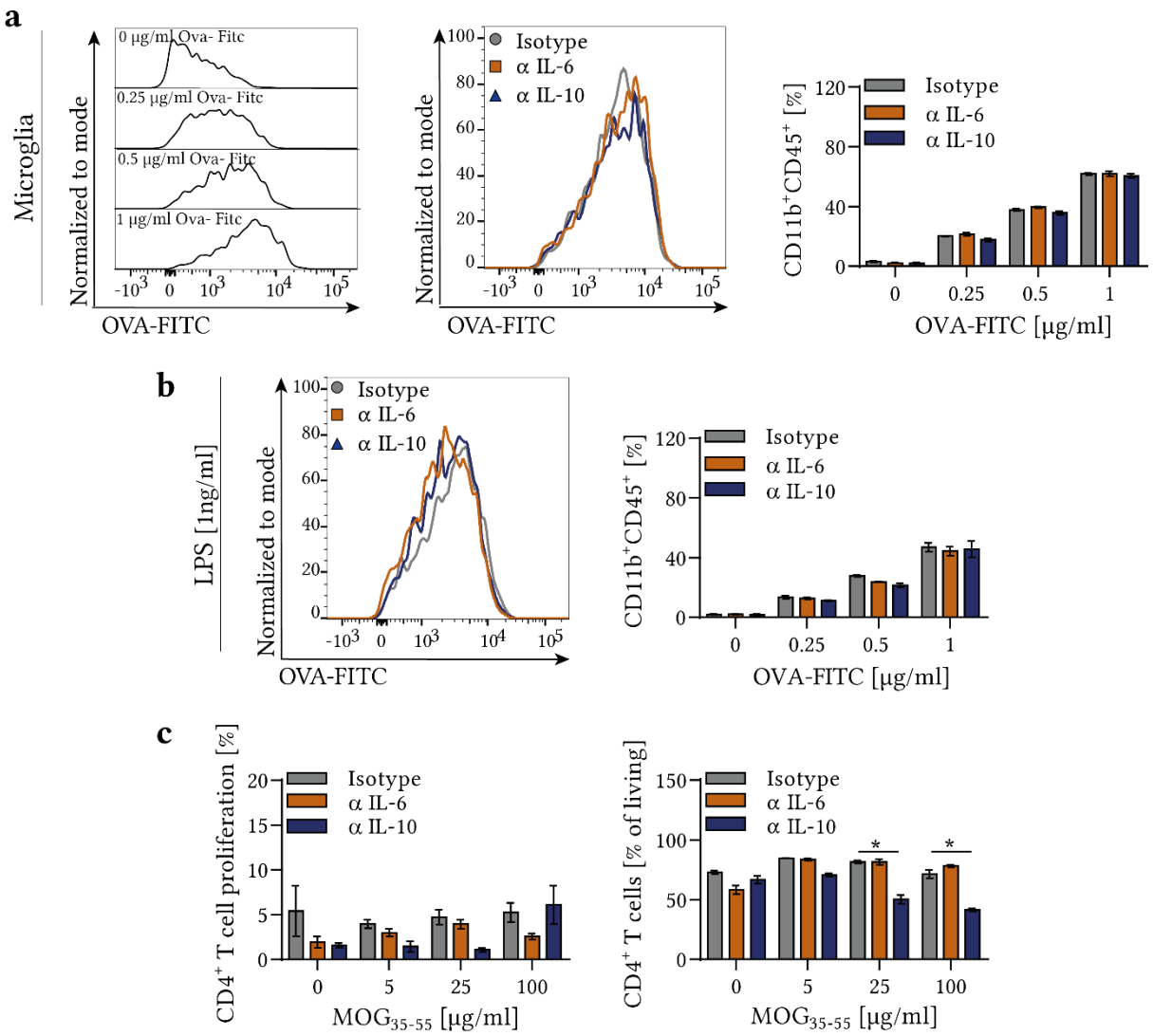

FIGURE 1.16: B CELL-DERIVED IL-10 REGULATES T CELL SURVIVAL. Primary microglia were stimulated with 1 ng/ml LPS and co-cultured with IL-6 or IL-10 neutralized B cell supernatant for 24 h. **a, b)** Cells were washed and OVA-FITC was added. After 2 h the cells were harvested and stained for flow cytometry analysis. Frequency of OVA-FITC$^+$ microglia cells ± SEM; n=3. **b)** Microglia were stimulated with 1 ng/ml LPS **c)** After incubation with B cell supernatant microglia cells were co-cultured with CFSE stained MOG-specific 2D2 T cells and MOG_{35-55} peptide. After 72 h T cells were harvested and stained for flow cytometry. Frequency of CD4$^+$ T cell proliferation by CFSE dilution; Frequency of living of CD4$^+$ T cells; Mean ± SEM; n=3. Representative data of 2-3 independent experiments; one-way ANOVA with Holm-Sidak post hoc test; *p<0.05

3.1.5 B CELL-DERIVED MOLECULES MODULATE ASTROCYTE PHENOTYPE

Alongside microglia, astrocytes are supposed to play also a critical role in disease progression of MS and may contribute to B cell survival, maturation, and proliferation through production

of B cell-activating factors. These observations support the concept of a direct interaction of B cells and astrocytes. To assess if B cells regulate the astrocyte phenotype, astrocytes were exposed to B cell supernatant and activated by IFN-γ and IL-1β. Under homeostatic conditions LPS activated B cells upregulated the expression of the pro-inflammatory cytokines CCL2 and CCL5 (Fig. 1.17b). Furthermore, the secretion of these cytokines and CXCL1 was enhanced while the viability remained unchanged (Fig. 1.17c). B cells activated by CpG did not changes the astrocyte phenotype (Fig.1.17d-f).

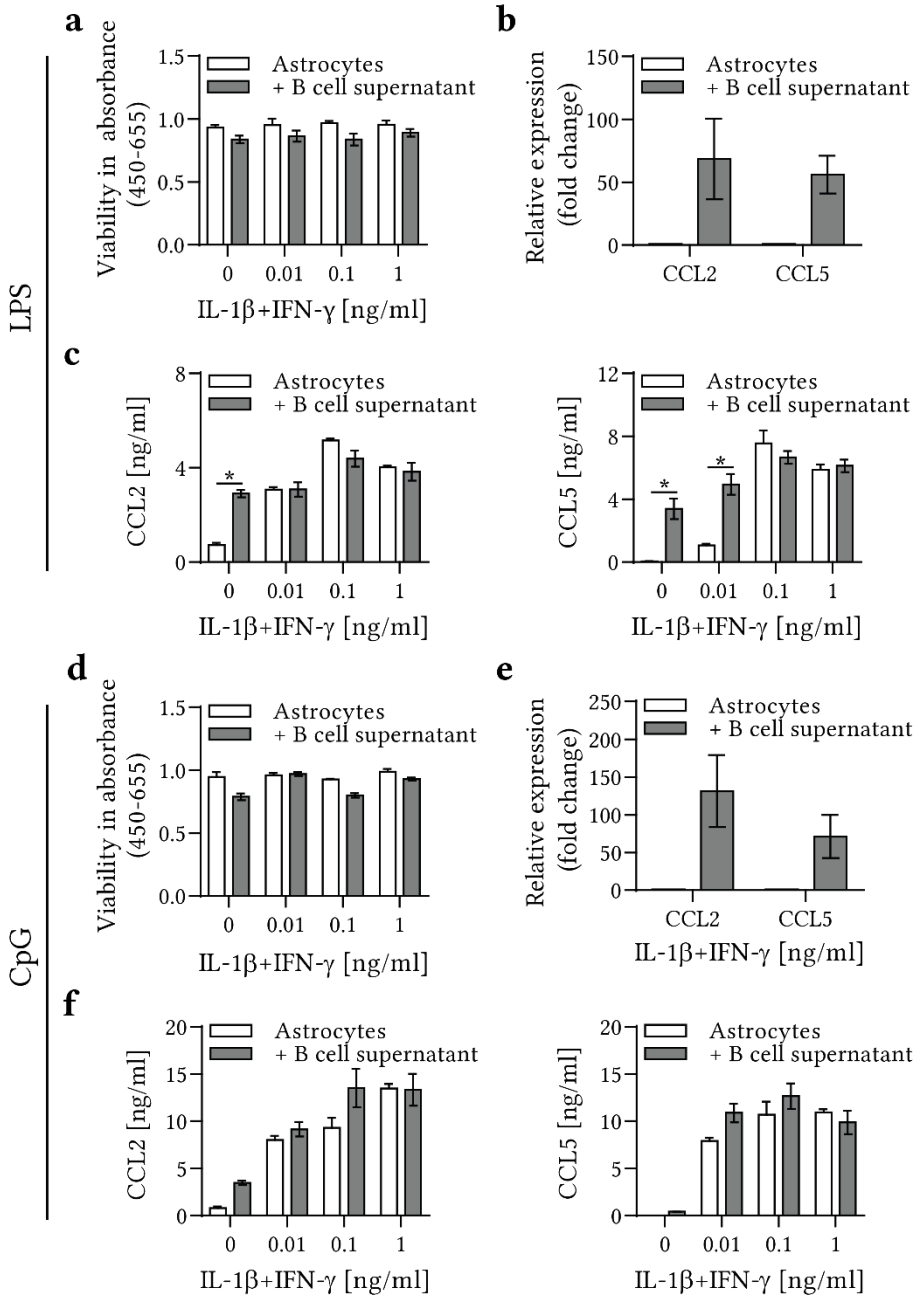

FIGURE 1.17: B CELL-DERIVED FEATURES CHANGE THE ASTROCYTE PHENOTYPE. Purified primary astrocytes were left unstimulated or stimulated with IFN-ɣ/IL-1β and were cultured in the presence of B cell supernatant stimulated with LPS (a, b) or CpG (c, d). **a, d)** Viability was assessed by WST-1 assay. **b, e)** Cytokine expression was analyzed by qPCR. **c, f)** Cytokine production measured by ELISA; mean cytokine concentration ± SEM; n=3; Representative data of 2-3 independent experiments; unpaired t-test, *p<0.05.

3.1.6 DIFFERENT B CELL FEATURES THAN IL-6 OR IL-10 ARE REQUIRED TO REGULATE ASTROCYTE ACTIVITY

Next, it was investigated whether IL-6, IL-10 and/or TGF-β may have an impact on the astrocyte phenotype. Therefore, astrocytes were incubated with increasing concentrations of IL-1β/IFN-ɣ in the presence of rIL-6, rIL-10 or rTGF-β. In both, homeostatic and inflammatory conditions, neither of the cytokines showed a significant effect on the phenotype of astrocytes. However, rTGF-β showed a trend towards downregulating CCL5 (Fig. 1.18).

Yet, the effect of blocking IL-6 or IL-10 in the supernatant derived by LPS or CPG activated B cells was analyzed and revealed that lack of these cytokines in B cell derived supernatant had no implications on the cytokine expression or production by astrocytes (Fig. 1.19).

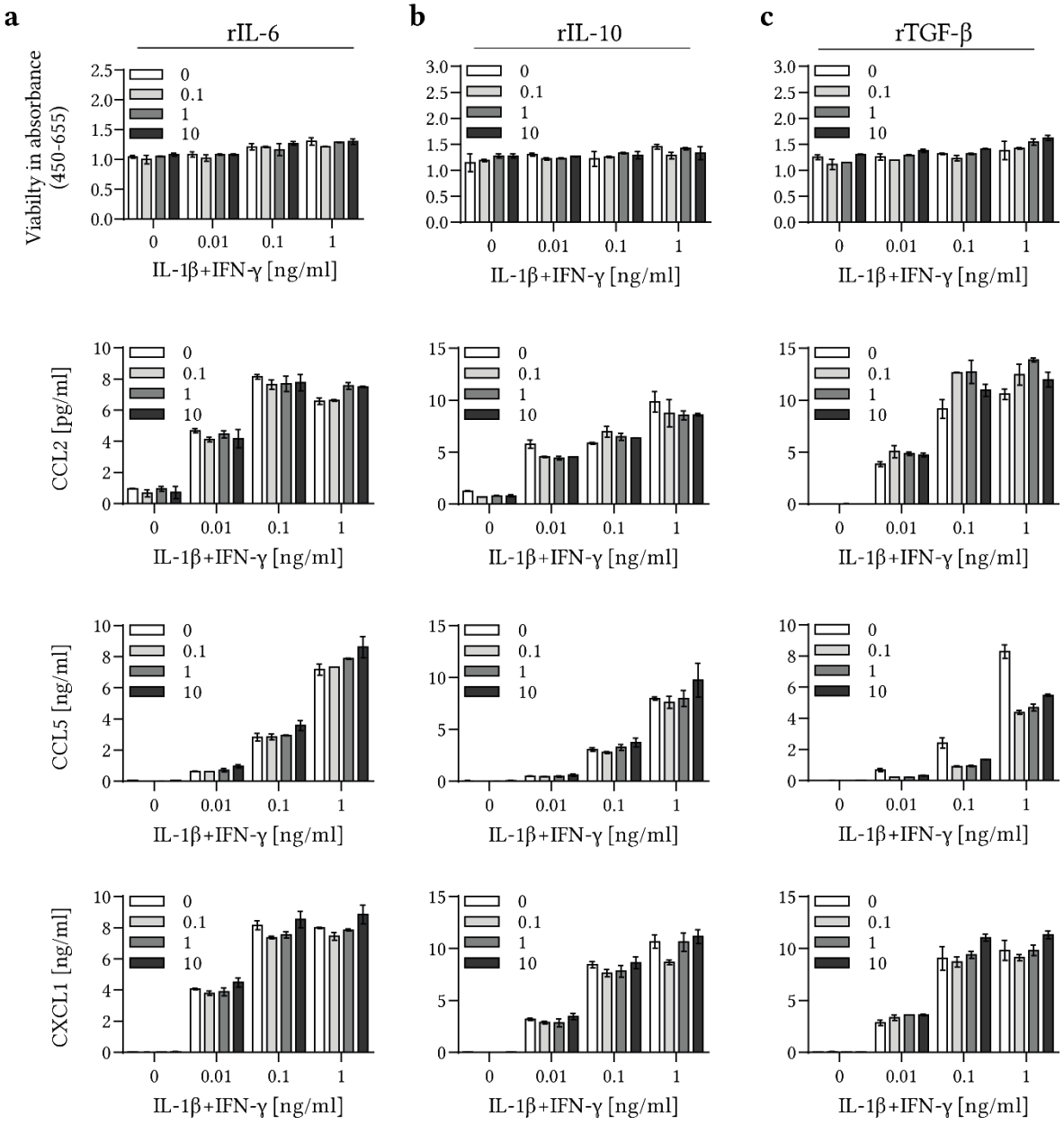

FIGURE 1.18: IL-6 AND IL10 HAVE NO EFFECT ON THE ASTROCYTE PHENOTYPE. Primary astrocytes were left either unstimulated or stimulated with IFN-γ/IL-1β and were cultured in the presence of indicated concentrations of rIL-6, rIL-10 or rTGF-β. **a-c)** Viability of the cells determined by WST-1 assay; Mean ± SEM, cytokine production measured by ELISA; Mean cytokine concentration ± SEM; n=3, **c)** Mean cytokine concentration ± SEM; n=2; Representative data of 2-3 independent experiments.

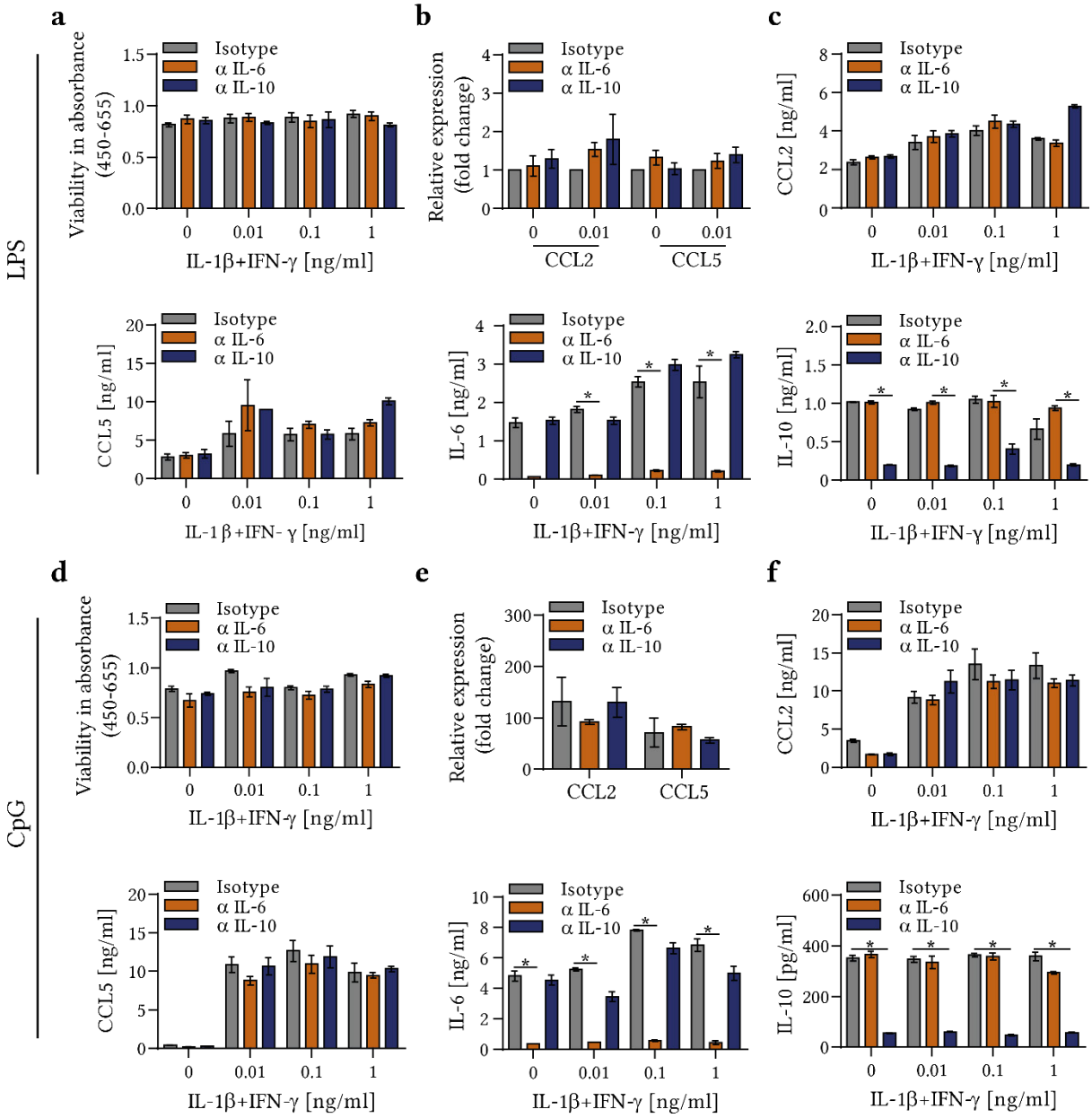

FIGURE 1.19: DIFFERENT B CELL FEATURES THAN IL-6 OR IL-10 ARE REQUIRED TO REGULATE ASTROCYTE ACTIVITY. Purified primary astrocytes were either left unstimulated or stimulated with IFN-γ/IL-1β and were cultured in the presence of B cell supernatant generated by stimulation of B cells with either LPS (a, b) or CpG (c, d) followed by neutralization of IL-6 or IL-10. **a, d)** Viability was assessed by WST-1 assay. **b, e)** Cytokine expression was analyzed by qPCR. **c, f)** Cytokine production measured by ELISA; mean cytokine concentration ± SEM; n=3; Representative data of 2-3 independent experiments; one-way ANOVA with Holm-Sidak post hoc test; *p<0.05.

3.2 PROJECT 2: THE THERAPEUTIC POTENTIAL OF BTK INHIBITION IN CHRONIC CNS AUTOIMMUNITY

Controlling MS progression by therapeutic agents remains a major challenge. Small molecules inhibiting BTK may be promising candidates to target innate immunity within the CNS, which is associated with disease progression. In the present study, the effect of the BTK inhibitor evobrutinib was analyzed on CNS-resident cells in vitro and in vivo in animal models of MS.

3.2.1 BTK IS EXPRESSED IN MICROGLIA AND INCREASES UNDER INFLAMMATION

At first, the expression of BTK in microglia was assessed in primary cell cultures and in adult mice during EAE, an animal model of MS. While there is a strong and consistent expression of BTK RNA in primary microglia as well as in isolated splenic B cells, astrocytes and T cells are lacking BTK expression completely (Fig. 2.1a). Along the same line, ex vivo analysis of microglia isolated from brain and spinal cord of adult mice showed BTK expression, which was upregulated during EAE induced by MOG_{35-55} peptide immunization (Fig. 2.1b, d). The upregulation of BTK under inflammation was confirmed by splenic lymphocytes, macrophages and neutrophils (Fig. 2.1c). Additionally, the expression of some markers associated with activation and antigen presentation was induced in microglia upon immunization (Fig. 2.1f).

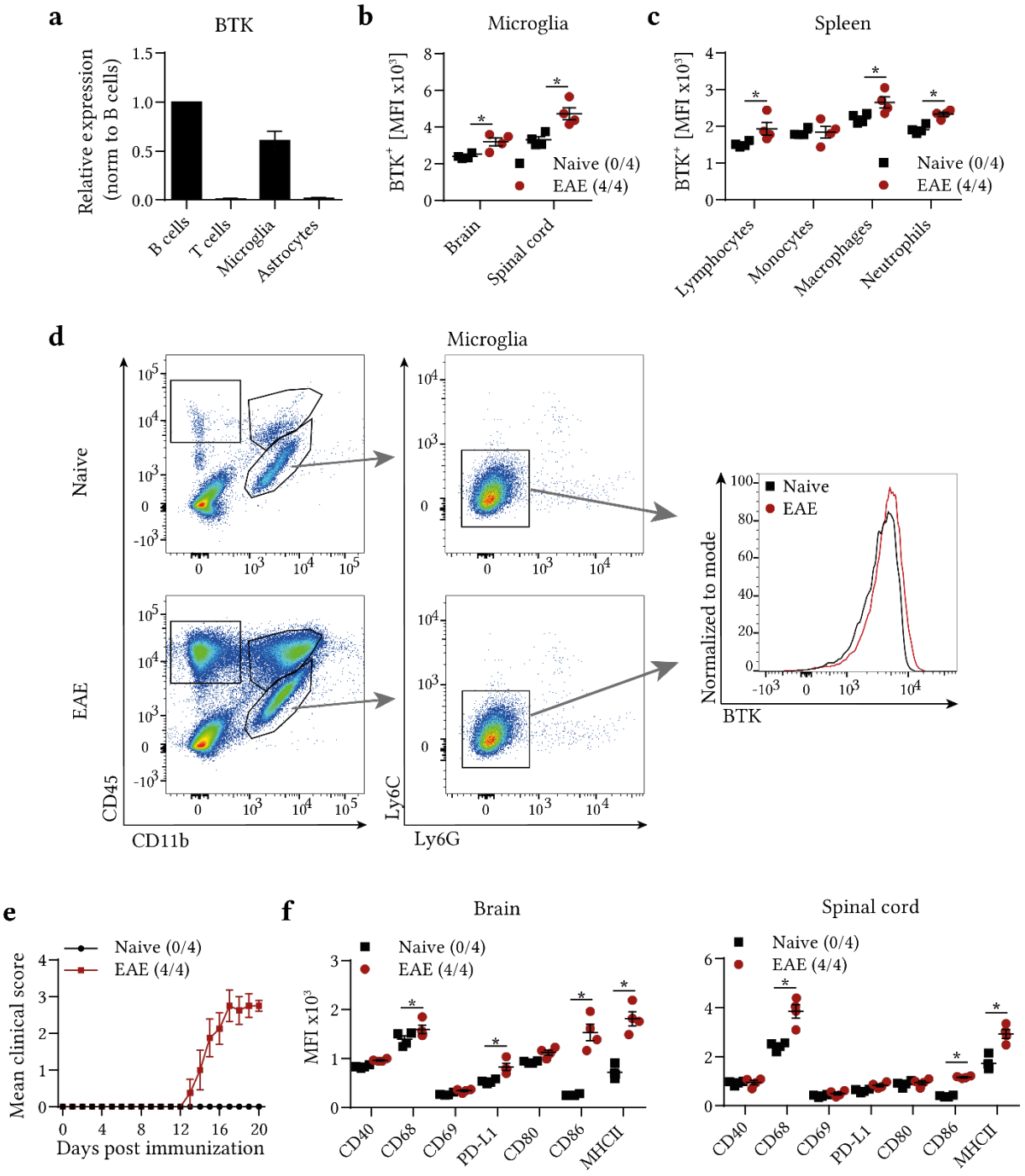

FIGURE 2.1: BTK IS EXPRESSED IN MICROGLIA BUT NOT ASTROCYTES AND IS UPREGULATED UNDER INFLAMMATION. a) Primary cell cultures were harvested and lysed for RNA extraction; relative expression normalized to GapDH ± SEM **b-f)** Mice were left untreated or immunized with MOG_{35-55} peptide. On day 20 after immunization, cells were isolated and stained for flow cytometry, **e)** Mean clinical score ± SEM. **b, c, f)** Mean fluorescence intensity ± SEM; n=4; Mann-Whitney U test *p<0.05. **d)** Representative histograms and gating strategy.

3.2.2 EVOBRUTINIB INHIBITION ON MICROGLIA IN VITRO

3.2.2.1 BTK INHIBITION DOWNREGULATES PD-L1 EXPRESSION ON MICROGLIA IN VITRO

Next, the modulatory effect of the BTK inhibitor evobrutinib was analyzed in vitro on microglia, stimulated with LPS (Fig. 2.2) or a mixture of cytokines (Fig. 2.3) to induce a pro-inflammatory microglial phenotype. Here, a down-regulation of the marker PD-L1 was observed, which was independent of the stimulation (Fig. 2.2a b, 2.3a-c). Other investigated markers for activation, antigen presentation as well as cytokine production remained relatively stable (Fig. 2.2a, 2.3a, c).

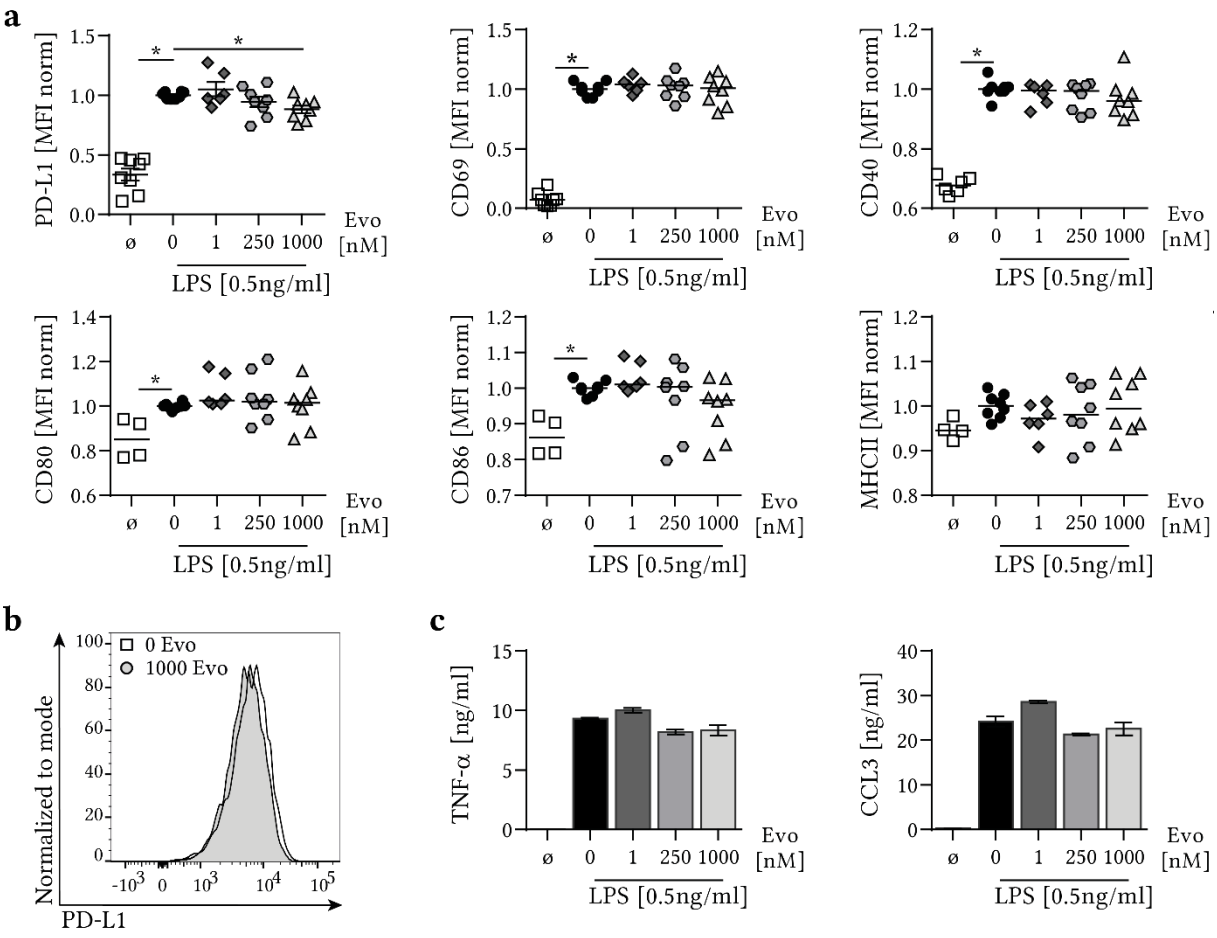

FIGURE 2.2: EVOBRUTINIB AFFECTS LPS-INDUCED MICROGLIAL PD-L1 EXPRESSION IN VITRO. Primary microglia were pre-treated with the indicated evobrutinib concentrations for 30 minutes prior to stimulation with 0.5 ng/ml LPS. After 6 h the cells were harvested and stained for flow cytometry analysis. **a)** Mean fluorescence intensity ± SEM; n=4-8, pooled from 2-3 independent experiments; Kruskal-Wallis with Dunn's post hoc test; *p<0.05. **b)** Representative histogram. **c)** Mean cytokine production ± SEM; n=3.

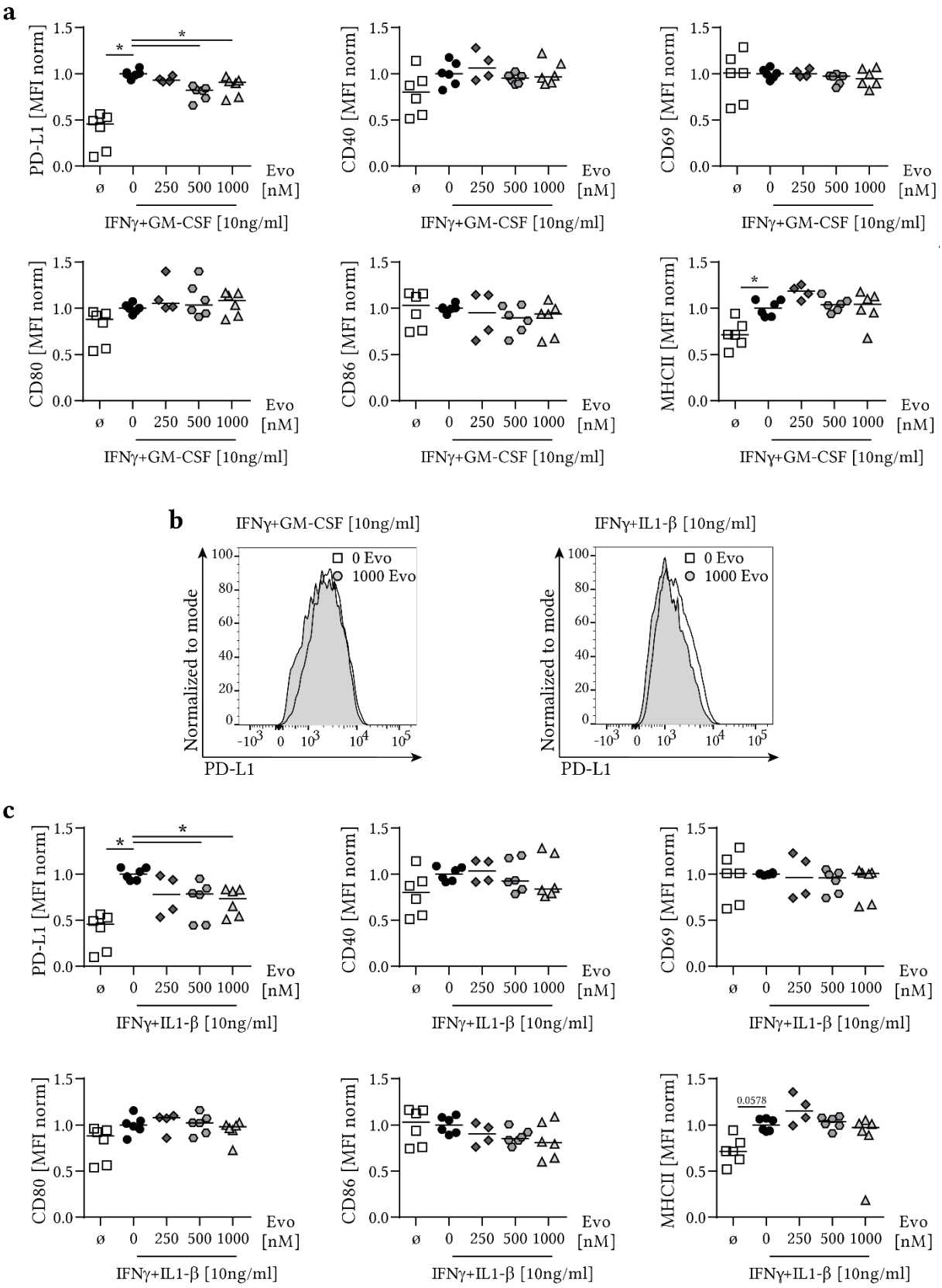

FIGURE 2.3: EVOBRUTINIB DOWNREGULATES CYTOKINE-INDUCED MICROGLIAL PD-L1 EXPRESSION IN VITRO. Primary microglia were pre-treated with the indicated evobrutinib concentrations for 30 minutes prior to stimulation with 10 ng/ml of the indicated cytokines. After 18 h the cells were harvested and stained for flow cytometry analysis. **a, c)** Mean fluorescence intensity ± SEM; n=4-8, pooled from 2-3 independent experiments; Kruskal-Wallis with Dunn's post hoc test; *p<0.05. **b)** Representative histograms.

3.2.2.2 EVOBRUTINIB SPECIFICALLY INHIBITS LPS-INDUCED MICROGLIAL M1 DIFFERENTIATION

Since inhibition of BTK in B cells directly interferes with BCR-mediated B cell differentiation, it was next investigated if BTK inhibition influences the differentiation of microglial phenotypes into M1 phenotype using LPS stimulation versus M2 phenotype using a combination of recombinant IL-4, IL-10 and IL-13 in vitro. While the overall induction of the M1 and M2 phenotype by the specific stimulation was dose-dependently inducible (Fig. 2.4a, b), treatment with evobrutinib led to a reduction in the LPS-induced iNOS expression (Fig 2.4c, d). Of note, there were no changes in the M2 differentiation observed, independent of the induced differentiation (Fig 2.4c).

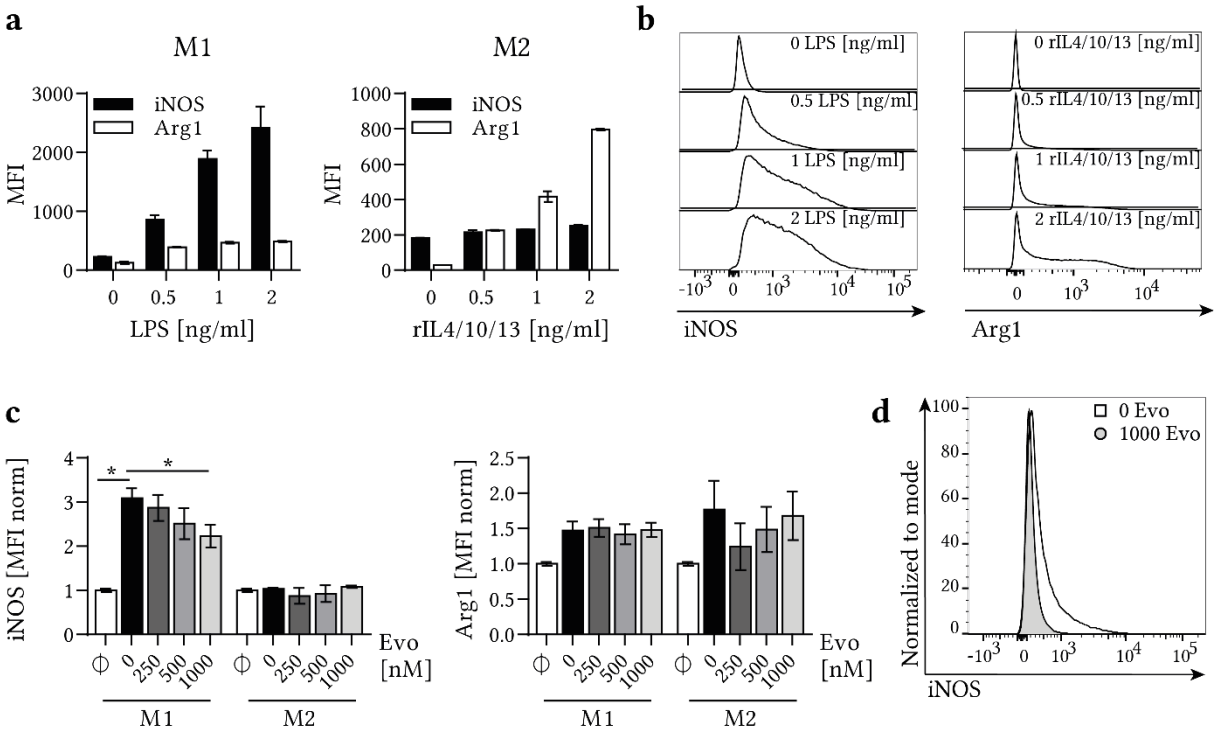

FIGURE 2.4: EVOBRUTINIB SPECIFICALLY INHIBITS LPS-INDUCED MICROGLIAL M1 DIFFERENTIATION. Primary microglia were pre-treated with the indicated evobrutinib concentrations for 30 minutes prior to differentiation into M1 (LPS) or M2 (rIL-4/10/13) phenotype. After 48 h the cells were harvested and stained using the BD PhosFlow protocol. **a)** Mean fluorescence intensity ± SEM; n=2, **b)** representative histograms, **c)** Mean fluorescence intensity ± SEM; n=4-8, pooled from 2-3 independent experiments; Kruskal-Wallis with Dunn's post hoc test; *p<0.05. **d)** Representative histogram.

Furthermore it was investigated if the changes in the differentiation of the M1 phenotype have an impact on the phagocytic capacity of microglia. Interestlingly, independent on the differentiation of microglia, evobrutinib led to a seemingly unspecific increase in overall phagocytosis (Fig. 2.5).

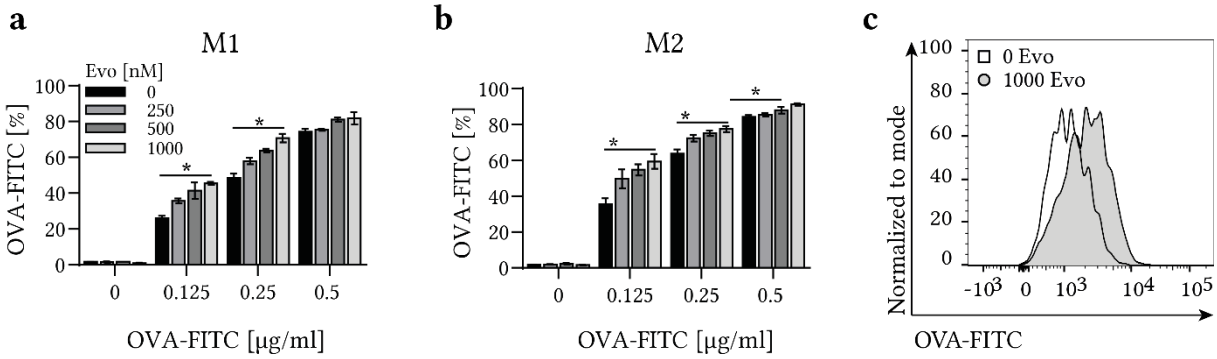

FIGURE 2.5: EVOBRUTINIB PROMOTES PHAGOCYTOSIS CAPACITY. Primary microglia were left unstimulated or differentiated into M1 or M2 microglia. 30 minutes prior to the phagocytosis assay the cells were treated with evobrutinib with indicated concentrations. Thereafter the cells were incubated for 2 h with indicated concentrations of OVA-FITC, harvested and stained for flow cytometry analysis. **a, b)** Frequency of OVA-FITC$^+$ microglia cells ± SEM; n=3, Kruskal-Wallis with Dunn's post hoc test; *p<0.05. **c)** Representative histogram of M1 microglia.

3.2.3 EVOBRUTINIB HAS NO EFFECT ON ASTROCYTES

To control for any toxic or off-target effects of evobrutinib, astrocytes which do not express BTK were exposed to evobrutinib. No inhibitory effect of evobrutinib was detected either in unstimulated or in IFN-γ/IL1-β stimulated astrocytes (Fig. 2.6).

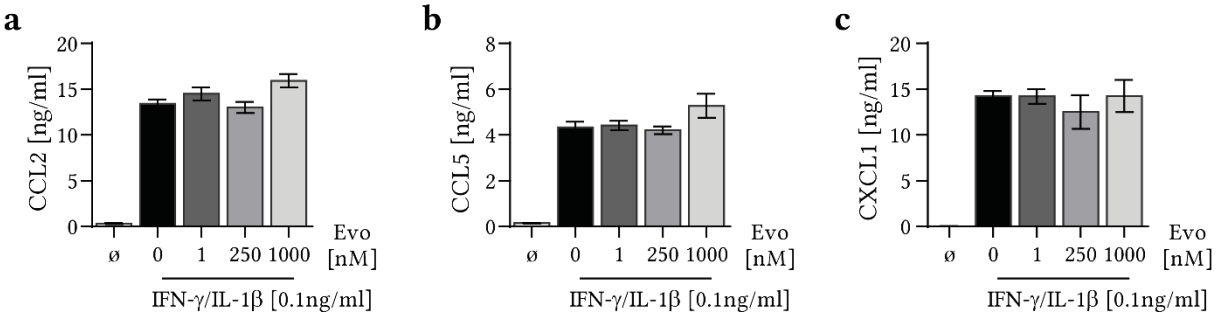

FIGURE 2.6: EVOBRUTINIB DOES NOT ALTER THE CYTOKINE PATTERN OF ASTROCYTES. Purified primary astrocytes were pre-treated with the indicated evobrutinib concentrations for 30 minutes prior to stimulation with 0.1 ng/ml IFN-γ/IL-1β. **a-c)** Cytokine production measured by ELISA; mean cytokine concentration ± SEM; n=3; representative data of 2 independent experiments.

3.2.4 EFFECT OF EVOBRUTINIB IN VIVO

To investigate the effect of evobrutinib on microglia in in vivo models of MS which reflects partly progression and progressive disease, the cuprizone, the passive EAE model and the chronic EAE model were used. In all experiments mice were treated daily with 10 mg/kg evobrutinib or vehicle control.

3.2.4.1 CUPRIZONE-INDUCED DEMYELINATION WAS NOT AFFECTED BY EVOBRUTINIB

Since, evobrutinib reduced M1 microglia while enhancing phagocytosis in vitro, the cuprizone model was used to investigate if evobrutinib controls microglial activity in the context of de- and remyelination. In this model, microglia gain their full activation status and phagocyte myelin debris between week 3-5 upon cuprizone exposure. Therefore, to study the impact of evobrutinib on microglia activity, mice were treated prophylactically for 3 days with evobrutinib, followed by simultaneously treatment with 0.25 % cuprizone for 5 weeks.

After 4 days of cuprizone diet, mice showed a profound body weight loss which was unaffected by evobrutinib (Fig. 2.7a). Previous studies with evobrutinib showed a shift in the B cell differentiation into a less activated phenotype due to evobrutinib during EAE (Torke et al., 2020). This effect was confirmed in the cuprizone model with an accumulation of follicular (Fo) II splenic B cells and corresponding reduction of Fo I B cells in mice treated with evobrutinib, while other B cell subsets remained stable (Fig 2.7b). Furthermore, neither B cells, nor T cells showed any changes in terms of activation and expression of co-stimulatory molecules upon evobrutinib treatment (Fig. 2.7c). By contrast, $CD11b^+$ myeloid cells showed a downregulation of CD69, while CD86 was upregulated in evobrutinib treated mice (Fig. 2.7c). Of note, the cuprizone model is a toxic demyelinating model without major influences on the peripheral immune system. Comparing naïve mice with cuprizone fed mice, no changes were observed in the analyzed peripheral immune cells (Fig. 2.7c). In contrast, brain derived microglia upregulated the expression of CD40, PD-L1, CD68, CD80 and CD86, upon cuprizone diet (Fig. 2.7d). However, no changes were observed in evobrutinib treated animals. Expression of the analyzed marker in microglia isolated from the spinal cord remained relatively stable under cuprizone diet compared to naïve mice as well as upon evobrutinib treatment compared to vehicle control (data not shown). In addition, the same results were reached by analyzing mice after 2, 3, 4 and 6 weeks of cuprizone diet (data not shown).

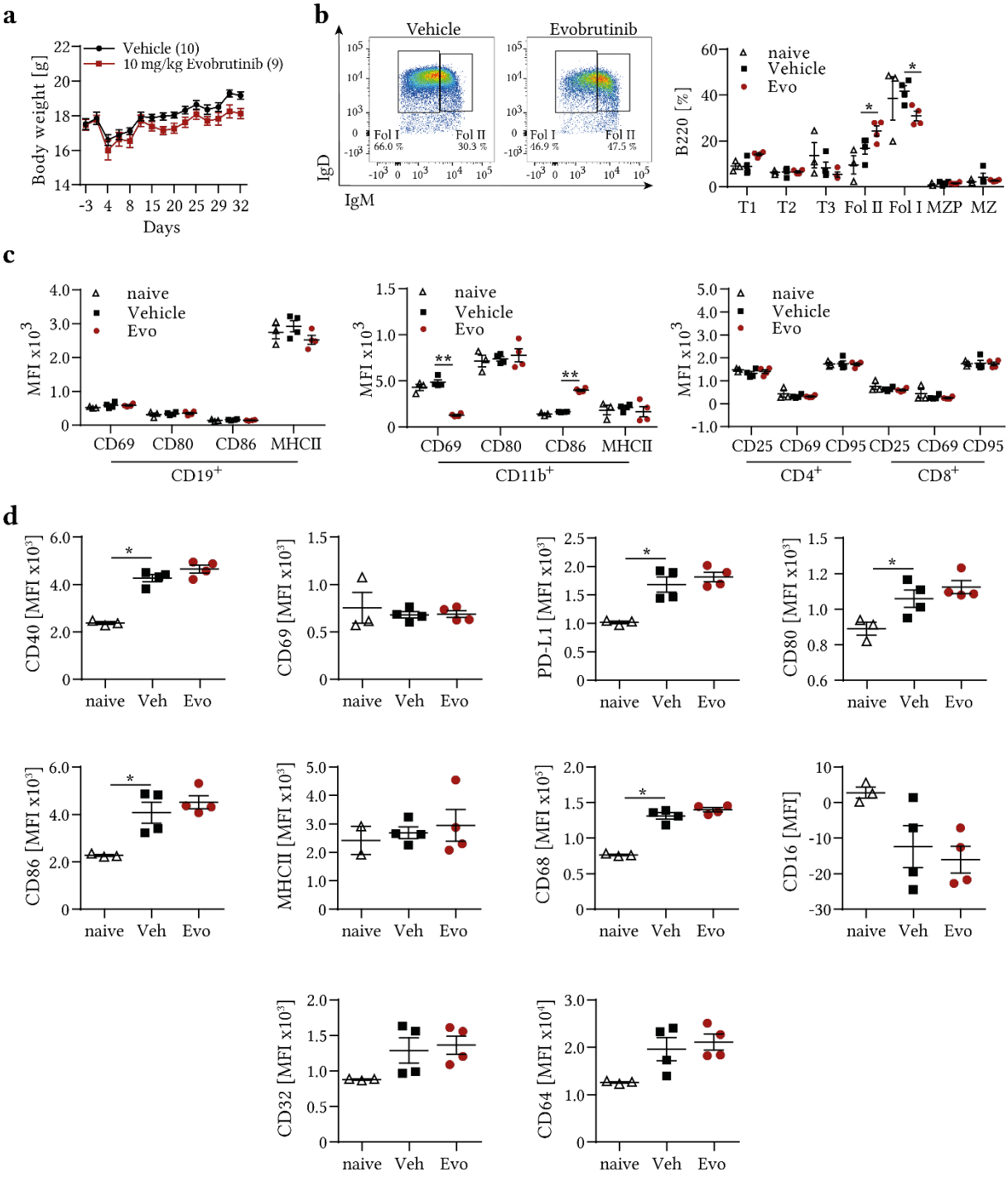

FIGURE 2.7: EVOBRUTINIB INHIBITS THE MATURATION OF B CELLS IN THE CUPRIZONE MODEL. C57BL/6 mice were fed with 0.25 % cuprizone for 5 weeks and treated with evobrutinib starting from d-3-d32. On day 32 the cells were isolated and analyzed by flow cytometry. **a)** Mean body weight ± SEM; n=10. **b)** Mean frequency of $B220^+$ cells ± SEM, n=3-4. **c)** Mean fluorescence intensity ± SEM; n=3-4. **d)** Microglia activation in the brain; mean fluorescence intensity ± SEM, n=3-4, representative data of two independent experiments; Kruskal-Wallis with Dunn's post hoc test; *p<0.05

Besides the phenotype analysis of microglia, histological analysis were performed to assess the impact of evobrutinib on demyelination and the number of CNS-resident cells (Fig. 2.8). Typically, a complete demyelination of the corpus callosum (CC) occurs after 5 weeks of cuprizone exposure. Brain sections of control and evobrutinib treated mice were examined and analyzed for demyelination of the CC by LFB-PAS and proteolipid protein (PLP) staining (Fig. 2.8a, b). Myelin appears blue in the LFB-PAS staining and brown in the PLP staining. The extent of myelin, both in the LFB-PAS and in the PLP staining was similar in both groups. After 5 weeks of cuprizone diet the occurring demyelination together with the activation of microglia and astrocytes, triggers the activation and recruitment of oligodendrocyte precursor cells (OPCs). Thus, the number of $Olig2^+$ oligodendrocytes was measured in the CC. However, evobrutinib treatment did not alter the number of $Olig2^+$ cells after 5 weeks of cuprizone exposure (Fig. 2.8c). Cuprizone-mediated demyelination led to an increased accumulation of microglia and a higher number of astrocytes. To assess the number of those cells immunohistochemistry (IHC) for the marker Iba1 and GFAP was performed. The number of $Iba1^+$ or $GFAP^+$ cells remained comparable in both groups (Fig. 2.8d, e).

In the cuprizone model, the exchange of the cuprizone diet by the standard diet leads to a rapid remyelination. To investigate the potential of evobrutinib to increase remyelination, mice were exposed to 0.25 % cuprizone for 5 weeks and were analyzed using histology after 3 days of cuprizone withdrawal (Fig. 2.9). In this approach, the body weight of both groups remained comparable (data not shown). However, evobrutinib treatment increased remyelination, measured by LFB-PAS staining, while the extent of myelin in the PLP staining remained similar (Fig. 2.9a, b). Interestingly, the number of $Olig2^+$ oligodendrocytes was enhanced in evobrutinib-treated animals compared to control mice (Fig. 2.9c). The number of microglia cells usually decreases in the CC with the onset of remyelination after removal of cuprizone. However, evobrutinib did not alter the number of both, microglia and astrocytes (Fig. 2.9d, e).

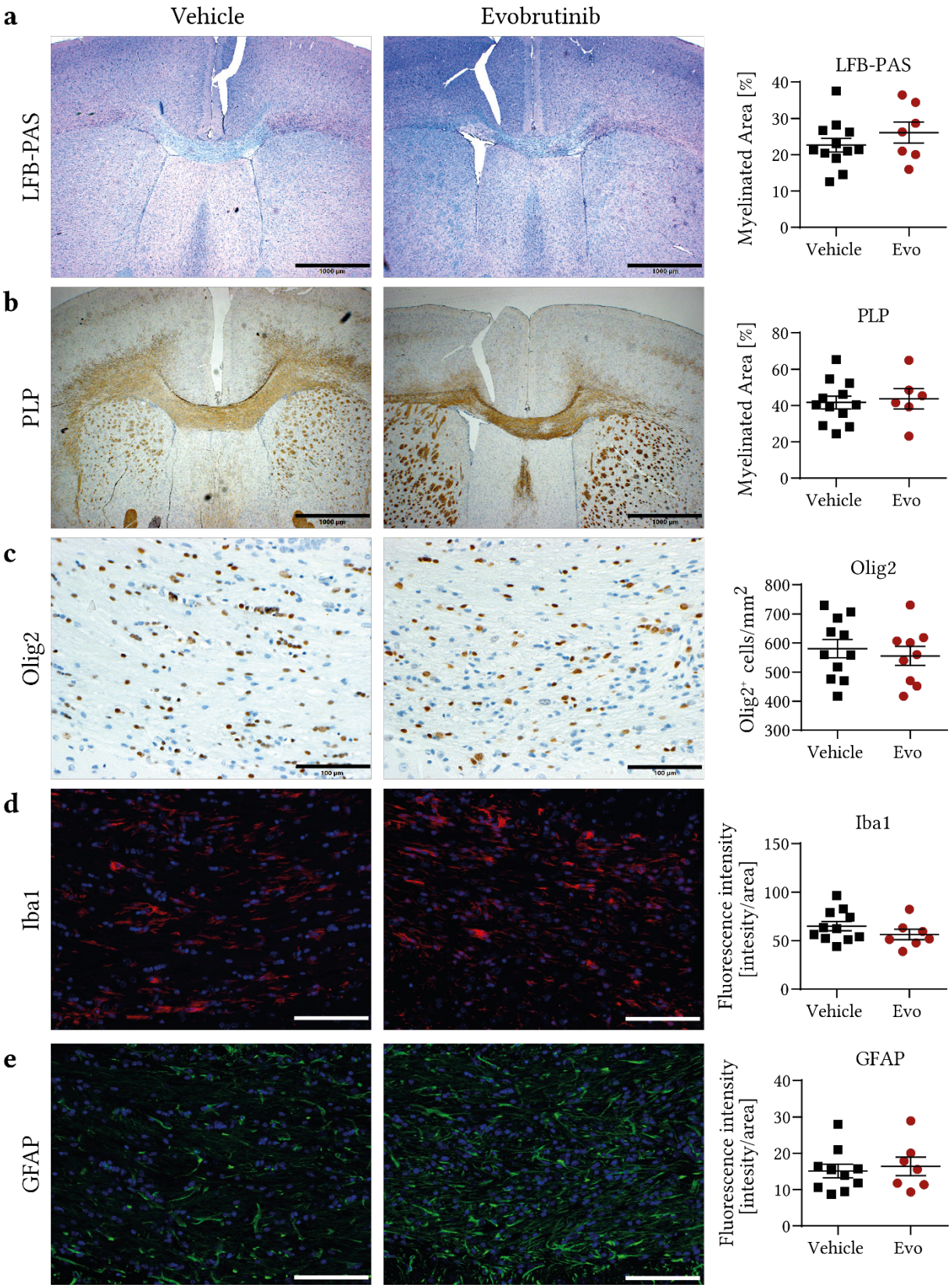

FIGURE 2.8: EVOBRUTINIB DOES NOT ALTER THE HISTOPATHOLOGICAL PATTERN OF CUPRIZONE-INDUCED DEMYELINATION. C57BL/6 mice were treated daily with evobrutinib starting 3 days prior to the 0.25 % cuprizone diet for 5 weeks. **a, b**) Myelin was visualized by LFB-PAS staining and anti-PLP IHC; scale bar = 1000 µm. **c)** OPCs were visualized by anti-Olig2 IHC; scale bar = 100 µm. **d, e**) Microglia activation was visualized by anti-Iba1 IHC and astrocyte activation by anti-GFAP IHC; scale bar =100 µm. Data are shown as mean ± SEM; n=6-10.

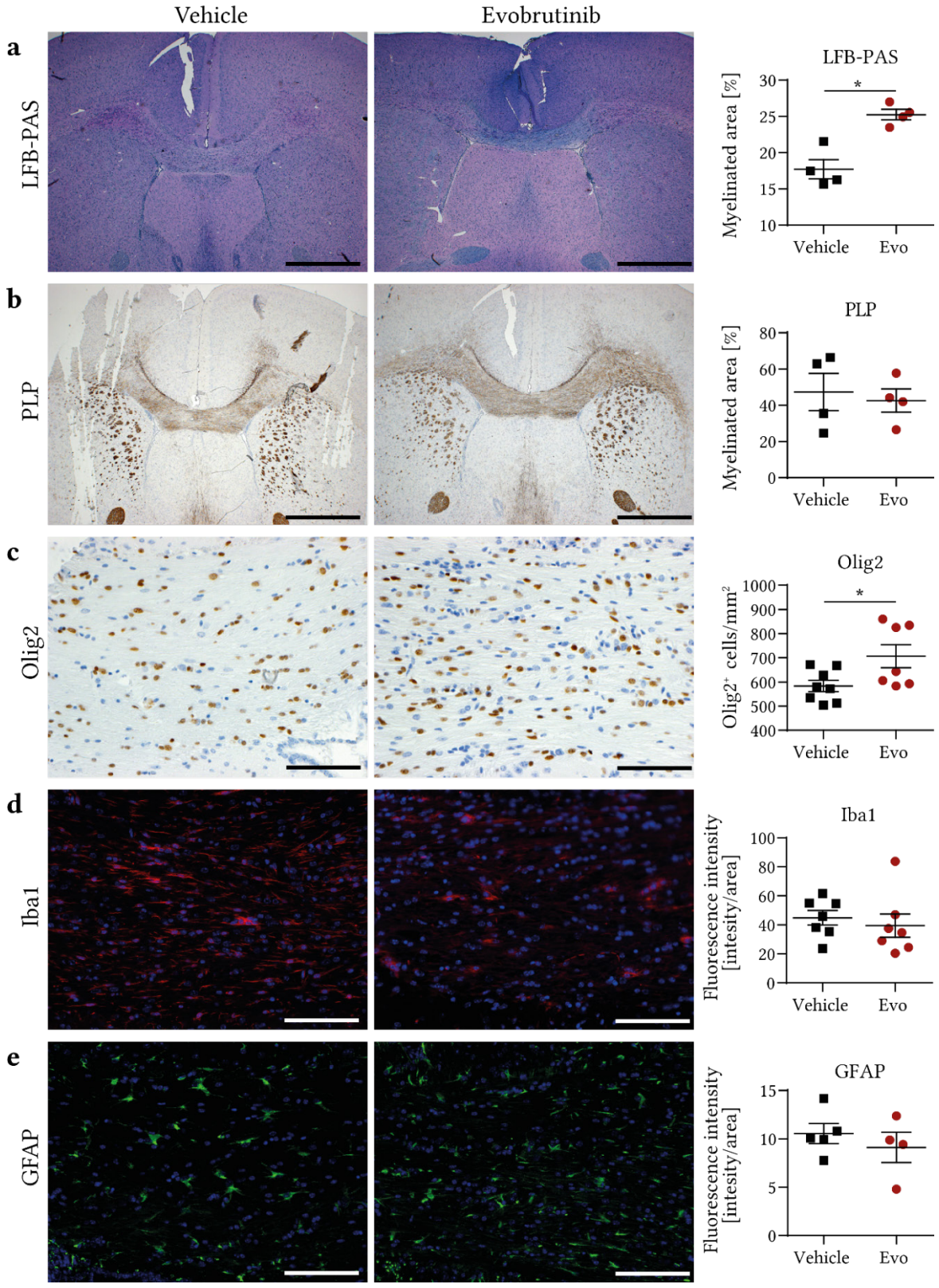

FIGURE 2.9: EVOBRUTINIB INCREASES OLIGODENDROCYTE RECRUITMENT AND ENHANCES REMYELINATION UPON CUPRIZONE WITHDRAWAL. C57BL/6 mice were treated daily with evobrutinib 3 days before starting the diet with 0.25 % cuprizone for 5 weeks followed by 3 days of normal diet. **a, b**) Myelin was visualized by LFB-PAS staining and anti-PLP IHC; scale bar = 1000 µm. **c)** OPCs were visualized by anti-Olig2 IHC; scale bar = 100 µm. **d, e**) Microglia activation was visualized by anti-Iba1 IHC and astrocyte activation by anti-GFAP IHC; scale bar =100 µm. Data are shown as mean ± SEM; n=4-6; unpaired t test *p<0.05.

3.2.4.2 EVOBRUTINIB DAMPENS PATHOGENIC T CELL-INDUCED MICROGLIA ACTIVITY

As the cuprizone model reflects only some aspects of MS, a second model, which allows to study CNS-intrinsic mechanisms while separating the induction phase of EAE, was used to analyze the effect of evobrutinib on microglial cells. In this model, pathogenic T cells were transferred into recipient mice, which were treated with evobrutinib or vehicle. The purification of the pathogenic T cells provided roughly 92 % $CD4^+$ and $CD8^+$ T cells and less than 2 % remaining B cells, which were afterwards transferred into the recipient mice treated with evobrutinib or vehicle (Fig. 2.10a). Treatment with evobrutinib led to a reduced clinical severity (Fig. 2.10b). While the cellular composition of the spleen did not change, evobrutinib treatment inhibited B cell maturation at the specific conversion from Fo II to Fo I B cells (Fig. 2.10c-e). Furthermore, the splenic cells showed no activation compared to naïve mice as well as evobrutinib showed no modulation compared to vehicle treated mice (Fig. 2.10f).

The transfer of pathogenic T cells to the recipient mice, led to an infiltration of T cells, B cells, macrophages and dendritic cells into the brain and spinal cord (Fig. 2.11a). Within the spinal cord, the number of microglia increased upon transfer of pathogenic T cells, which was downregulated by evobrutinib (Fig. 2.11b). The transferred T cells enhanced the expression of almost all investigated markers including marker for activation, antigen presentation and Fc receptor expression on microglial cells compared to naïve mice, both in the brain and in the spinal cord (Fig. 2.11c, d). Evobrutinib was able to reduce the upregulated expression of CD80, CD86, CD68, CD16 in the brain and CD86 and CD68 in the spinal cord (Fig. 2.11c, d).

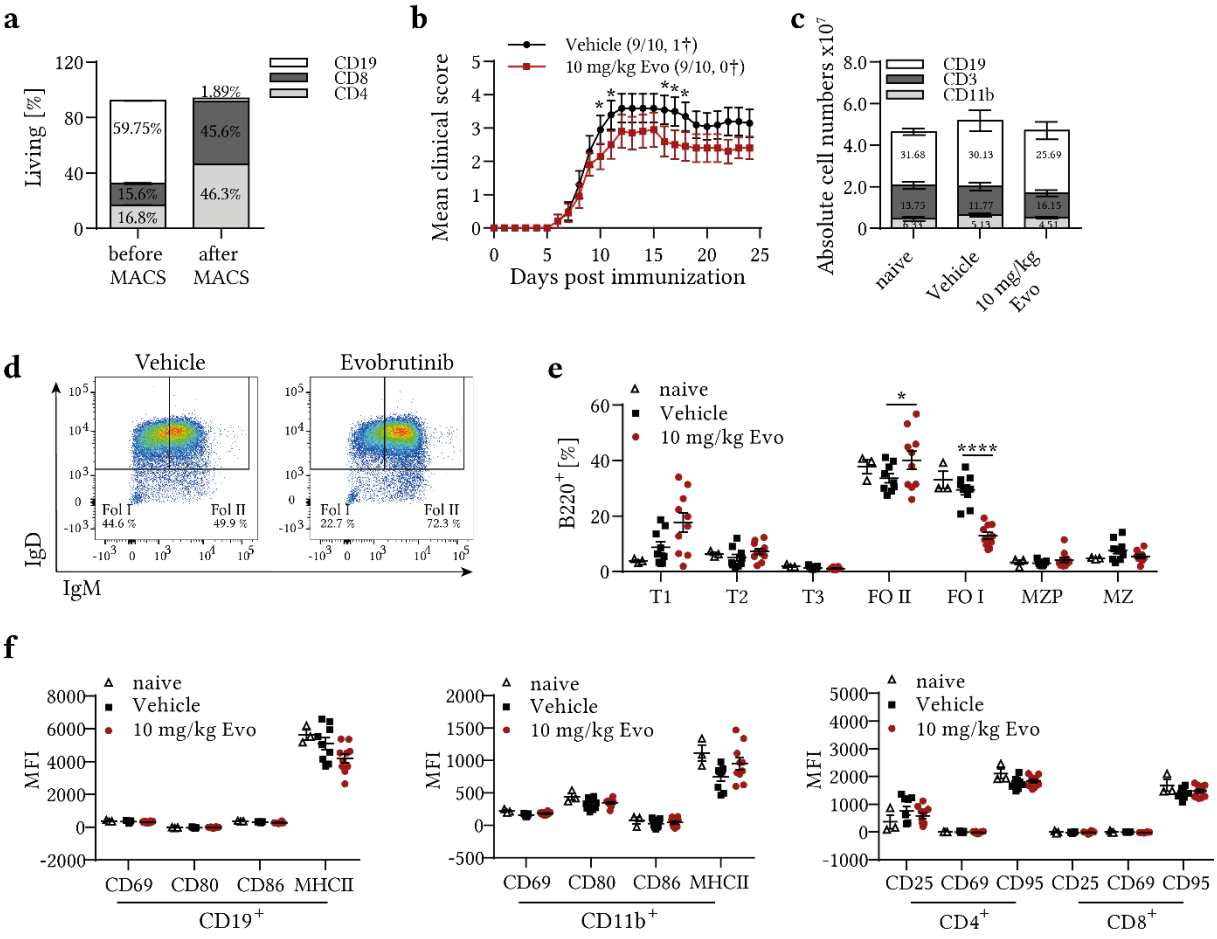

FIGURE 2.10: EVOBRUTINIB AMELIORATES EAE SEVERITY AND INHIBITS B CELL MATURATION IN A PASSIVE EAE MODEL. C57BL/6 mice were immunized with 200 µg MOG_{35-55} peptide. After 11-12 days, the inguinal lymph nodes were isolated and cultivated for 3 days at a density of 2-2.5x10^6 cells in the presence of 20 µg/ml anti-IFN-γ, rIL-12 and 25 µg/ml MOG_{35-55} peptide. Subsequently, T cells were purified by a magnetic-bead associated removal of B cells. Recipient mice, pre-treated for 3 days with evobrutinib or vehicle control, received 1.83x10^6 cells intraperitoneally. **a)** Mean cell composition ± SEM of pathogenic T cells before transfer **b)** Mean clinical score ± SEM. **c)** Absolute cell number ± SEM. **d)** Representative histograms. **e, f)** Mean fluorescence intensity ± SEM. n=3-10; Unpaired t test; *p<0.05, **p<0.01, ****p<0.0001.

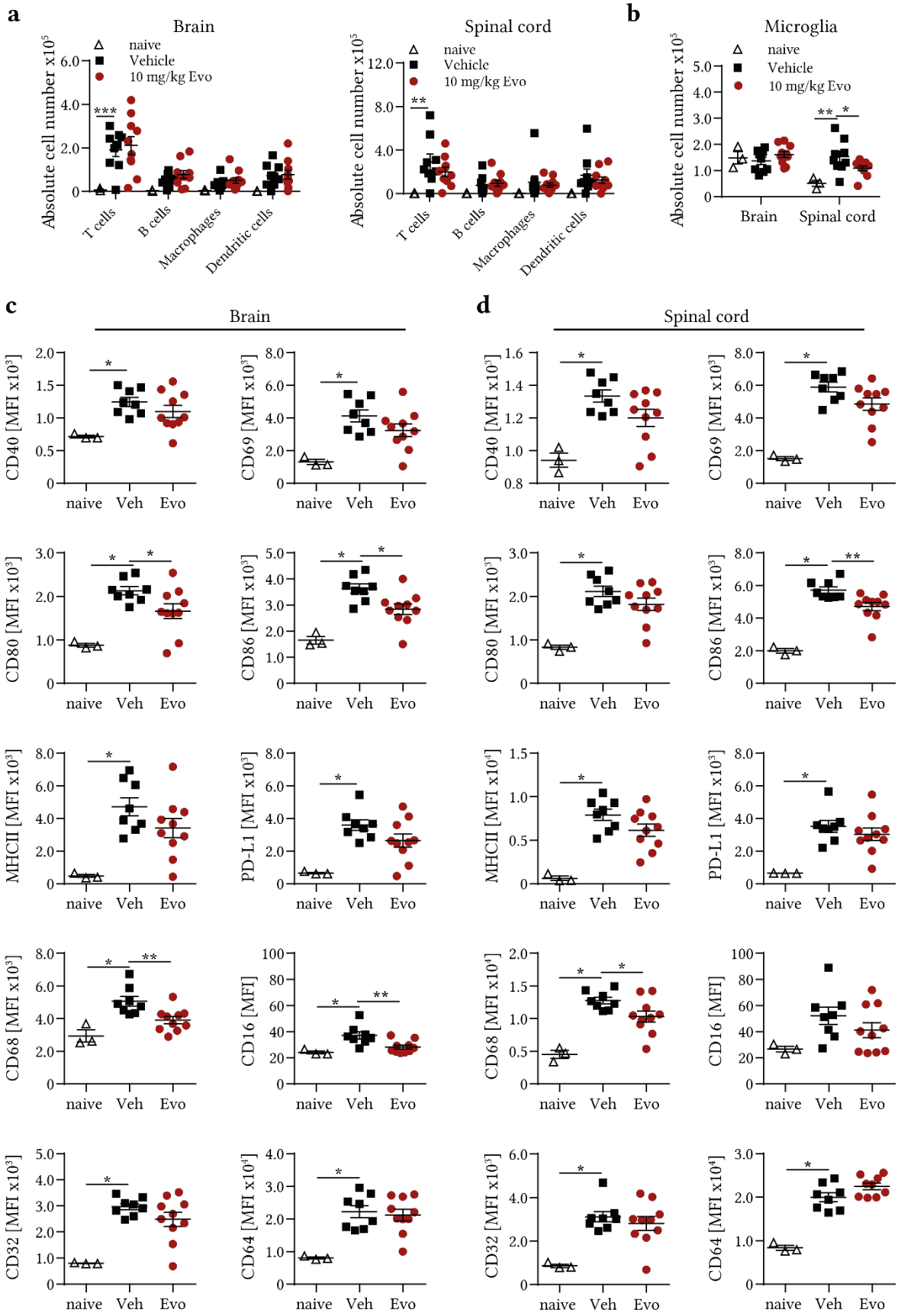
a
Brain
naive
Vehicle
10 mg/kg Evo
Absolute cell number x10^5
T cells
B cells
Macrophages
Dendritic cells
Spinal cord
b
Microglia
Brain
Spinal cord
c
Brain
d
Spinal cord
CD40 [MFI x10^3]
CD69 [MFI x10^3]
CD80 [MFI x10^3]
CD86 [MFI x10^3]
MHCII [MFI x10^3]
MHCII [MFI x10^4]
PD-L1 [MFI x10^3]
CD68 [MFI x10^3]
CD68 [MFI x10^4]
CD16 [MFI]
CD32 [MFI x10^3]
CD64 [MFI x10^4]
naive
Veh
Evo

FIGURE 2.11: ADOPTIVE TRANSFER OF PATHOGENIC T CELLS LEADS TO A STRONG MICROGLIA ACTIVATION, A PROCESS THAT CAN BE DAMPENED BY EVOBRUTINIB. C57BL/6 mice were immunized with 200 µg MOG_{35-55} peptide. After 11-12 days, the inguinal lymph nodes were isolated and cultivated for 3 days at a density of 2-2.5x10^6 cells in the presence of 20 µg/ml anti-IFN-γ, rIL-12 and 25 µg/ml MOG_{35-55} peptide. Subsequently, T cells were purified by a magnetic-bead associated removal of B cells. Recipient mice, pre-treated for 3 days with evobrutinib or vehicle control, received 1.83x10^6 cells intraperitoneally. On day 25 cells were isolated and analyzed by flow cytometry. **a, b)** Absolute cell numbers ± SEM; **c)** Microglia activation in the brain. **d)** Microglia activation in the spinal cord; mean fluorescence intensity ± SEM; n=3-10. Mann-Whitney U test *p<0.05 or Unpaired T test; *p<0.05, **p<0.01.

3.2.4.3 BTK INHIBITION IN CHRONIC DISEASE STAGE

After active immunization with MOG_{35-55} peptide, mice develop a chronic disease which reflects stable disease on a moderate level of neurological disability (Lassmann & Bradl, 2017). Thus, to investigate if BTK inhibition has an impact on microglial activation in a chronic disease stage, the chronic EAE model was used. Mice were treated with evobrutinib or vehicle after development of a stable disease on day 40 post immunization. Evobrutinib had no effect on the disease course (Fig. 2.12a). Moreover, the number of infiltrating cells and microglia did not change upon evobrutinib treatment and the activation of the analyzed B cells, T cells, macrophages and dendritic cells remained stable (Fig. 2.12b, c). Evobrutinib downregulated the expression of CD80 and CD86 in microglia isolated from the brain (Fig. 2.13a) as well as reduced the expression of CD80 and MHCII in microglia derived from the spinal cord (Fig. 2.13b).

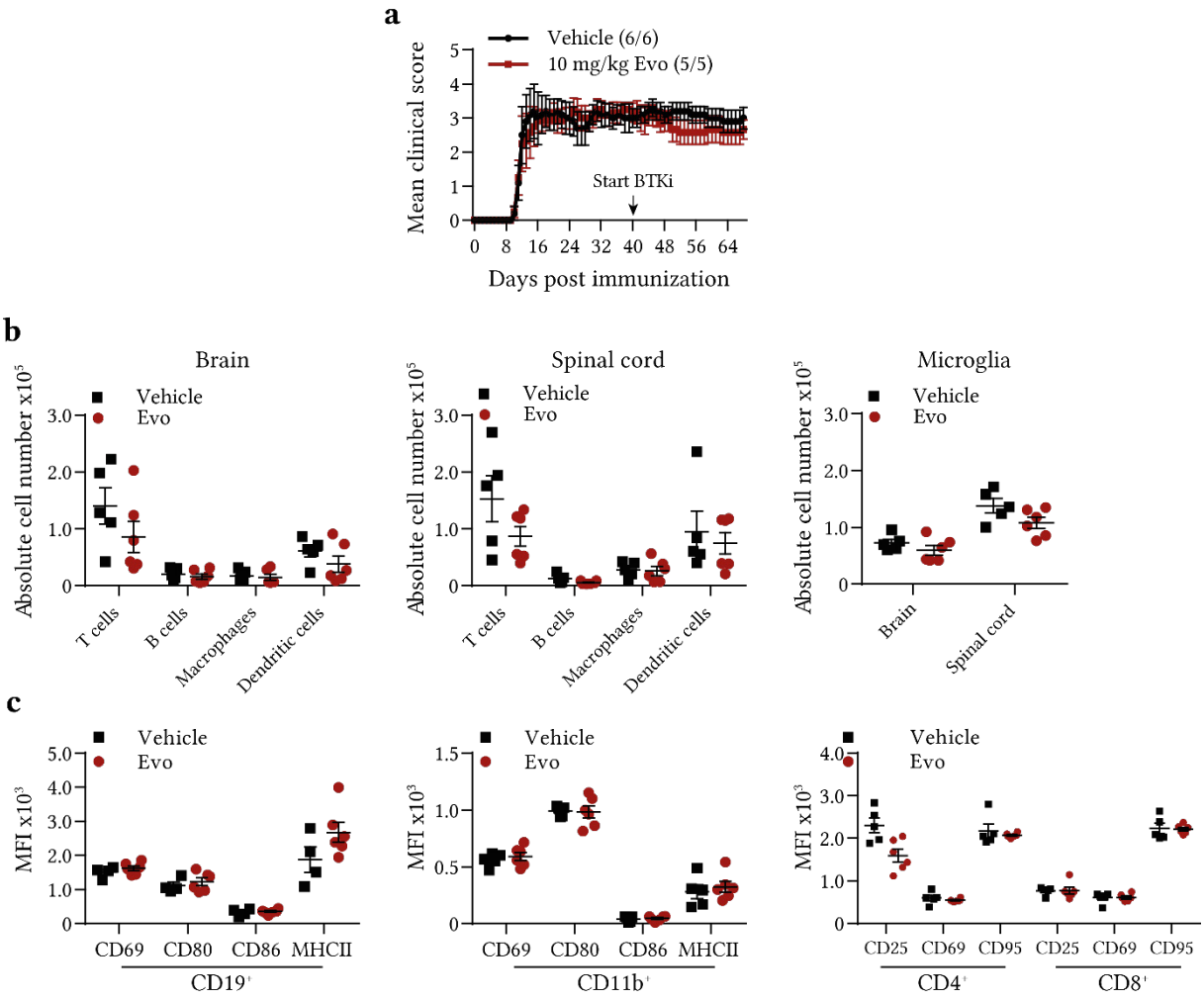

FIGURE 2.12: THERAPEUTIC TREATMENT OF EVOBRUTINIB HAD NO EFFECT ON PERIPHERAL IMMUNE CELLS IN A CHRONIC DISEASE MODEL. C57BL/6 mice were immunized with 75 µg MOG_{35-55} peptide. Mice were treated with evobrutinib or vehicle starting at day 40 post immunization. On day 70 cells were isolated and analyzed by flow cytometry. **a)** Mean clinical score ± SEM. **b)** Absolute cell number ± SEM. **c)** Mean fluorescence intensity ± SEM; n=5-6.

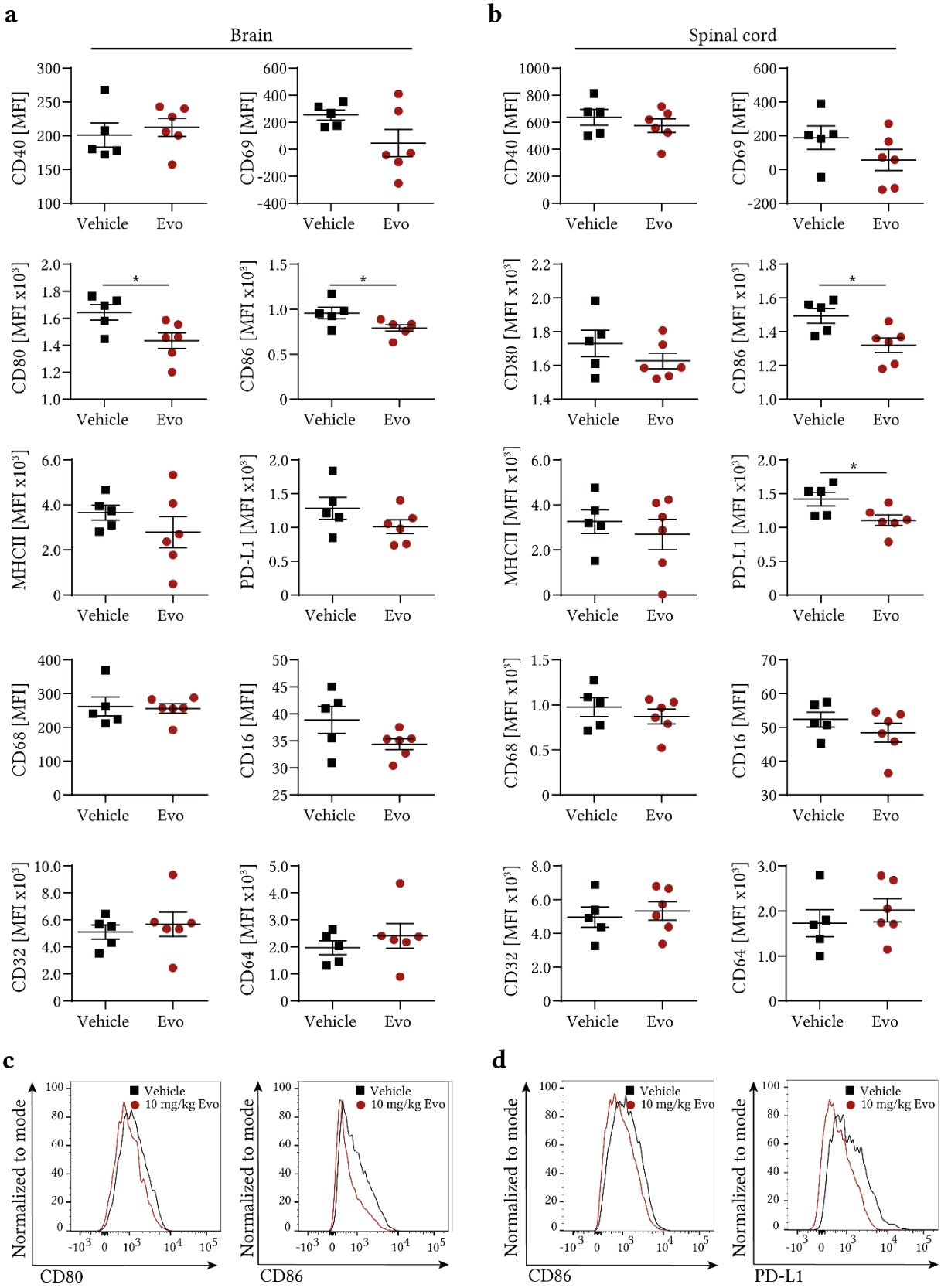

FIGURE 2.13: EVOBRUTINIB ALTER THE MICROGLIA PHENOTYPE IN CHRONIC EAE MODEST. C57BL/6 mice were immunized with 75 µg MOG_{35-55} peptide. Mice were treated with evobrutinib or vehicle starting at day 40 post immunization. On day 70 cells were isolated and analyzed by flow cytometry. **a)** Microglia activation in the brain. **b)** Microglia activation in the spinal cord; mean fluorescence intensity ± SEM; n=5-6. Mann-Whitney U test *p<0.05 or Unpaired T test; *p<0.05, **p<0.01. **c, d)** Representative histograms.

4 DISCUSSION

This thesis consists of two projects. The first part focuses on the interaction of CNS-resident cells and B cells in understanding the role of B cells in regulating CNS-established inflammation in MS. The second part aimed at analyzing the potential of BTK inhibition as a therapeutic strategy on CNS-resident cells, on slowing disease progression. The individual projects will be discussed separately in the following chapters.

4.1 PROJECT 1: THE ROLE OF REGULATORY B CELLS IN CONTAINMENT OF CHRONIC CNS INFLAMMATION

In the current view, chronic progression of MS is attributed to a self-sustained inflammatory circuit between CNS-established and CNS-resident cells, which may explain why peripherally acting MS drugs fail to prevent chronic progression in the absence of focal inflammation. The persistence of B cells in the CNS of MS patients highlighted that B cells may contribute to disease-relevant immune responses, not only by antibody production but also through antigen presentation and cytokine secretion. Thus, identifying cellular and molecular factors which may inhibit MS progression and promote CNS recovery is of essential importance.

The present study provides insights into cellular mechanisms of B cells in controlling chronic progression by dampening the activity of CNS-resident cells. Through a series of direct co-culture experiments, transwell experiments and the use of B cell-derived supernatant it was demonstrated that soluble products of both, toll-like receptor (TLR)-activated B cells and their supernatant induced pro-inflammatory properties of homeostatic microglia and astrocytes. By contrast, the pro-inflammatory cytokine production of LPS-induced M1-like microglia, known to be present in the inflamed brain of MS patients were reduced upon incubation with activated B cells or their supernatant. Interestingly, the ability of microglia to activate T cells and the microglial phagocytic capacity was reduced by B cell supernatant. The observation that these effects were mediated through B cell-secreted factors and do not require direct cell contact is notable since neuropathological studies have shown the presence of demyelination and axonal damage in the cortical and deep grey matter of MS patients, which are associated with activity of CNS-resident cells while lymphocytes are located in the meninges (Magliozzi et al., 2007). Therefore, it is likely that the activation of microglia and astrocytes is driven by soluble factors produced by B cells in the CNS of MS patients.

To identify which factor could modulate microglia and astrocyte activation, first the repertoire of molecules produced by TLR-activated B cells was investigated. As expected, IL-6

and IL-10 were produced in high amounts. IL-6 is a pro-inflammatory cytokine known to be produced by B cells and may play a major role in the resolution and propagation of MS (Ireland, Monson, & Davis, 2015). For example, peripheral B cells isolated from MS patients produce enhanced levels of IL-6 compared to healthy controls (Barr et al., 2012), supporting the concept that peripheral B cells in MS act as potent APCs for activation and differentiation of encephalitogenic T cells. Besides their pro-inflammatory function, B cells or B cell subsets have anti-inflammatory properties by producing substantial amounts of regulatory IL-10, which dampens the activity of myeloid APCs, such as monocytes and dendritic cells (Fillatreau et al., 2002). If these B cell-derived molecules are capable of diminishing CNS-intrinsic inflammation by their interaction with CNS-resident cells remains still unknown. Therefore, IL-6 and IL-10 were functionally neutralized in B cell-derived supernatants by specific antibodies in or the direct effects of rIL-6 and rIL-10 were analyzed separately. While treatment with rIL-6 and blocking of IL-6 showed no impact on microglia and astrocyte phenotype and function, rIL-10 reduced the pro-inflammatory cytokine secretion of microglia but not astrocytes and blocking of IL-10 led to an enhanced pro-inflammatory microglial phenotype. Consistent with these observed results, IL-10 has been shown to directly reduce the pro-inflammatory cytokine production of microglia (Ledeboer et al., 2002).

IL-10 is one of the most studied immunoregulatory molecules of the immune system. Its production in the brain has also been described, but the cellular source and regulatory molecular mechanisms are much less known than those in the periphery. Astrocytes are supposed to be a major source of IL-10 but CNS-established B cells may also display an important source of IL-10 in the inflamed MS brain. In particular, IL-10 production of B cells has been implicated in controlling the extent of immune reposes associated with CNS autoimmunity (M. E. Duddy, Alter, & Bar-Or, 2004; Fillatreau et al., 2002). The first study, demonstrated the anti-inflammatory role of IL-10 produced by B cell production in EAE (Fillatreau et al., 2002), while the second study investigated the distinct production of IL-10 dependent on the stimulation of human B cells. Interestingly, peripheral blood mononuclear (PBMC)-derived B cells isolated from RRMS and PPMS patients showed an impaired IL-10 secretion upon TLR and BCR activation (M. E. Duddy et al., 2004). The observation that these abnormalities were apparent upon stimulation suggests that the B cell pool at large is deregulated in individuals with MS. However, if CNS-established B cells display the same phenotype remains still unknown but remarkably, plasma cells were found to be one major source of IL-10 in the lesions of MS patients (Machado-Santos et al., 2018). Together with the present observation that blocking of IL-10 in the supernatant of B cells induced a pro-

inflammatory microglia phenotype, B cell and/or plasma cell derived IL-10 might be protective in MS by regulating microglial function.

Therefore, the functional outcome of B cell-derived IL-10 within the CNS was investigated on microglial cells. Besides their function as phagocytes, microglia also act as antigen presenting cells by activating T cells. As IL-6 did not change the microglial phenotype, it was not surprising that IL-6 had no impact on the phagocytic capacity of microglia or their capacity to activate T cells, while rIL-10 reduced the phagocytic capacity. Interestingly, blocking of IL-10 had no effects on the ability of microglia to phagocyte, probably due to the overall low level of phagocytosis upon treatment with B cell supernatant. Somewhat surprisingly, the ability to activate T cells was unchanged by IL-10 ablation, probably also due to the overall low proliferation rate. Moreover, the viability of these T cells was reduced. In comparison, the treatment with B cell supernatant led to a reduced T cell proliferation while T cell viability remained unchanged. However, the direct stimulation of microglia with rIL-10, reduced T cell proliferation but did not altered the viability of these cells. Importantly, neutralization of IL-10 did not only block IL-10 secretion by B cells, but also blocked IL-10 production by microglia. A study showed that the level of IL-10 production was enhanced upon co-culture of microglia and T cells, probably dependent on cell-cell contact (Chabot, Williams, Hamilton, Sutherland, & Yong, 1999). Lacking IL-10 in microglia may induce a microglial phenotype which affects T cell survival and leads to enhanced inflammation during MS progression. However, microglia and T cells can interact through various other pathways, for example CD40 or PD-L1, therefore it would be interesting to investigate the T cell phenotype in the context of activation, differentiation or regulatory T cell properties.

In vivo data from our lab showed the pro-inflammatory activity of microglia and astrocytes isolated from the CNS of mice depleted of naïve B cells upon immunization with MOG^{35-55} peptide (Häusler et al., unpublished Data). Depletion of B cells was associated with increased clinical severity, spinal cord infiltration, white matter demyelination as well as enhanced microglia activation and upregulation of pro-inflammatory gene products in astrocytes. Moreover in vivo adoptively transferred B cells deficient for IL-6 or IL-10 into B cell depleted recipient mice, showed that IL-6-deficient B cells had no impact on EAE severity or microglial activity, while IL-10-deficient B cells worsened clinical severity and increased the number of CNS-infiltrating immune cells. Exacerbation was associated with an enhanced expression of molecules involved in antigen presentation on microglia cells (Häusler et al., unpublished Data). However, in vitro neither IL-6 nor IL-10 directly or derived by B cells changed the astrocyte phenotype. Plasma and regulatory B cells have shown to secrete other anti-

inflammatory cytokines like IL-35 or TGF-β (Bjarnadottir et al., 2016; Shen et al., 2014). Both cytokines are essential for the resolution of CNS autoimmunity, as mice deficient for IL-35 fail to recover from EAE, even chronically deteriorate and B cell-derived TGF-β limits EAE severity (Bjarnadottir et al., 2016; Shen et al., 2014). However, treatment of microglia or astrocytes with rTGF-β showed no effect as well as TGF-β was not produced by TLR-activated B cells. Therefore, investigating the potential of other cytokines, such as B cell-derived IL-35 would be of interest. Nevertheless, the data provided in this study point towards an interaction of B cells and astrocytes. Since it has already been shown that astrocytes in the MS brain secrete high amounts of BAFF, which is known as a survival factor for B cells and B cell subsets (Touil et al., 2018), a bi-directional interaction of B cells and astrocytes is likely. Supporting the concept that glial cells in an inflammatory environment may contribute to a local B cell and plasma cell fostering environment, promoting a regulatory role of B cells in the MS-affected CNS.

Taken together the current study points toward a regulatory function of B cells through the production of IL-10 in limiting CNS inflammation by modulating the pro-inflammatory phenotype of microglia which may be potential in promoting CNS recovery.

4.2 PROJECT 2: THE THERAPEUTIC POTENTIAL OF BTK INHIBITION IN CHRONIC CNS AUTOIMMUNITY

The therapeutic control of disease progression in MS patients remains a major challenge. Until now, only two drugs, ocrelizumab and siponimod, are approved for the treatment of progressive MS ("European Medicines Agency Press Release. New medicine for multiple sclerosis," 2017; "U.S. Food and Drug Administration News Release. FDA approves new drug to treat multiple sclerosis. First drug approved for Primary Progressive MS," 2018). While both drugs mainly act on the focal inflammatory component of the disease, which is not absent during progression, their potential in limiting disease progression by itself remains questionable. Several mechanisms have been proposed to drive disease progression (Rommer et al., 2019). In this regard, microglia activation and microglia-driven neuroinflammation are considered key events in the onset, progression and resolution of MS. Inhibition of BTK may represent a promising treatment strategy to target disease progression, not only by inhibiting pathogenic B cell subsets, but also by targeting chronically activated microglia.

In the present study the potential of BTK inhibition by the novel drug evobrutinib as a therapeutic strategy to target disease progression was evaluated. This study revealed that the

majority of CNS-resident cells expressing BTK are microglial cells and that the level of BTK increases upon inflammation in the EAE animal model. However, another study investigated the expression of BTK in cerebellar organotypic slices and showed that astrocytes express BTK on a low level (Martin et al., 2020). This observation is in apparent contradiction with the finding of the present study, probably due to the use of different models and detection method of BTK expression. Of note, the expression of BTK in astrocytes was only investigated in primary cultures, therefore analyzing the BTK expression of adult astrocytes ex vivo would be interesting. However, treatment of evobrutinib on primary astrocytes had no effect, suggesting that microglia are the main target for BTK inhibition.

The LPS- and cytokine-induced activation of microglia in vitro seemed relatively unaffected by evobrutinib. Interestingly only the expression of the marker PD-L1 was decreased independent of the stimulation. The PD-1/PD-L1 axis has been shown to play a crucial role in maintaining immune homeostasis, which is best characterized in T cells. PD-1 blocks the activation of cytotoxic effector T cells during acute inflammation, while ligation of PD-1 on regulatory T cells fosters their expansion and stability (Francisco et al., 2009). Furthermore, an impairment of PD-1 inhibitory signalling on T cells as a result of a PD-1 polymorphism is associated with progression of MS (Kroner et al., 2005). However, samples of progressive MS patients revealed that CNS-established T cells do not express PD-1 (Bell, Lenhart, Rosenwald, Monoranu, & Berberich-Siebelt, 2019). Therefore, the mode of action of the PD-1/PD-L1 axis within the CNS in progressive MS is probably independent of T cells. B cells, macrophages, dendritic cells, microglia and neurons also express PD-1 (Zhao, Roberts, Wang, Savage, & Ji, 2021). PBMC-derived B cells have shown to upregulate PD-1 expression while the ligation of its ligands reduced their proliferation and cytokine production (Thibult et al., 2013). Whether CNS-established B cells in progressive MS express PD-1 and if the ligation of microglial PD-L1 has an inhibitory or regulatory effect on B cells is uncertain. Interestingly, B- and T cells themselves express PD-L1, which is further upregulated upon activation. Similarly, microglia also upregulate PD-1 upon infection induced inflammation (Zhao et al., 2021). It might be possible that microglia interact with themselves through the PD-1/PD-L1 pathway. In inflammatory models, the PD-1/PD-L1 pathway attenuates inflammatory responses and promotes neuronal repair through induction of the M2 phenotype (Yao et al., 2014). However, more studies are needed to understand the reduced PD-L1 expression upon evobrutinib treatment in microglia. Of note, in the cuprizone model and the passive EAE model, which both only display some aspects of MS, PD-L1 expression remained unchanged by evobrutinib.

Progression of MS is supposed to be triggered by an CNS-compartmentalized inflammation, whereby microglia exhibit a chronically activated M1 phenotype, characterized by the secretion of pro-inflammatory cytokines and upregulation of iNOS (Gordon & Taylor, 2005). One approach in halting disease progression is the induction of the neuroprotective M2 microglia which secrete anti-inflammatory cytokines and Arg1 (Gordon & Taylor, 2005). In the present study, evobrutinib treatment reduced the M1 polarization of microglia, as assessed by iNOS expression, while evobrutinib had no impact on the M2 polarization. Consistent with these data, a study using human macrophages showed that BTK inhibition with evobrutinib hindered the M1 macrophage differentiation and triggered the M2 polarization (Y-B Alankus, R Grenningloh, P Haselmayer, A Bender, & Bruttger, 2019).

One important function of microglia is the phagocytosis of myelin debris. Most interestingly, evobrutinib induced the phagocytosis capacity independent of the microglial polarization in vitro. Furthermore, the recruitment of $Olig2^+$ oligodendrocytes as well as the remyelination, as measured by LFB-PAS staining, were enhanced in the cuprizone model after treatment with evobrutinib and upon cuprizone withdrawal. These data points toward a more neuroprotective microglial phenotype, especially a more phagocyting microglia, which might mediate the recruitment of OPCs and thereby induce remyelination upon BTK inhibition. Since one mechanism leading to progression is the unbalance between damage and repair, more neuroprotective microglia, inducing repair would be desirable. Along the same line, a human study using macrophages showed increased phagocytosis by M2 macrophages upon evobrutinib treatment (Y-B Alankus et al., 2019). Furthermore, another study reported the potential of evobrutinib favoring remyelination in ex vivo mouse cerebellar slices and in vivo in transgenic Xenopus laevis, two models of demyelination independent on the adaptive immunity (Martin et al., 2020). The same study investigated the BTK expression of oligodendrocytes, which was lower than 1 %. Therefore, the increased remyelination is probably based on the enhanced phagocytosis and reduced pro-inflammatory microglial phenotype initiated by BTK inhibition.

Since the compartmentalized inflammation during progressive MS is triggered by the interaction of CNS-established hematopoietic cells and activated resident cells, the passive EAE and a chronic EAE model were used to investigate the potential of evobrutinib in modulation of CNS-intrinsic inflammation. In the passive EAE model, the BBB is relatively closed and pathogenic T cells need to be reactivated by CNS-resident APCs, such as microglia, leading to a strong microglial activation, which could be partly dampened by BTK inhibition.

However, only mild differences were observed in microglia activation in the therapeutic treatment of evobrutinib during the chronic course of EAE.

Of note, in the cuprizone model, the passive EAE model and the therapeutic treatment of active EAE, B cell differentiation was blocked from transitioning from Fo II to the Fo I state by evobrutinib. This differentiation is known to be a BTK-dependent step in the B cell maturation and was already shown to be inhibited by evobrutinib in a B cell-dependent EAE model (Torke et al., 2020). Interestingly, the animal models used in this study are models which show CNS-intrinsic mechanisms of MS, while sparing the peripheral immune system. Therefore, it was not surprising that neither of the analyzed cells of the adaptive immune system showed an upregulation of the analyzed markers compared to naïve mice, and yet evobrutinib was able to reduce the differentiation of B cells. These data demonstrate the efficiency of evobrutinib not only by blocking the differentiation of activated but also of naïve B cells. Already blocking the differentiation of naïve B cells may also play an important role in halting disease progression.

Taken together, the present study highlights the therapeutic potential of evobrutinib in progression of MS. Since there are several BTK inhibitors developed with variations in their mechanism of action, binding mode and potential to cross the BBB, it remains to be investigated which BTK inhibitor is most efficient in modulating microglia and therefore halting disease progression. Evobrutinib has already met its primary endpoint in the treatment of RRMS, defined as total number of T1 gadolinium-enhancing lesions in a phase II clinical trial, while it showed no effect on progression of disability (Montalban et al., 2019). In contrast the noncovalent BTK inhibitor fenebrutinib is currently in a phase III trial in PPMS (Gheen et al., 2020). The ideal BTK inhibitor would be rapidly reversible, BBB-penetrant as well as highly selective and therefore could potentially reduce disease activity and slow disease progression.

5 OUTLOOK

5.1 PROJECT 1: THE ROLE OF REGULATORY B CELLS IN CONTAINMENT OF CHRONIC CNS INFLAMMATION

In the first project of this thesis it has been revealed that B cells are capable of modulating the activity of CNS-resident cells in an anti-inflammatory manner. In particular, diminishing the inflammatory response of microglia in vitro. Unpublished data from our lab revealed similar

results in vivo in a murine model of MS. These findings can have important implications, as they show that the B cell pool within the CNS is not by definition associated with pathogenic functions. B cells can also be immunoregulatory and potentially relevant for controlling CNS-intrinsic inflammation associated with disease progression.

Since in the present study, TGF-β and IL-10 was investigated and it is known that B cells produce other anti-inflammatory molecules like IL-35, it would be interesting to investigate the potential of other cytokines on microglia and astrocyte function, especially since B cell-derived IL-10 seemed to have no impact on astrocyte activity.

To further confirm the results of this study, it would be interesting to analyze the phenotype of B cell subsets within the CNS. Finally, by using VLA-4 deficient B cells, which cannot enter the CNS it would be possible to clarify whether B cells have to enter the CNS to induce clinical recovery.

Since mouse models are limited due to significant differences to humans, another approach investigating the ability of B cells in halting disease progression might be the use of induced pluripotent stem cell (iPSC)-derived microglia and/or astrocytes in the presence of PBMC-derived B cells. Furthermore, in this setup, both iPSC-derived microglia and astrocytes as well as B cells could be isolated from MS patients.

5.2 PROJECT 2: THE THERAPEUTIC POTENTIAL OF BTK INHIBITION IN CHRONIC CNS AUTOIMMUNITY

The second part of the study provides evidence that BTK inhibition has the potential to limit innate immune activation in the CNS, which is proposed to be a key driver of MS progression.

Evobrutinib showed an induction of remyelination by enhancing the OPC number in the early remyelinating cuprizone model. It would therefore be interesting to analyze the effect of evobrutinib at a later stage of remyelination, for example on day 7 post cuprizone withdrawal. Since, in vitro microglia revealed a more neuroprotective phenotype and downregulation of PD-L1, investigating the PD-1/PD-L1 axis within the CNS may be interesting to understand the biological relevance of PD-L1 inhibition by BTK.

Further research is required to investigate to which extent evobrutinib reaches the CNS, specifically in models when the BBB is relatively closed, which is the case for progressive MS. Since there are several other BTK inhibitors developed with different properties, it is crucial to clarify which BTK inhibitor would be most efficient in silencing disease progression. A

study directly comparing the most promising candidates in vitro and in vivo would be most outstanding in resolving the question how BTK inhibition is most efficient in halting disease progression.

6 REFERENCE

Aguzzi, A., Barres, B. A., & Bennett, M. L. (2013). Microglia: scapegoat, saboteur, or something else? *Science, 339*(6116), 156-161. doi:10.1126/science.1227901

Aharoni, R., Eilam, R., & Arnon, R. (2021). Astrocytes in Multiple Sclerosis-Essential Constituents with Diverse Multifaceted Functions. *Int J Mol Sci, 22*(11). doi:10.3390/ijms22115904

Barr, T. A., Shen, P., Brown, S., Lampropoulou, V., Roch, T., Lawrie, S., . . . Gray, D. (2012). B cell depletion therapy ameliorates autoimmune disease through ablation of IL-6-producing B cells. *J Exp Med, 209*(5), 1001-1010. doi:10.1084/jem.20111675

Bell, L., Lenhart, A., Rosenwald, A., Monoranu, C. M., & Berberich-Siebelt, F. (2019). Lymphoid Aggregates in the CNS of Progressive Multiple Sclerosis Patients Lack Regulatory T Cells. *Front Immunol, 10*, 3090. doi:10.3389/fimmu.2019.03090

Bettelli, E., Pagany, M., Weiner, H. L., Linington, C., Sobel, R. A., & Kuchroo, V. K. (2003). Myelin oligodendrocyte glycoprotein-specific T cell receptor transgenic mice develop spontaneous autoimmune optic neuritis. *J Exp Med, 197*(9), 1073-1081. doi:10.1084/jem.20021603

Bjarnadottir, K., Benkhoucha, M., Merkler, D., Weber, M. S., Payne, N. L., Bernard, C. C. A., . . . Lalive, P. H. (2016). B cell-derived transforming growth factor-beta1 expression limits the induction phase of autoimmune neuroinflammation. *Sci Rep, 6*, 34594. doi:10.1038/srep34594

Bottcher, C., van der Poel, M., Fernandez-Zapata, C., Schlickeiser, S., Leman, J. K. H., Hsiao, C. C., . . . Priller, J. (2020). Single-cell mass cytometry reveals complex myeloid cell composition in active lesions of progressive multiple sclerosis. *Acta Neuropathol Commun, 8*(1), 136. doi:10.1186/s40478-020-01010-8

Boyd, A., Zhang, H., & Williams, A. (2013). Insufficient OPC migration into demyelinated lesions is a cause of poor remyelination in MS and mouse models. *Acta Neuropathol, 125*(6), 841-859. doi:10.1007/s00401-013-1112-y

Brosnan, C. F., & Raine, C. S. (2013). The astrocyte in multiple sclerosis revisited. *Glia, 61*(4), 453-465. doi:10.1002/glia.22443

Bruck, W. (2005). The pathology of multiple sclerosis is the result of focal inflammatory demyelination with axonal damage. *J Neurol, 252 Suppl 5*, v3-9. doi:10.1007/s00415-005-5002-7

Brullo, C., Villa, C., Tasso, B., Russo, E., & Spallarossa, A. (2021). Btk Inhibitors: A Medicinal Chemistry and Drug Delivery Perspective. *Int J Mol Sci, 22*(14). doi:10.3390/ijms22147641

Caldwell, R. D., Qiu, H., Askew, B. C., Bender, A. T., Brugger, N., Camps, M., . . . Liu-Bujalski, L. (2019). Discovery of Evobrutinib: An Oral, Potent, and Highly Selective, Covalent Bruton's Tyrosine Kinase (BTK) Inhibitor for the Treatment of Immunological Diseases. *J Med Chem, 62*(17), 7643-7655. doi:10.1021/acs.jmedchem.9b00794

Campbell, G. R., Ziabreva, I., Reeve, A. K., Krishnan, K. J., Reynolds, R., Howell, O., . . . Mahad, D. J. (2011). Mitochondrial DNA deletions and neurodegeneration in multiple sclerosis. *Ann Neurol, 69*(3), 481-492. doi:10.1002/ana.22109

Carnero Contentti, E., & Correale, J. (2020). Bruton's tyrosine kinase inhibitors: a promising emerging treatment option for multiple sclerosis. *Expert Opin Emerg Drugs, 25*(4), 377-381. doi:10.1080/14728214.2020.1822817

Chabot, S., Williams, G., Hamilton, M., Sutherland, G., & Yong, V. W. (1999). Mechanisms of IL-10 production in human microglia-T cell interaction. *J Immunol, 162*(11), 6819-6828. Retrieved from https://www.ncbi.nlm.nih.gov/pubmed/10352303

Chhor, V., Le Charpentier, T., Lebon, S., Ore, M. V., Celador, I. L., Josserand, J., . . . Fleiss, B. (2013). Characterization of phenotype markers and neuronotoxic potential of

polarised primary microglia in vitro. *Brain Behav Immun, 32*, 70-85. doi:10.1016/j.bbi.2013.02.005
Chung, W. S., Allen, N. J., & Eroglu, C. (2015). Astrocytes Control Synapse Formation, Function, and Elimination. *Cold Spring Harb Perspect Biol, 7*(9), a020370. doi:10.1101/cshperspect.a020370
Clarke, L. E., & Barres, B. A. (2013). Emerging roles of astrocytes in neural circuit development. *Nat Rev Neurosci, 14*(5), 311-321. doi:10.1038/nrn3484
Colton, C. A., & Gilbert, D. L. (1987). Production of superoxide anions by a CNS macrophage, the microglia. *FEBS Lett, 223*(2), 284-288. doi:10.1016/0014-5793(87)80305-8
De Groot, C. J., Bergers, E., Kamphorst, W., Ravid, R., Polman, C. H., Barkhof, F., & van der Valk, P. (2001). Post-mortem MRI-guided sampling of multiple sclerosis brain lesions: increased yield of active demyelinating and (p)reactive lesions. *Brain, 124*(Pt 8), 1635-1645. doi:10.1093/brain/124.8.1635
Deeks, E. D. (2017). Ibrutinib: A Review in Chronic Lymphocytic Leukaemia. *Drugs, 77*(2), 225-236. doi:10.1007/s40265-017-0695-3
Dendrou, C. A., Fugger, L., & Friese, M. A. (2015). Immunopathology of multiple sclerosis. *Nat Rev Immunol, 15*(9), 545-558. doi:10.1038/nri3871
Ding, A. H., Nathan, C. F., & Stuehr, D. J. (1988). Release of reactive nitrogen intermediates and reactive oxygen intermediates from mouse peritoneal macrophages. Comparison of activating cytokines and evidence for independent production. *J Immunol, 141*(7), 2407-2412. Retrieved from https://www.ncbi.nlm.nih.gov/pubmed/3139757
Duddy, M., Niino, M., Adatia, F., Hebert, S., Freedman, M., Atkins, H., . . . Bar-Or, A. (2007). Distinct effector cytokine profiles of memory and naive human B cell subsets and implication in multiple sclerosis. *J Immunol, 178*(10), 6092-6099. doi:10.4049/jimmunol.178.10.6092
Duddy, M. E., Alter, A., & Bar-Or, A. (2004). Distinct profiles of human B cell effector cytokines: a role in immune regulation? *J Immunol, 172*(6), 3422-3427. doi:10.4049/jimmunol.172.6.3422
European Medicines Agency Press Release. New medicine for multiple sclerosis. (2017). *https://www.ema.europa.eu/en/news/new-medicine-multiple-sclerosis*.
Faissner, S., Plemel, J. R., Gold, R., & Yong, V. W. (2019). Progressive multiple sclerosis: from pathophysiology to therapeutic strategies. *Nat Rev Drug Discov, 18*(12), 905-922. doi:10.1038/s41573-019-0035-2
Fillatreau, S., Sweenie, C. H., McGeachy, M. J., Gray, D., & Anderton, S. M. (2002). B cells regulate autoimmunity by provision of IL-10. *Nat Immunol, 3*(10), 944-950. doi:10.1038/ni833
Francisco, L. M., Salinas, V. H., Brown, K. E., Vanguri, V. K., Freeman, G. J., Kuchroo, V. K., & Sharpe, A. H. (2009). PD-L1 regulates the development, maintenance, and function of induced regulatory T cells. *J Exp Med, 206*(13), 3015-3029. doi:10.1084/jem.20090847
Franklin, R. J., & Goldman, S. A. (2015). Glia Disease and Repair-Remyelination. *Cold Spring Harb Perspect Biol, 7*(7), a020594. doi:10.1101/cshperspect.a020594
Frischer, J. M., Bramow, S., Dal-Bianco, A., Lucchinetti, C. F., Rauschka, H., Schmidbauer, M., . . . Lassmann, H. (2009). The relation between inflammation and neurodegeneration in multiple sclerosis brains. *Brain, 132*(Pt 5), 1175-1189. doi:10.1093/brain/awp070
Fulmer, C. G., VonDran, M. W., Stillman, A. A., Huang, Y., Hempstead, B. L., & Dreyfus, C. F. (2014). Astrocyte-derived BDNF supports myelin protein synthesis after cuprizone-induced demyelination. *J Neurosci, 34*(24), 8186-8196. doi:10.1523/JNEUROSCI.4267-13.2014
Gardner, C., Magliozzi, R., Durrenberger, P. F., Howell, O. W., Rundle, J., & Reynolds, R. (2013). Cortical grey matter demyelination can be induced by elevated pro-inflammatory

cytokines in the subarachnoid space of MOG-immunized rats. *Brain, 136*(Pt 12), 3596-3608. doi:10.1093/brain/awt279

Gheen, M., Hauser, S., Bar-Or, A., Francis, G., Giovannoni, G., Kappos, L., . . . Goodyear, A. (2020). Examination of fenebrutinib, a highly selective BTKi, on disease progression of multiple sclerosis. P0211. *MSVirtual2020*.

Giannetti, P., Politis, M., Su, P., Turkheimer, F., Malik, O., Keihaninejad, S., . . . Piccini, P. (2014). Microglia activation in multiple sclerosis black holes predicts outcome in progressive patients: an in vivo [(11)C](R)-PK11195-PET pilot study. *Neurobiol Dis, 65*, 203-210. doi:10.1016/j.nbd.2014.01.018

Gilmore, C. P., Donaldson, I., Bo, L., Owens, T., Lowe, J., & Evangelou, N. (2009). Regional variations in the extent and pattern of grey matter demyelination in multiple sclerosis: a comparison between the cerebral cortex, cerebellar cortex, deep grey matter nuclei and the spinal cord. *J Neurol Neurosurg Psychiatry, 80*(2), 182-187. doi:10.1136/jnnp.2008.148767

Ginhoux, F., Lim, S., Hoeffel, G., Low, D., & Huber, T. (2013). Origin and differentiation of microglia. *Front Cell Neurosci, 7*, 45. doi:10.3389/fncel.2013.00045

Glendenning, L., Gruber, R., Dufault, M., Chretien, N., Proto, J., Zhang, M., . . . Ofengeim, D. (2020). Decoding Bruton's tyrosine kinase signalling in neuroinflammation. *MSVirtual2020*.

Goddard, D. R., Berry, M., & Butt, A. M. (1999). In vivo actions of fibroblast growth factor-2 and insulin-like growth factor-I on oligodendrocyte development and myelination in the central nervous system. *J Neurosci Res, 57*(1), 74-85. doi:10.1002/(SICI)1097-4547(19990701)57:1<74::AID-JNR8>3.0.CO;2-O

Gordon, S., & Taylor, P. R. (2005). Monocyte and macrophage heterogeneity. *Nat Rev Immunol, 5*(12), 953-964. doi:10.1038/nri1733

Goverman, J. (2009). Autoimmune T cell responses in the central nervous system. *Nat Rev Immunol, 9*(6), 393-407. doi:10.1038/nri2550

Green, A. J., McQuaid, S., Hauser, S. L., Allen, I. V., & Lyness, R. (2010). Ocular pathology in multiple sclerosis: retinal atrophy and inflammation irrespective of disease duration. *Brain, 133*(Pt 6), 1591-1601. doi:10.1093/brain/awq080

Hametner, S., Wimmer, I., Haider, L., Pfeifenbring, S., Bruck, W., & Lassmann, H. (2013). Iron and neurodegeneration in the multiple sclerosis brain. *Ann Neurol, 74*(6), 848-861. doi:10.1002/ana.23974

Hauser, S. L., Waubant, E., Arnold, D. L., Vollmer, T., Antel, J., Fox, R. J., . . . Group, H. T. (2008). B-cell depletion with rituximab in relapsing-remitting multiple sclerosis. *N Engl J Med, 358*(7), 676-688. doi:10.1056/NEJMoa0706383

Hendriks, R. W., Yuvaraj, S., & Kil, L. P. (2014). Targeting Bruton's tyrosine kinase in B cell malignancies. *Nat Rev Cancer, 14*(4), 219-232. doi:10.1038/nrc3702

Hochmeister, S., Grundtner, R., Bauer, J., Engelhardt, B., Lyck, R., Gordon, G., . . . Lassmann, H. (2006). Dysferlin is a new marker for leaky brain blood vessels in multiple sclerosis. *J Neuropathol Exp Neurol, 65*(9), 855-865. doi:10.1097/01.jnen.0000235119.52311.16

Howell, O. W., Reeves, C. A., Nicholas, R., Carassiti, D., Radotra, B., Gentleman, S. M., . . . Reynolds, R. (2011). Meningeal inflammation is widespread and linked to cortical pathology in multiple sclerosis. *Brain, 134*(Pt 9), 2755-2771. doi:10.1093/brain/awr182

Humphries, L. A., Dangelmaier, C., Sommer, K., Kipp, K., Kato, R. M., Griffith, N., . . . Rawlings, D. J. (2004). Tec kinases mediate sustained calcium influx via site-specific tyrosine phosphorylation of the phospholipase Cgamma Src homology 2-Src homology 3 linker. *J Biol Chem, 279*(36), 37651-37661. doi:10.1074/jbc.M311985200

Ireland, S. J., Monson, N. L., & Davis, L. S. (2015). Seeking balance: Potentiation and inhibition of multiple sclerosis autoimmune responses by IL-6 and IL-10. *Cytokine, 73*(2), 236-244. doi:10.1016/j.cyto.2015.01.009

Karamita, M., Barnum, C., Mobius, W., Tansey, M. G., Szymkowski, D. E., Lassmann, H., & Probert, L. (2017). Therapeutic inhibition of soluble brain TNF promotes remyelination by increasing myelin phagocytosis by microglia. *JCI Insight, 2*(8). doi:10.1172/jci.insight.87455

Keaney, J., Gasser, J., Gillet, G., Scholz, D., & Kadiu, I. (2019). Inhibition of Bruton's Tyrosine Kinase Modulates Microglial Phagocytosis: Therapeutic Implications for Alzheimer's Disease. *J Neuroimmune Pharmacol, 14*(3), 448-461. doi:10.1007/s11481-019-09839-0

Kettenmann, H., Hanisch, U. K., Noda, M., & Verkhratsky, A. (2011). Physiology of microglia. *Physiol Rev, 91*(2), 461-553. doi:10.1152/physrev.00011.2010

Konjevic Sabolek, M., Held, K., Beltran, E., Niedl, A. G., Meinl, E., Hohlfeld, R., . . . Dornmair, K. (2019). Communication of CD8(+) T cells with mononuclear phagocytes in multiple sclerosis. *Ann Clin Transl Neurol, 6*(7), 1151-1164. doi:10.1002/acn3.783

Korn, T., Mitsdoerffer, M., Croxford, A. L., Awasthi, A., Dardalhon, V. A., Galileos, G., . . . Oukka, M. (2008). IL-6 controls Th17 immunity in vivo by inhibiting the conversion of conventional T cells into Foxp3+ regulatory T cells. *Proc Natl Acad Sci U S A, 105*(47), 18460-18465. doi:10.1073/pnas.0809850105

Kreutzberg, G. W. (1996). Microglia: a sensor for pathological events in the CNS. *Trends Neurosci, 19*(8), 312-318. doi:10.1016/0166-2236(96)10049-7

Kroner, A., Mehling, M., Hemmer, B., Rieckmann, P., Toyka, K. V., Maurer, M., & Wiendl, H. (2005). A PD-1 polymorphism is associated with disease progression in multiple sclerosis. *Ann Neurol, 58*(1), 50-57. doi:10.1002/ana.20514

Krumbholz, M., Theil, D., Derfuss, T., Rosenwald, A., Schrader, F., Monoranu, C. M., . . . Meinl, E. (2005). BAFF is produced by astrocytes and up-regulated in multiple sclerosis lesions and primary central nervous system lymphoma. *J Exp Med, 201*(2), 195-200. doi:10.1084/jem.20041674

Kuhlmann, T., Ludwin, S., Prat, A., Antel, J., Bruck, W., & Lassmann, H. (2017). An updated histological classification system for multiple sclerosis lesions. *Acta Neuropathol, 133*(1), 13-24. doi:10.1007/s00401-016-1653-y

Kutzelnigg, A., & Lassmann, H. (2014). Pathology of multiple sclerosis and related inflammatory demyelinating diseases. *Handb Clin Neurol, 122*, 15-58. doi:10.1016/B978-0-444-52001-2.00002-9

Lampron, A., Larochelle, A., Laflamme, N., Prefontaine, P., Plante, M. M., Sanchez, M. G., . . . Rivest, S. (2015). Inefficient clearance of myelin debris by microglia impairs remyelinating processes. *J Exp Med, 212*(4), 481-495. doi:10.1084/jem.20141656

Lassmann, H., & Bradl, M. (2017). Multiple sclerosis: experimental models and reality. *Acta Neuropathol, 133*(2), 223-244. doi:10.1007/s00401-016-1631-4

Lassmann, H., Bruck, W., & Lucchinetti, C. F. (2007). The immunopathology of multiple sclerosis: an overview. *Brain Pathol, 17*(2), 210-218. doi:10.1111/j.1750-3639.2007.00064.x

Ledeboer, A., Breve, J. J., Wierinckx, A., van der Jagt, S., Bristow, A. F., Leysen, J. E., . . . Van Dam, A. M. (2002). Expression and regulation of interleukin-10 and interleukin-10 receptor in rat astroglial and microglial cells. *Eur J Neurosci, 16*(7), 1175-1185. doi:10.1046/j.1460-9568.2002.02200.x

Li, R., Rezk, A., Miyazaki, Y., Hilgenberg, E., Touil, H., Shen, P., . . . Canadian, B. c. i. M. S. T. (2015). Proinflammatory GM-CSF-producing B cells in multiple sclerosis and B cell depletion therapy. *Sci Transl Med, 7*(310), 310ra166. doi:10.1126/scitranslmed.aab4176

Liddelow, S. A., & Barres, B. A. (2017). Reactive Astrocytes: Production, Function, and Therapeutic Potential. *Immunity, 46*(6), 957-967. doi:10.1016/j.immuni.2017.06.006

Liddelow, S. A., Guttenplan, K. A., Clarke, L. E., Bennett, F. C., Bohlen, C. J., Schirmer, L., . . . Barres, B. A. (2017). Neurotoxic reactive astrocytes are induced by activated microglia. *Nature, 541*(7638), 481-487. doi:10.1038/nature21029

Link, H., & Huang, Y. M. (2006). Oligoclonal bands in multiple sclerosis cerebrospinal fluid: an update on methodology and clinical usefulness. *J Neuroimmunol, 180*(1-2), 17-28. doi:10.1016/j.jneuroim.2006.07.006

Linker, R. A., Lee, D. H., Demir, S., Wiese, S., Kruse, N., Siglienti, I., . . . Gold, R. (2010). Functional role of brain-derived neurotrophic factor in neuroprotective autoimmunity: therapeutic implications in a model of multiple sclerosis. *Brain, 133*(Pt 8), 2248-2263. doi:10.1093/brain/awq179

Lisak, R. P., Benjamins, J. A., Bealmear, B., Nedelkoska, L., Studzinski, D., Retland, E., . . . Land, S. (2009). Differential effects of Th1, monocyte/macrophage and Th2 cytokine mixtures on early gene expression for molecules associated with metabolism, signaling and regulation in central nervous system mixed glial cell cultures. *J Neuroinflammation, 6*, 4. doi:10.1186/1742-2094-6-4

Lopez-Herrera, G., Vargas-Hernandez, A., Gonzalez-Serrano, M. E., Berron-Ruiz, L., Rodriguez-Alba, J. C., Espinosa-Rosales, F., & Santos-Argumedo, L. (2014). Bruton's tyrosine kinase--an integral protein of B cell development that also has an essential role in the innate immune system. *J Leukoc Biol, 95*(2), 243-250. doi:10.1189/jlb.0513307

Lublin, F. D., Reingold, S. C., Cohen, J. A., Cutter, G. R., Sorensen, P. S., Thompson, A. J., . . . Polman, C. H. (2014). Defining the clinical course of multiple sclerosis: the 2013 revisions. *Neurology, 83*(3), 278-286. doi:10.1212/WNL.0000000000000560

Lucchinetti, C., Bruck, W., Parisi, J., Scheithauer, B., Rodriguez, M., & Lassmann, H. (2000). Heterogeneity of multiple sclerosis lesions: implications for the pathogenesis of demyelination. *Ann Neurol, 47*(6), 707-717. doi:10.1002/1531-8249(200006)47:6<707::aid-ana3>3.0.co;2-q

Machado-Santos, J., Saji, E., Troscher, A. R., Paunovic, M., Liblau, R., Gabriely, G., . . . Lassmann, H. (2018). The compartmentalized inflammatory response in the multiple sclerosis brain is composed of tissue-resident CD8+ T lymphocytes and B cells. *Brain, 141*(7), 2066-2082. doi:10.1093/brain/awy151

Magliozzi, R., Howell, O., Vora, A., Serafini, B., Nicholas, R., Puopolo, M., . . . Aloisi, F. (2007). Meningeal B-cell follicles in secondary progressive multiple sclerosis associate with early onset of disease and severe cortical pathology. *Brain, 130*(Pt 4), 1089-1104. doi:10.1093/brain/awm038

Magraner, M. J., Bosca, I., Simo-Castello, M., Garcia-Marti, G., Alberich-Bayarri, A., Coret, F., . . . Casanova, B. (2012). Brain atrophy and lesion load are related to CSF lipid-specific IgM oligoclonal bands in clinically isolated syndromes. *Neuroradiology, 54*(1), 5-12. doi:10.1007/s00234-011-0841-7

Mahad, D. H., Trapp, B. D., & Lassmann, H. (2015). Pathological mechanisms in progressive multiple sclerosis. *Lancet Neurol, 14*(2), 183-193. doi:10.1016/S1474-4422(14)70256-X

Mahad, D. J., Ziabreva, I., Campbell, G., Lax, N., White, K., Hanson, P. S., . . . Turnbull, D. M. (2009). Mitochondrial changes within axons in multiple sclerosis. *Brain, 132*(Pt 5), 1161-1174. doi:10.1093/brain/awp046

Martin, E., Marie-Stephane Aigrota, Roland Grenninglohb, Bruno Stankoffa, Catherine Lubetzkia, Ursula Boscherte, & Zalc, B. (2020). Bruton's Tyrosine Kinase Inhibition Promotes Myelin Repair. *Brain Plasticity*.

Martinez, F. O., Sica, A., Mantovani, A., & Locati, M. (2008). Macrophage activation and polarization. *Front Biosci, 13*, 453-461. doi:10.2741/2692

Mayo, L., Trauger, S. A., Blain, M., Nadeau, M., Patel, B., Alvarez, J. I., . . . Quintana, F. J. (2014). Regulation of astrocyte activation by glycolipids drives chronic CNS inflammation. *Nat Med, 20*(10), 1147-1156. doi:10.1038/nm.3681

Michel, L., Touil, H., Pikor, N. B., Gommerman, J. L., Prat, A., & Bar-Or, A. (2015). B Cells in the Multiple Sclerosis Central Nervous System: Trafficking and Contribution to CNS-

Compartmentalized Inflammation. *Front Immunol, 6*, 636. doi:10.3389/fimmu.2015.00636

Miklos, D., Cutler, C. S., Arora, M., Waller, E. K., Jagasia, M., Pusic, I., . . . Jaglowski, S. (2017). Ibrutinib for chronic graft-versus-host disease after failure of prior therapy. *Blood, 130*(21), 2243-2250. doi:10.1182/blood-2017-07-793786

Montalban, X., Arnold, D. L., Weber, M. S., Staikov, I., Piasecka-Stryczynska, K., Willmer, J., . . . Evobrutinib Phase 2 Study, G. (2019). Placebo-Controlled Trial of an Oral BTK Inhibitor in Multiple Sclerosis. *N Engl J Med, 380*(25), 2406-2417. doi:10.1056/NEJMoa1901981

Murphy, M. P. (2009). How mitochondria produce reactive oxygen species. *Biochem J, 417*(1), 1-13. doi:10.1042/BJ20081386

Nave, K. A., & Trapp, B. D. (2008). Axon-glial signaling and the glial support of axon function. *Annu Rev Neurosci, 31*, 535-561. doi:10.1146/annurev.neuro.30.051606.094309

Nutt, S. L., Hodgkin, P. D., Tarlinton, D. M., & Corcoran, L. M. (2015). The generation of antibody-secreting plasma cells. *Nat Rev Immunol, 15*(3), 160-171. doi:10.1038/nri3795

Pal Singh, S., Dammeijer, F., & Hendriks, R. W. (2018). Role of Bruton's tyrosine kinase in B cells and malignancies. *Mol Cancer, 17*(1), 57. doi:10.1186/s12943-018-0779-z

Parish, C. R. (1999). Fluorescent dyes for lymphocyte migration and proliferation studies. *Immunol Cell Biol, 77*(6), 499-508. doi:10.1046/j.1440-1711.1999.00877.x

Park, J. K., Byun, J. Y., Park, J. A., Kim, Y. Y., Lee, Y. J., Oh, J. I., . . . Lee, E. B. (2016). HM71224, a novel Bruton's tyrosine kinase inhibitor, suppresses B cell and monocyte activation and ameliorates arthritis in a mouse model: a potential drug for rheumatoid arthritis. *Arthritis Res Ther, 18*, 91. doi:10.1186/s13075-016-0988-z

Perry, V. H., & Gordon, S. (1988). Macrophages and microglia in the nervous system. *Trends Neurosci, 11*(6), 273-277. doi:10.1016/0166-2236(88)90110-5

Ponath, G., Park, C., & Pitt, D. (2018). The Role of Astrocytes in Multiple Sclerosis. *Front Immunol, 9*, 217. doi:10.3389/fimmu.2018.00217

Ponath, G., Ramanan, S., Mubarak, M., Housley, W., Lee, S., Sahinkaya, F. R., . . . Pitt, D. (2017). Myelin phagocytosis by astrocytes after myelin damage promotes lesion pathology. *Brain, 140*(2), 399-413. doi:10.1093/brain/aww298

Ragheb, S., Li, Y., Simon, K., VanHaerents, S., Galimberti, D., De Riz, M., . . . Lisak, R. (2011). Multiple sclerosis: BAFF and CXCL13 in cerebrospinal fluid. *Mult Scler, 17*(7), 819-829. doi:10.1177/1352458511398887

Rivera, A., Chen, C. C., Ron, N., Dougherty, J. P., & Ron, Y. (2001). Role of B cells as antigen-presenting cells in vivo revisited: antigen-specific B cells are essential for T cell expansion in lymph nodes and for systemic T cell responses to low antigen concentrations. *Int Immunol, 13*(12), 1583-1593. doi:10.1093/intimm/13.12.1583

Rommer, P. S., Milo, R., Han, M. H., Satyanarayan, S., Sellner, J., Hauer, L., . . . Stuve, O. (2019). Immunological Aspects of Approved MS Therapeutics. *Front Immunol, 10*, 1564. doi:10.3389/fimmu.2019.01564

Roskoski, R., Jr. (2020). Properties of FDA-approved small molecule protein kinase inhibitors: A 2020 update. *Pharmacol Res, 152*, 104609. doi:10.1016/j.phrs.2019.104609

Rossi, S., Motta, C., Studer, V., Barbieri, F., Buttari, F., Bergami, A., . . . Centonze, D. (2014). Tumor necrosis factor is elevated in progressive multiple sclerosis and causes excitotoxic neurodegeneration. *Mult Scler, 20*(3), 304-312. doi:10.1177/1352458513498128

Rothhammer, V., Borucki, D. M., Tjon, E. C., Takenaka, M. C., Chao, C. C., Ardura-Fabregat, A., . . . Quintana, F. J. (2018). Microglial control of astrocytes in response to microbial metabolites. *Nature, 557*(7707), 724-728. doi:10.1038/s41586-018-0119-x

Rouach, N., Koulakoff, A., Abudara, V., Willecke, K., & Giaume, C. (2008). Astroglial metabolic networks sustain hippocampal synaptic transmission. *Science, 322*(5907), 1551-1555. doi:10.1126/science.1164022

Schetters, S. T. T., Gomez-Nicola, D., Garcia-Vallejo, J. J., & Van Kooyk, Y. (2017). Neuroinflammation: Microglia and T Cells Get Ready to Tango. *Front Immunol, 8*, 1905. doi:10.3389/fimmu.2017.01905

Serafini, B., Rosicarelli, B., Magliozzi, R., Stigliano, E., & Aloisi, F. (2004). Detection of ectopic B-cell follicles with germinal centers in the meninges of patients with secondary progressive multiple sclerosis. *Brain Pathol, 14*(2), 164-174. doi:10.1111/j.1750-3639.2004.tb00049.x

Shen, P., Roch, T., Lampropoulou, V., O'Connor, R. A., Stervbo, U., Hilgenberg, E., . . . Fillatreau, S. (2014). IL-35-producing B cells are critical regulators of immunity during autoimmune and infectious diseases. *Nature, 507*(7492), 366-370. doi:10.1038/nature12979

Shillitoe, B., & Gennery, A. (2017). X-Linked Agammaglobulinaemia: Outcomes in the modern era. *Clin Immunol, 183*, 54-62. doi:10.1016/j.clim.2017.07.008

Smith, K. J., & McDonald, W. I. (1999). The pathophysiology of multiple sclerosis: the mechanisms underlying the production of symptoms and the natural history of the disease. *Philos Trans R Soc Lond B Biol Sci, 354*(1390), 1649-1673. doi:10.1098/rstb.1999.0510

Smolders, J., Heutinck, K. M., Fransen, N. L., Remmerswaal, E. B. M., Hombrink, P., Ten Berge, I. J. M., . . . Hamann, J. (2018). Tissue-resident memory T cells populate the human brain. *Nat Commun, 9*(1), 4593. doi:10.1038/s41467-018-07053-9

Sofroniew, M. V., & Vinters, H. V. (2010). Astrocytes: biology and pathology. *Acta Neuropathol, 119*(1), 7-35. doi:10.1007/s00401-009-0619-8

Stadelmann, C., Kerschensteiner, M., Misgeld, T., Bruck, W., Hohlfeld, R., & Lassmann, H. (2002). BDNF and gp145trkB in multiple sclerosis brain lesions: neuroprotective interactions between immune and neuronal cells? *Brain, 125*(Pt 1), 75-85. doi:10.1093/brain/awf015

Thibult, M. L., Mamessier, E., Gertner-Dardenne, J., Pastor, S., Just-Landi, S., Xerri, L., . . . Olive, D. (2013). PD-1 is a novel regulator of human B-cell activation. *Int Immunol, 25*(2), 129-137. doi:10.1093/intimm/dxs098

Torke, S., Pretzsch, R., Hausler, D., Haselmayer, P., Grenningloh, R., Boschert, U., . . . Weber, M. S. (2020). Inhibition of Bruton's tyrosine kinase interferes with pathogenic B-cell development in inflammatory CNS demyelinating disease. *Acta Neuropathol, 140*(4), 535-548. doi:10.1007/s00401-020-02204-z

Touil, H., Kobert, A., Lebeurrier, N., Rieger, A., Saikali, P., Lambert, C., . . . Canadian, B. C. T. i. M. S. (2018). Human central nervous system astrocytes support survival and activation of B cells: implications for MS pathogenesis. *J Neuroinflammation, 15*(1), 114. doi:10.1186/s12974-018-1136-2

Trapp, B. D., & Stys, P. K. (2009). Virtual hypoxia and chronic necrosis of demyelinated axons in multiple sclerosis. *Lancet Neurol, 8*(3), 280-291. doi:10.1016/S1474-4422(09)70043-2

U.S. Food and Drug Administration News Release. FDA approves new drug to treat multiple sclerosis. First drug approved for Primary Progressive MS. (2018). *https://www.fda.gov/news-events/press-announcements/fda-approves-new-drug-treat-multiple-sclerosis*.

van der Poel, M., Ulas, T., Mizee, M. R., Hsiao, C. C., Miedema, S. S. M., Adelia, . . . Huitinga, I. (2019). Transcriptional profiling of human microglia reveals grey-white matter heterogeneity and multiple sclerosis-associated changes. *Nat Commun, 10*(1), 1139. doi:10.1038/s41467-019-08976-7

Walton, C., King, R., Rechtman, L., Kaye, W., Leray, E., Marrie, R. A., . . . Baneke, P. (2020). Rising prevalence of multiple sclerosis worldwide: Insights from the Atlas of MS, third edition. *Mult Scler, 26*(14), 1816-1821. doi:10.1177/1352458520970841

Wang, D., Ayers, M. M., Catmull, D. V., Hazelwood, L. J., Bernard, C. C., & Orian, J. M. (2005). Astrocyte-associated axonal damage in pre-onset stages of experimental autoimmune encephalomyelitis. *Glia, 51*(3), 235-240. doi:10.1002/glia.20199

Y-B Alankus, R Grenningloh, P Haselmayer, A Bender, & Bruttger, J. (2019). Inhibition of Bruton's tyrosine kinase prevents inflammatory macrophage differentiation: a potential role in multiple sclerosis. *Annual Meeting of the Consortium of Multiple Sclerosis Centers; May 28–June 1, 2019; Seattle, WA, USA, Poster*.

Yao, A., Liu, F., Chen, K., Tang, L., Liu, L., Zhang, K., . . . Wang, J. (2014). Programmed death 1 deficiency induces the polarization of macrophages/microglia to the M1 phenotype after spinal cord injury in mice. *Neurotherapeutics, 11*(3), 636-650. doi:10.1007/s13311-013-0254-x

Zhang, J. M., & An, J. (2007). Cytokines, inflammation, and pain. *Int Anesthesiol Clin, 45*(2), 27-37. doi:10.1097/AIA.0b013e318034194e

Zhao, J., Roberts, A., Wang, Z., Savage, J., & Ji, R. R. (2021). Emerging Role of PD-1 in the Central Nervous System and Brain Diseases. *Neurosci Bull, 37*(8), 1188-1202. doi:10.1007/s12264-021-00683-y

ACKNOWLEDGMENT

Ich möchte an dieser Stelle die Gelegenheit nutzen, meinen Dank an diejenigen zu richten, die mich während meiner Doktorarbeit motiviert, unterstützt und inspiriert haben.

Allen voran gilt mein besonderer Dank meinem Betreuer Prof. Dr. Martin S. Weber. Ich bin Ihm sehr dankbar für seinen Enthusiasmus, seine Geduld und Motivation. Die Zusammenarbeit hat mir immer viel Spaß gemacht und hat mich auf professioneller wie auf privater Ebene über mich hinauswachsen lassen.

Ich bedanke mich bei Prof. Dr. Hannelore Ehrenreich und Prof. Dr. Jutta Gärtner für ihr Interesse, ihre Ideen und die Unterstützung während der Promotion.

Ich bedanke mich bei allen anderen Kolleg:innen der Neuropathologie und des Promotionsprogramms Molekulare Medizin.

Besonderer Dank gilt Dr. Darius Häusler, der immer ein offenes Ohr für mich und meine Ideen hatte. Ich hätte mir keine bessere Betreuung wünschen können und Ich freue mich auf eine weitere erfolgreiche Zusammenarbeit.

Dr. Sebastian Torke möchte Ich nicht nur für die unzähligen Kaffeepausen danken, sondern auch für sein fachliches Feedback und die gemeinsamen Brainstorming Momente.

Unendlich dankbar bin ich Katja Grondey und Julian Koch für die Unterstützung, wann immer sie nötig war. Ohne euch wäre diese Arbeit nicht möglich gewesen und nur halb so spaßig.

Ich möchte mich bei der gesamten Arbeitsgruppe bedanken, nicht nur für den Austausch der Ideen, sondern vor allem für die großartige Atmosphäre und Unterstützung. Besonderer Dank gilt meiner Kaffeepartnerin Sarah, meiner Milchmäuse Versorgerin und Rückenmasseurin Jasmin, meinen Sektbuddies Marie und Adriane, meiner Kurzzeit Labor Mitbewohnerin Roxanne und meiner Motivationsstütze Silke.

Des Weiteren möchte ich mich bei Prof. Dr. Katrin Streckfuß-Bömeke bedanken, die mir als Mentorin zur Seite stand.

Außerdem bedanke ich mich bei all meinen Mitbewohner:innen, die die B24 während dieser Zeit zu meinem Zuhause gemacht haben.

Großer Dank geht an meine Familie für ihre Unterstützung. Insbesondere bedanke ich mich bei meiner Schwester Helena, ohne die ich nicht die Person wäre, die ich bin.

Abschließend bedanke ich mich bei all meinen Herzensmenschen, die mir auf dieser Reise so viel Akzeptanz und Geduld entgegengebracht haben. Danke für eure Freundschaft: Sina, Paddy, Katja, Alina, Julia, Esther, Lina, Kai, und Paul.